POLITECNICO
MILANO 1863

SCUOLA DI INGEGNERIA INDUSTRIALE
E DELL'INFORMAZIONE

L.I.F.E. sensorized garments for noninvasive and continuous respiratory monitoring: validation in different experimental conditions

Tesi di Laurea Magistrale in
Biomedical Engineering - Ingegneria Biomedica

Author: **Matteo Scotti**

Student ID: 928337
Advisor: Prof. Andrea Aliverti
Co-advisors: Silvia De Nadai, Francesco De Grazia
Academic Year: 2021-22

Abstract

Continuous monitoring of ventilatory parameters is of critical importance to assess the health state of patient in critical conditions, such as intensive care units and post-operative scenarios, and in presence of ventilatory or cardiac diseases. Nowadays there exist several accurate and reliable options to assess the health status of a subject in the clinical practice and structures, but their application is limited to clinical environment and can be performed by trained staff only. Furthermore, they only offer "snapshot in time" informations abut the health status of the subject, and cannot be used to continuously monitor ventilatory functions without at least discomfort.
These limitations in traditional measuring systems could be overcame by wearable biomedical devices, which allow a continuous monitoring of ventilatory and cardiac conditions during daily-life, in every environment and during every activity. The main drawback of these innovative technologies is to match the accuracy and reliability of standard measurement methods used in the clinical practice.
This work of thesis is focused on this problem, and its purpose is to validate three wearable devices from L.I.F.E. Italia S.r.l. in static and dynamic conditions. L.I.F.E. Healer R1, R2 and R3 garments integrate a sensors network able to measure ventilatory, cardiac functions and other physiological parameters of the subject. Ventilatory parameters have been evaluated following a static protocol in different body positions and a dynamic protocol.
Results proved the feasibility of using the three L.I.F.E. devices to monitor respiratory temporal and rate parameters in both static and dynamic conditions, while volumetric parameters could not be considered accurate enough due to the large variance of measurements. To improve the accuracy and reliability of volume measurement, it is suggested to prefer a slim and tight fit of the wearable device and to perform a calibration phase for every subject.

Keywords: continuous monitoring, wearable, validation, ventilatory functions, strain gauges.

Abstract in lingua italiana

Il monitoraggio continuo dei parametri ventilatori è considerato di importanza cruciale per la valutazione dello stato di salute di pazienti in condizioni critiche, per esempio in terapia intensiva o in un contesto post-operatorio, e in presenza di patologie cardiache e respiratorie. Ad oggi esistono diverse opzioni accurate e affidabili utilizzate per valutare queste condizioni in strutture ospedaliere, ma la loro applicazione è limitata all'ambiente clinico e può essere effettuata solamente da personale formato. Inoltre, questi strumenti offrono informazioni sulla condizione del soggetto in esame per un intervallo temporale limitato, e non possono essere utilizzate per monitorare in maniera continua le funzioni respiratorie. Le limitazioni dei sistemi di misura tradizionali possono essere superate utilizzando dispositivi indossabili, che permettono il monitoraggio continuo delle condizioni ventilatorie e cardiache del paziente nella vita di tutti i giorni, in qualsiasi ambiente e durante qualsiasi attività. Il principale svantaggio di questi strumenti innovativi è la loro inferiore accuratezza e affidabilità rispetto alle tecnologie convenzionali usate comunemente nella pratica clinica.

Lo scopo di questo lavoro di tesi è la validazione di tre dispositivi indossabili di L.I.F.E. Italia S.r.l. in condizioni sia statiche che dinamiche. I dispositivi indossabili di L.I.F.E., Healer R1, R2 ed R3, integrano una rete interconnessa di sensori in grado di misurare le funzioni ventilatorie e cardiache, così come altri parametri fisiologici di interesse. I parametri ventilatori, centrali in questo studio, sono stati valutati attraverso un protocollo statico ripetuto in diverse posizioni e uno dinamico.

I risultati hanno confermato la possibilità di utilizzare i tre dispositivi indossabili di L.I.F.E. per monitorare i parametri temporali e di frequenza respiratoria sia in condizioni statiche che dinamiche. I parametri volumetrici, tuttavia, non possono essere considerati sufficientemente accurati a causa dell'ampia dispersione delle misurazioni. Per migliorare accuratezza e affidabilità delle misure di questi parametri volumetrici è consigliabile utilizzare garment con un taglio snello e aderente, e calibrare i dispositivi in maniera personalizzata per ogni singolo paziente.

Parole chiave: monitoraggio continuo, dispositivo indossabile, validazione, funzionalità ventilatoria, strain gauges.

Contents

Introduction

The monitoring of ventilatory parameters is of fundamental importance in the clinical practice to assess ventilation function and to diagnose and supervise the progression of lung and heart diseases. Nowadays the laboratory instrumentation and tests are well affirmed as gold standard to assess health condition of the respiratory system, with spirometry being one of the most diffused. It is a non-invasive method which can accurately and reliably measure ventilatory parameters, but it is not feasible for continuous monitoring and requires the cooperation of the subject under test. Like spirometry, the existing tests and instrumentation in the clinical practice provide informations in a "snapshot in time" approach, and even if they are becoming more and more portable, they are yet unfeasible for long continuous monitoring and assessment of the health conditions of the respiratory system.
For this reason, wearable devices are spreading during the last years as great candidates for continuous monitoring scenarios. Wearable devices can be whatever object that can be worn, from chest belts to sensorized garments, and allow to monitor various ventilatory and heart-related parameters during daily-life activities with minimized constriction on mobility. Anyway, the major limitations they have shown until now is the limited reliability and accuracy of the measured data with respect to the gold standard measures, which prevents the application of such wearables systems in a valuable clinical practice.
The aim of this thesis work is to validate L.I.F.E. Italia S.r.l. Healer R1, R2 and R3 wearable garments for the continuous monitoring of respiratory parameters, namely inspiratory volume (both absolute and normalized), inspiratory time and respiration rate in both static and dynamic conditions. Such validation is needed to assess if the wearable garments under analysis are able to accurately and reliably measure ventilatory parameters in concordance with a gold standard spirometer or, otherwise, to investigate the reasons of such inaccuracy to address future improvements of the L.I.F.E. devices.
The structure of this study is as follow:

- Chapter 1 describes the state of the art of ventilatory monitoring technologies, both used in the clinical practice and newer solutions exploiting wearable devices. Measuring principles of the fundamental wearable devices used in this field will be

introduced. Theoretical and anatomical information, essential to understand the remaining body of the thesis, are also recalled in this first chapter. A particular focus is given to the L.I.F.E. measuring principle of ventilatory parameters.

- Chapter 2 deals with the materials, technologies and methods employed in the validation of the three L.I.F.E. Healer devices, which are here characterized together with the gold standard MicroQuark spirometer by COSMED. The validation protocol is here explained in detail, as the processing steps used to derive the ventilatory parameters of interest.
- Chapter 3 presents the comparison between the ventilatory parameters derived using L.I.F.E. Healer devices and MicroQuark spirometer through qualitative and quantitative analysis.
- Chapter 4 reports the conclusions achieved during the validation process of L.I.F.E. Healer R1, R2 and R3 suits with respect to the considered gold standard instrumentation.

1 State of the art

1.1. Ventilation monitoring

Ventilation is the act of moving air in and out the lungs to allow gas exchange between the circulatory system and the external environment, which occurs in the lungs between alveolar air and the blood of the pulmonary capillaries. The motion of air inside and outside the lungs is created by a change in volume of the chest wall thanks to the action of the respiratory muscles. The chest wall is defined as all the parts surrounding the lungs and moving with them during breathing, hence the thoracic and abdominal wall. This subdivision defines two parallel ventilation pathways both contributing to ventilation. Monitoring pulmonary ventilation means monitor time, volume, and flow parameters listed in Section 1.2 [1]. These parameters are fundamental to assess ventilation function, to diagnose or monitor the progression of respiratory diseases. For example, breathing frequency is an indicator used to assess abnormalities in the respiratory system, but even as predictor for several severe clinical events, such as cardiac arrest or admission to the intensive care unit. Respiratory rate, as breathing activity in broad term, should be continuously monitored since it is affected by many heart and lung diseases, even more while dealing with particularly sensitive cases, as could be mechanical ventilation assisted patients or post-operative ones [2, 3, 4, 5, 6].

1.2. Spirometry

As already mentioned, measuring ventilatory parameters is crucial in order to assess the conditions of the breathing system. Pulmonary function tests permit accurate, reproducible assessment of the functional state of the respiratory system. Such evaluation can be performed, among a large variety of lungs function tests, by spirometry, in which relative lungs volume and volume variations are measured as function of time during inspirations and expirations. Spirometry is a invaluable screening test of general respiratory health, as diagnostic, monitoring and rehabilitative tool.
A spirometry test is currently performed by asking the patient to breath through a mouth-

piece linked to an instrument, a spirometer, which measures the flow and/or volume of moved air while breathing spontaneously at rest, or forcibly during the execution of breathing maneuvers. Through a spirometric test it is possible to measure and quantify different relative volume parameters, as it can be seen in Figure 2.6 which shows a typical recording of this functional test.

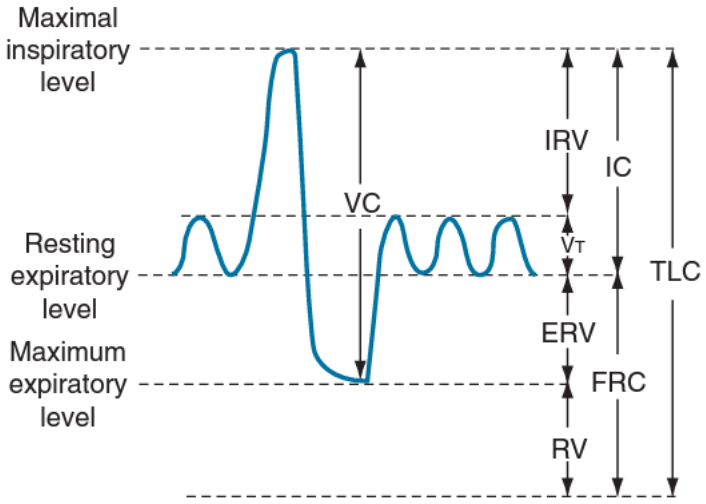

Figure 1.1: Spirogram

Lung volume and capacities can be characterized within the volume recordings in the spirogram in Figure 1.1. More in detail there are four distinct, non-overlapping volumes:

1. tidal volume (V_T): volume of gas inhaled or exhaled during each respiratory cycle at rest;
2. inspiratory reserve volume (IRV): maximal volume of gas inspired from end-inspiration at rest;
3. expiratory reserve volume (ERV): maximal volume of gas exhaled from resting end-expiration;
4. residual volume (RV): volume of gas remaining in the lungs following a maximal forced exhalation.

In addition there are four capacities, each of which contains two or more primary volumes:

1. total lung capacity (TLC): amount of gas contained in the lungs at maximal forced inspiration;
2. vital capacity (VC): volume change at the mouth between the position of full inspiration and complete expiration;

3. inspiratory capacity (IC): is the maximal volume of gas that can be inspired from the resting expiratory level;
4. functional residual capacity (FRC): volume of gas in the lungs at resting end-expiration.

Upon all these different lungs characterizations, the VC and IC will be the main ones under analysis in this work, as described later on in Section 2.2.1. In particular the Slow Vital Capacity (SVC) can be derived in two ways: through the expiratory vital capacity (EVC), which is the maximal volume of air exhaled from the point of maximal inhalation, and through the inspiratory vital capacity (IVC) as the maximal volume of air inhaled from the point of maximal exhalation, achieved by a slow expiration from end-tidal inspiration. These manoeuvres are unforced, except at the point of reaching RV or TLC, respectively, where extra effort is required. Maximum inhaled and exhaled volumes should be reached maintaining a relative constant flow: inspiration and expiration should not be excessively slow, as this can lead to underestimation of VC.
Regarding IC, it is the volume change recorded at the mouth when taking a slow full inspiration with no hesitation, from a position of passive end-tidal expiration (FRC) to a position of maximum inspiration (TLC). These two maneuvers are shown in the two spirograms in Figure 1.2 [7, 8, 9].

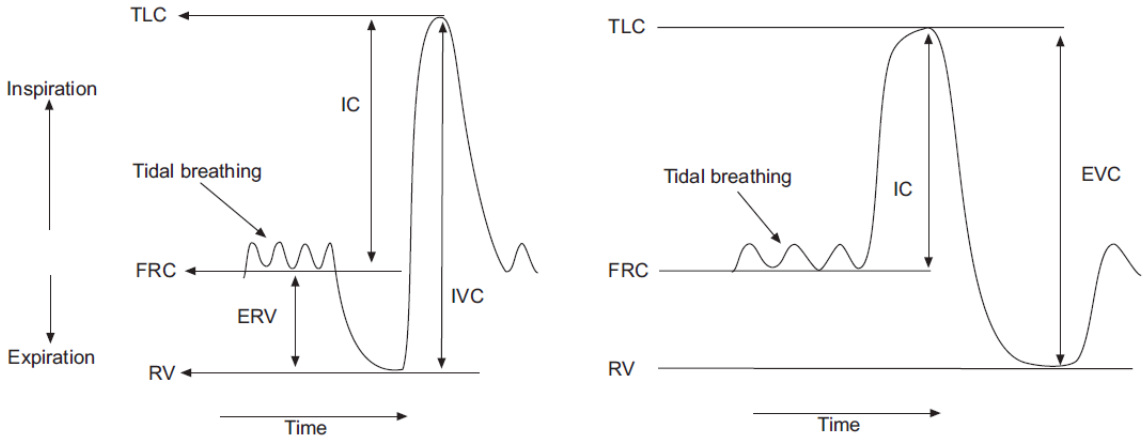

Figure 1.2: Spirogram showing IC, IVC and EVC maneuvers.

Along with volumes and capacities, also breathing temporal parameters must be measured. The main are the breathing frequency (f_B), or respiratory rate, expressed as breathing events per minute; inspiratory time (T_I) and expiratory time (T_E) whose sum determines the breathing period (T_{tot}). The duty cycle (DC) is the ratio between inspiratory time and total respiratory time, and is another key parameters in respiratory

ventilation monitoring and assessment.
Starting from these three subsets of primary parameters, another group of so called secondary parameters can be derived. It comprehends the minute respiratory volume (MV), product between tidal volume and respiratory rate; forced expiratory volume (FEV), which measures the volume of gas exhaled performing a forced expiration during the first (FEV1), second (FEV2) or third second (FEV3). It is also possible to measure the forced expiratory flow (FEF) as the flow of expired gas at fixed ratios of the FVC (25%, 50% and 75%), so obtaining FEV25, FEV50 and FEV75 [7, 8, 9].

1.2.1. The spirometer

The spirometer is the instrument used to measure the flow and/or volume of inspired/expired gas through the mouth. Various types of spirometers are available, and they differ from each other thanks to the sensors integrated inside the device. The most used and established are the following:

- Ultrasonic spirometer: a couple of ultrasonic transducers is placed transversal to the pipe in which the gas flows, as represented in Figure 1.3.

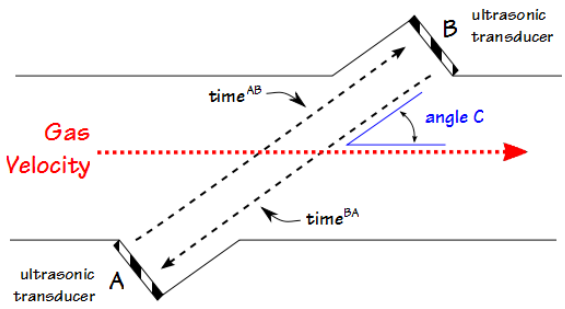

Figure 1.3: Ultrasonic spirometer working principle

The working principle is based on the time-of-fligth (TOF) measurement of the ultrasonic wave between the two transducers, which depends on the velocity and direction of the gas flow within the tubing. In fact, pulses that travel in the same direction of the gas flow will take less time to travel between the transducers, while pulses traveling against the gas direction will take longer. More in detail, the time-of-flight of an ultrasonic pulse depends on the distance between the two transducers (D), the angle of the ultrasound pulses relative to the gas flow (θ), its velocity (V_g)

and the speed of sound (V_s) as stated in equations 1.1, 1.2, 1.3:

$$TOF_{AB} = \frac{D}{V_s + (V_g \cdot cos\theta)} \tag{1.1}$$

for ultrasonic pulse directed from A to B;

$$TOF_{BA} = \frac{D}{V_s - (V_g \cdot cos\theta)} \tag{1.2}$$

for ultrasonic pulse directed from B to A.
Finally the gas velocity can be derived and well approximated as:

$$V_g \simeq \frac{D}{2cos(\Theta} \cdot \frac{TOF_{AB} - TOF_{BA}}{\frac{TOF_{AB}+TOF_{BA}}{2}} \tag{1.3}$$

In this way the measured gas flow is insensitive to the speed of sound, which can be affected by gas temperature, composition and pressure [10, 11].

- Pneumotach: gas flow through a pneumotach is measured from the difference in pressure across a resistance and there are two main ways to induce a relative linear pressure drop. The first approach uses a set of narrow capillary tubes parallel to the direction of flow, while in the second the resistance is created by a variable number of narrow-mesh screens placed perpendicular to the direction of flow. These two approaches are shown in Figure 1.4.

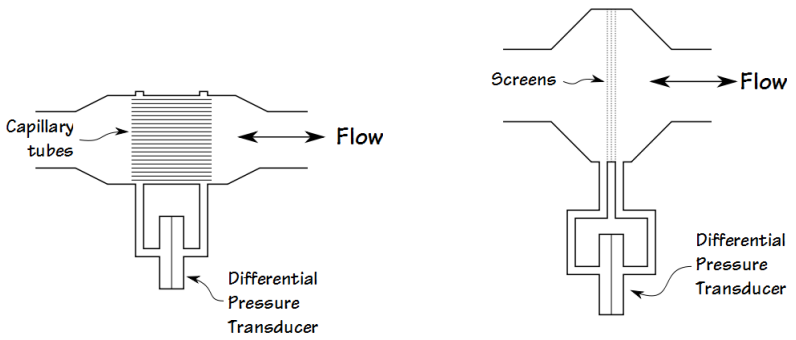

(a) Capillary-based pnemotachometer (b) Fine mesh-based pnemotachometer

Figure 1.4: Different working principles used in Pneumotachometry

Both of these two instruments have to be heated at $37\,°C$ in order to avoid con-

densation on the resistance element of water vapor at ambient temperature in the exhaled air. Condensation increases the resistance through the pneumotach in a variable and unpredictable measure, leading to an overestimation of the expiratory volume, after a series of breaths cycles, up to 7%. This gain in stability is paid by a reduction in portability of the pneumotach, since heating the internal resistance requires a fair amount of power [12, 13].

- Turbine spirometer: gas flow passing through a rotor is measured by a couple of diodes. The rate at which the infrared light beam is interrupted by the rotor is proportional to the gas flow, resulting in a decrease in current generated by the receiving diode. Across a relatively wide range of flow rates, each rotation of the fan is directly linked to the volume of gas flowing through the sensor. This is the simple principle on which is based the spirometer used in this work of thesis, which will be explained more in detail in Section 2.1.2, and a typical design is shown in Figure 1.5.

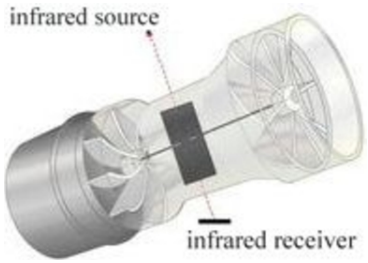

Figure 1.5: Turbine spirometer

In literature there are numerous studies comparing turbine and more conventional spirometers. Although the majority of these studies showed that turbine spirometers met the ATS/ERS guidelines, they also showed that FVC tended to be underestimated somewhat and that the FEV1/FVC ratio tended to be slightly overestimated. It must also be noted that there is no clear reason to believe that turbine spirometers are significantly less accurate than any other measurement technique [14, 15].

1.3. Wearable biomedical devices

In healthcare, the vast majority of diagnostic tools provide information in a "snapshot in time" approach. A complete monitoring is mainly performed in healthcare structures by using accurate, gold standard instrumentation yet unfeasible for long continuous measurement. Because of these limitations, one of the great future challenges is to continuously monitor the physiological parameters of a patient under daily-life conditions, in any envi-

ronment and during activity. These systems will allow to track and monitor both chronic and acute events and the general condition of patients in cities or even in rural areas, resulting in a increase of healthcare services efficiency and improving the patients comfort. All those innovative results could be obtained by the introduction of wearable devices.
A wearable device is any measurement device that can be worn without any restriction on mobility or daily activity. Nowadays there is a large and well established diffusion of wearables, as activity tracker or smart watches, but the majority of them cannot be considered reliable or accurate in the analysis of the health condition of the user. On the other hand, there is a significant number of sensors and devices that measure physiological parameters in a traditional, non-wearable, way. Therefore, a wearable biomedical device is considered any equipment able to accurately and reliably measure physiological parameters and that can be worn.
Main wearable solutions and measuring principles for pulmonary ventilation monitoring will be introduced in Section 1.3.1.

1.3.1. Wearables in pulmonary ventilation monitoring

There exist several technologies to monitor pulmonary ventilation through wearable devices. Among the various solutions, body surface sensors are one of the most common choices. This category of devices measures the movement of the chest wall, rib cage or abdomen through different methods and equipment.
A first approach is to measure the linear displacement of the chest along the anterior-posterior axis. Using accelerometers coupled with gyroscopes and magnetometers, it is possible to estimate the breathing frequency. It is also possible to use Micro-ElectroMechanical System technology (MEMS), which host in a miniaturised device three-axis accelerometers, three-axis gyroscopes and three-axis magnetometers, to reconstruct the three-dimensional movement of the chest wall [16, 17, 18].
Another option is to measure changes in chest circumference in a direct or indirect way. Strain gauges, elastic bands which changes electrical resistance with stretching, are used to directly measure the changes in thoracic or abdominal circumferences during breathing. Respiratory Inductive Plethysmography (RIP), on the opposite, indirectly derives the variations by measuring changes in electrical impedance between a pair of electrodes or wires incorporated into elastic bands placed around the chest and abdomen. More in detail:

- using two electrodes, a drive signal can be applied to the subject and, by recording voltage fluctuations, it is possible to obtain the impedance variations in the thoracic cavity due to the respiration. Therefore, the voltage fluctuations may be used to

determine the respiratory rate;

- using two inductive belts carrying alternating current and incorporated into cloth bands placed around the chest and abdomen, changes in cross-sectional area can be measured by RIP. These variations result in proportional changes in self-inductance, causing voltage signals measured across the terminal ends of the wires [19, 20, 21].

In the next paragraph the measuring principle used by strain gauges will be characterized in detail, since they are the sensors incorporated within L.I.F.E. devices and used in this work to measure chest wall variations in circumference.

Strain Gauges

A resistive strain gauge (SG) is a transducer able to convert mechanical strain (ϵ) into a change in electrical resistance (R). This particular property of materials is named piezoresistive effect.
Generally, the electrical resistance depends on geometrical and factors depending on the material, as described in the following equation:

$$R = \rho \cdot \frac{l}{A} \tag{1.4}$$

where ρ is the resistivity of the material, l the length of the transducer and A its surface, as shown in Figure 1.6.

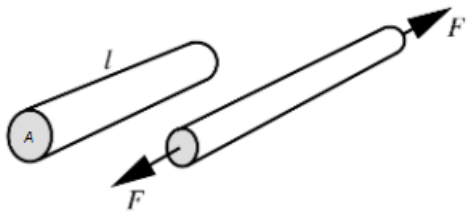

Figure 1.6: Geometrical model of a cylindrical strain gauge.

Under the hypothesis of applying a force F along the longitudinal axis of a cylindrical strain gauge, a change in electrical resistance, elicited by the mechanical stress, will be given by Equation 1.5

$$dR = \frac{\rho}{A}dl + \frac{l}{A}d\rho - \frac{l\rho}{A^2}dA \tag{1.5}$$

The change in resistance can be expressed as relative value by Equation 1.6, in which

are clearly expressed the dependencies of the change in electrical resistance by the length variation along the direction of the strain, the variation in resistivity and in the cross-sectional area.

$$\frac{dR}{R} = \frac{dl}{l} + \frac{d\rho}{\rho} - \frac{dA}{A} \tag{1.6}$$

There exist a third way to express the change in electrical resistance, for which it is necessary to introduce the Poisson's Ratio ν and the Gauge Factor G:

$$\begin{aligned} \nu &= -\frac{dA/A}{dl/l} \\ G &= \frac{dR/R}{dl/l} = 1 + 2\nu + \frac{d\rho/\rho}{dl/l} \end{aligned} \tag{1.7}$$

The Poisson's ratio characterises the mechanical properties of the material, while the Gauge Factor describes the resistance variation per unit of strain, which on turn depends on the variation of resistance due to longitudinal deformation, on the variation of cross-sectional area and lastly on the piezoresistive effect.
In conclusion, the change in relative electrical resistance can be expressed as in Equation 1.8, which includes all the dependencies discussed above.

$$\frac{dR}{R} = G\frac{dl}{l} = G\epsilon \tag{1.8}$$

In the interest of this work of thesis, it is important to note that resistance variation is linear with the strain under the assumption that the transducer is working in the elastic zone of the stress-strain curve, shown in Figure 1.7. In fact if the elastic limit is overcame, the material undergoes plastic deformation, which are non-linear and are irreversible [16, 22].

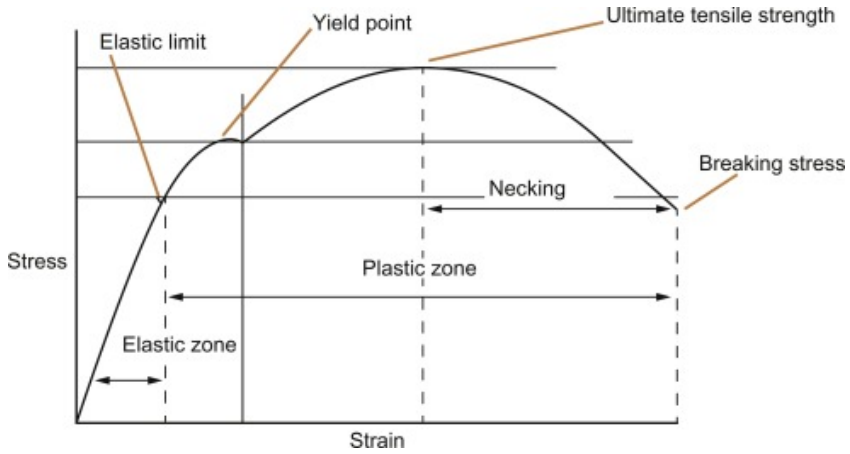

Figure 1.7: Stress-strain curve. In a strain-gauge, the linear behaviour of the resistance with strain is verified in the only case in which the stress and deformations of the material are constrained on the elastic zone of the curve.

2 | Material and Methods

In this chapter are explained all the materials and methodologies used in the acquisition and treatment of the measured data. In detail, in the first section are characterized the instrument to be validated and the one used as gold standard. Secondly the acquisition protocol and test pool are described. while in the third part the methods, algorithms used to process the acquired data are shown in detail.

2.1. Materials

2.1.1. LIFE garments

This study focused on the validation of three L.I.F.E. wearable devices named Healer R1, Healer R2, Healer R3. They are upper-body smart garments which integrate a sensor network to measure and monitor physiological signals and parameters. In particular, they record ECG (6 or 12 derivations), the ventilation mechanics on three channels, SpO2, body position, body temperature and activity level.
Every Healer is connected to a Logger device plugged on the upper-back of the suit, which controls the acquisition, processing, storage and transmission of the recorded data.
More specifically:

1. Healer R1: this T-shaped suit houses 10 dry ECG electrodes measuring the electrical activity of the heart along 12 derivations. 6 of such electrodes are placed on the thorax, two on the arms and two on the lower back. The device measures the respiratory mechanics by a set of three strain gauges placed in correspondence of the abdomen, xiphoid and thorax. The SpO2 is measured with a pulse oximeter produced by Nonin, which measures the blood oxygen-saturation at the fingertip; while an IMU located at the thoracic vertebra T3 measures the upper-body position and activity. Lastly the body-temperature is estimated in the armpit area through a temperature sensor.

2. Healer R2: this upper-body device is gilet-shaped and differs from the former Healer R1 by some few features. In particular, it measures the electrical activity of the heart

along 6 derivations through 4 dry ECG electrodes placed on the back; the SpO2 under the left armpit and the temperature under the right one. The ventilation mechanics (strain-gauges) and the position (IMU) sensors are placed as in the Healer R1.

3. Healer R3: gilet-shaped device, integrating the features of versions R1 and R2. It measures the ECG signal along 12 derivations through 10 dry electrodes, 6 located on thorax and four on the back; the respiratory signal by three strain-gauges as in the other two devices; qualitative blood-saturation and body-temperature as in R2 (in the armpit area). Healer R3 can additionally record the diagnostic SpO2 by the plugged-in pulse oximeter. Lastly, the upper-body position IMU sensor is placed at the thoracic vertebra T3 as in the two other suits.

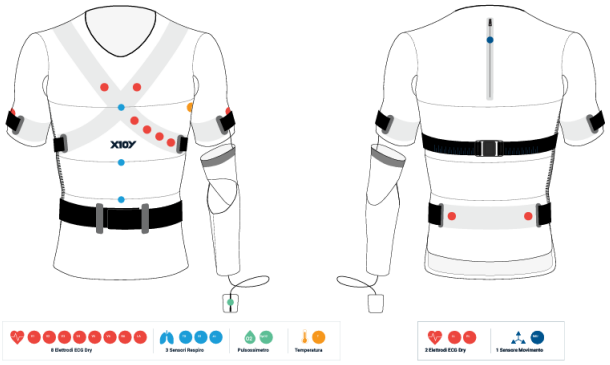

(a) Healer R1

(b) Healer R2

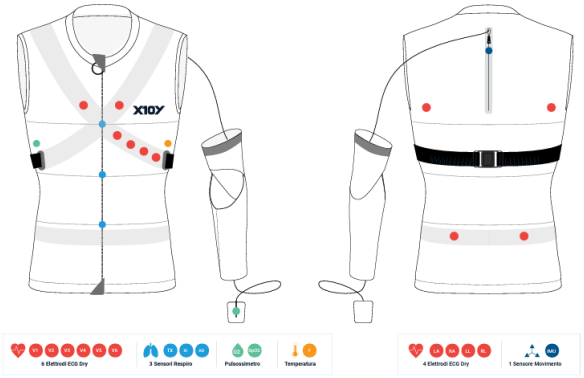

(c) Healer R3

Figure 2.1: Healer R1, R2, R3 garments

The three L.I.F.E. suits are produced in three different sizes (S, M and L) and in a male and female version, which differ in some structural features to better accommodate differences in anatomical features between the two versions. The three L.I.F.E. devices

differ, in addition to the number and position of the different sensors, by the way they fit when wore by the user. In fact, Healer R1 and Healer R3 shares the same shapes, proportions and dimensions, and are produced to be dressed in a comfortable and loose-like way. On the other hand, Healer R2 is characterized by a slim fit, resulting in a much tighter, yet comfortable fitting. Furthermore, there exist little differences in the positioning and length of the three silicon strain-gauges in the three suits.

LIFE strain-gauges sensors

In L.I.F.E. garments the ventilatory information is acquired through strain-gauges sensors. Such wire-like transducers are made by conductive silicon, and placed in correspondence of the thorax, xiphoid and abdomen. Recalling what said in Section 1.3.1, such sensors varies their resistance according to their stretch/relaxation in response to the expansion/compression of the body-district they sense. Regarding these sensors mounted on the three L.I.F.E. Healer garments R1, R2 and R3, the main differences between devices are found to be the relative position of the three stain gauges with respect to the body surface and their length, resulting in different pre-tensioning of the transducers.

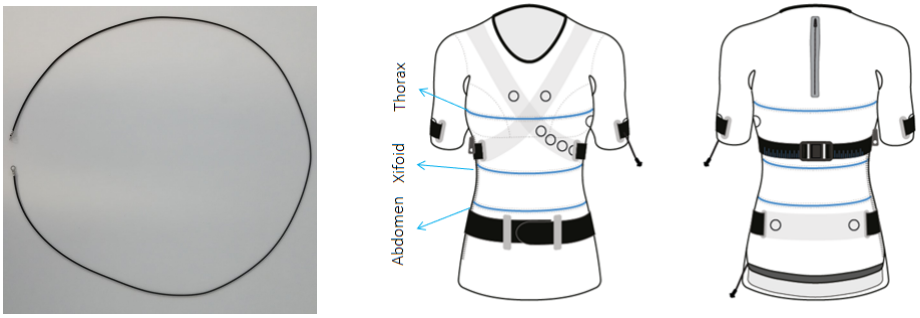

(a) Breath Strain-Gauge sensor

(b) Sensors placement

Figure 2.2: Breath sensors

The voltage across this variable resistor is read by the ADC in the micro controller housed in the Logger unit after a passive conditioning stage. Circuital and dimensional details about the conditioning circuit can not be divulged by L.I.F.E. Italia S.r.l. since they are sensitive material. The three strain-gauges are pre-stretched, allowing for measuring both compression and extensions with respect to their rest length. It must be noted that, after large inspiratory or expiratory breaths, the sensors come back to the resting length by an elastic-return dynamic which may drastically distort the following breaths. This behaviour can be seen by comparing the garment and spirometer volume recordings, as

shown in Figure 2.3, in which the dynamic is clearly observable in the case there is one or more breaths with a large difference in volume amplitude followed by one or more breaths with smaller volume variation. Such "recovery breaths" are characterized by a non-linear decreasing baseline, on top of which are summed the distorted breaths. The causes of this noisy-like behaviour can be found in the fact that the mechanical elastic-return dynamic of the strain-gauges is slower than the breathing dynamic of the ventilatory system sectors (thorax, xyphoidal complex and abdomen) sensed by the sensors on top. This difference leads to a limited and partial coupling in the change of length, or better circumference, of the strain-gauges with respect to the one of anatomical structures beneath them, resulting in a underestimated measurement of the length variation after a big elongation of the sensors, finally leading to an underestimation of the volume variations. In Section 2.3 the consequences of this distortion in the measured amplitudes will be discussed in detail.

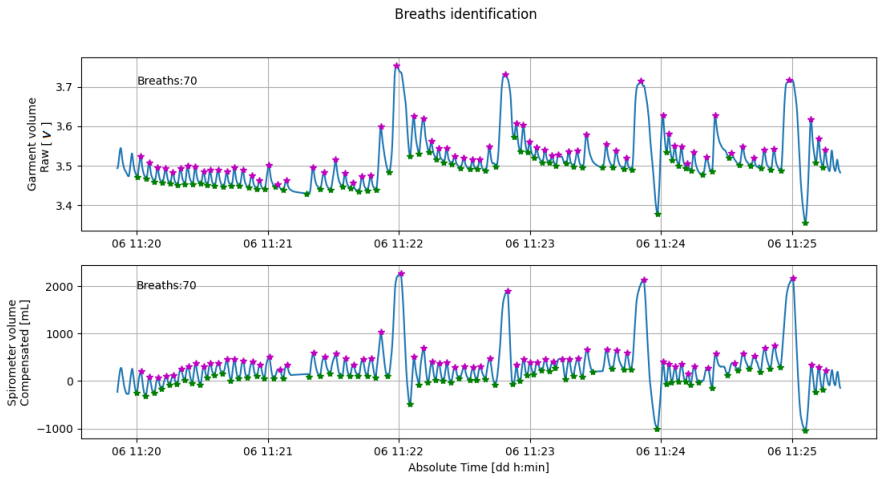

Figure 2.3: Elastic return dynamic in Healer volume signals.

2.1.2. COSMED MicroQuark spirometer

The MicroQuark spirometer from COSMED is a portable instrument which measures the flow of air passing through its turbine. It must be coupled with the OMNIA software from COSMED, and can perform standard spirometry tests, such as Forced Vital Capacity (FVC), Slow Vital Capacity (SVC) and Maximal Voluntary Ventilation (MVV), or record more freely the flow or volume of air passing through the turbine.

Figure 2.4: COSMED MicroQuark Spirometer

Components

1. Turbine flowmeter: this is the transducer to directly measure the flow passing through the turbine by means of a rotor and a photodiode/diode couple. The rotor (or turbine) is a removable piece which has to be inserted in the top-hole of the handle-shaped reader; the latter houses the electronics and circuitry to enable flow measurement.
   The infrared-light emitting photodiode is placed on one side of the hole in the reader, facing the receiving diode on the opposite side of the hole. The diode measures the intensity of the incident light by producing current proportionally to the received light's intensity.
   Whenever air flows through the turbine it will cause the rotor to rotate, blocking the infrared light beamed by the two diodes of the reader, hence reducing the intensity of the light received by the diode, and so reducing the current in output from the receiving diode. Every drop in current (hence interruption) corresponds to 1/4 of rotor cycle, allowing to measure the number of rotations in time, or rotation velocity. Since the rotation velocity is directly proportional to the airflow through the turbine, we can measure the flow of air passing through the transducer.

2. MicroQuark unit: it is the core of the device comprehending all the electronics and sensors used to measure the flow through the turbine flowmeter and communicate the data to an external device via USB cable. All those elements are housed in the handle of the device. Just as example, the unit controls the calibration of the instrument and can determine the volume of air moved through the flowmeter by flow integration.

3. Antibacterial filters: the use of disposable antibacterial filters has become almost mandatory to prevent the diffusion of droplets and aerosol in air in order to mini-

mize the transmission of infectious diseases. In this work, antiviral and antibacterial filters with integrated oval-shaped mouthpieces were used , much more comfortable and ergonomic than rounded cardboard mouthpieces. In table 2.1, all the characteristics of such filters are listed .

Bacterial filtering efficiency	99.999% (Staphylococcus aureus @ 30L/min)
Viral filtering efficiency	99.999% (Bacteriophage @ 30L/min)
Resistance	0.27cmH2O @ 30L/min 0.59cmH2O @60L/min 0.97cmH2O @ 90L/min
Dead Space	75ml

Table 2.1: Antibacterial filters characteristics

4. Nose clip: it is necessary to prevent respiration through the nasal cavity, so to minimize the loss of flow or volume during lung function testing maneuvers.

Calibration

The calibration is a procedure used to determine the relationship between the flow and volume signals measured by the flowmeter and the real effective flow and volume. Because of this, it is a crucial step to assure the spirometer is acquiring reliable flow and volume measurements. The turbine flow is not affected by pressure, humidity or temperature, so it does not require daily calibration. However it is strongly recommended to calibrate the system each week, or whenever the flowmeter is changed or if the ambient conditions, such as temperature, humidity and pressure, vary significantly[14]. Since the instrumentation is cleaned and disinfected between each subject, the spirometer has been calibrated before every acquisition as well.

The turbine spirometer is calibrated using a 3-liter calibration syringe connected to the spirometer through the in-line filter, since it will be used during the acquisitions, and by using the OMNIA software dedicated function "Flowmeter calibration". The piston of the syringe has to be moved in and out for six inspiratory and expiratory strokes with different timings in order to produce different flux at each stroke. The real-time flux/volume curves is shown on the screen, and at the end of the calibration phase the gains and measured volumes with relative inspiratory and expiratory errors (before and after calibration) will be visible. It has to be noted that during this phase the calibration syringe main body should not be held by hand to prevent any change in its internal temperature from the ambient one, allowing for an accurate calibration.

After the calibration procedure, a calibration verification procedure must be taken. After calibrating the flowmeter it is necessary to check that it is within calibration limits (±3%) by using the gains computed and stored at the end of the last calibration. This process must be performed at least daily, and if this test is failed a new calibration must be taken. This step requires to use another OMNIA software function, named "Flowmeter verification", by performing inspiratory and expiratory strokes at low, medium and high flows until the linearity check is completed [7, 14].

Hygiene and Infection Control

The goal of infection control is to prevent the transmission of infectious diseases to patience and staff members through either direct or indirect contact. The first is due to direct contact with surfaces such as mouthpieces, nose clips, spirometer body and other instrumentation; the latter indirectly through aerosol droplets expelled by the patient while expiring into the spirometer during test maneuvers. The need for infection and diseases control has been more urgent since the COVID-19 pandemic and is achieved by adopting several safety measures and protocols. They comprehend washing or sanitize the hands of the operator and of the subject under test, use of disposable in-line filters with integrated mouthpiece and its disposition for different patiences, and decontamination of the non-disposable instrumentation such as spirometer body and turbine [7].
Regarding decontamination, it is a multi-step process in which the two main phases are cleaning, together with rinsing, and a microbicidal treatment. The goal of this phase is to prevent and control the transmission of infectious diseases to subjects and staff members during the various tests and to avoid cross-contamination between subject. The purposes of cleaning and rinsing are to remove all adherent foreign material, to reduce the number of particulate, microorganisms, antigenic material and to increase the efficiency of the following disinfection. Instrumentation is normally cleaned using water with a neutral or near-neutral pH detergent solution since such solutions generally provide the best material compatibility profile and good soil removal.
Almost all parts in the COSMED MicroQuark spirometer are classified as non-critical items, while the turbine flowmeter is classified as semi-critical. Non-critical items are those that contacts intact skin, which acts as effective barrier against most microorganisms. It has been documented that there is virtually no risk for transmission of infectious agents to patients through noncritical items when they do not contact non-intact skin or mucous membranes. Such items can be disinfected where they are used by a sodium hypochlorite solution. Semi-critical items contact mucous membranes or non-intact skin, and include respiratory therapy instrumentation. These medical devices should be free

from all microorganisms; however, small numbers of bacterial spores are permissible since intact mucous membranes are generally resistant to infection by common bacterial spores but susceptible to other organisms, such as bacteria and viruses. Because of this, semi-critical items minimally require high-level disinfection, defined as complete elimination of all microorganisms in or on an instrument, except for small numbers of bacterial spores. Cleaning followed by high-level disinfection should eliminate enough pathogens to prevent transmission of infection. The recommended solution for high-level disinfection of the turbine flowmeter are sodium hypochlorite at two different concentrations: 0.5% to be used within 24 hours, or 1% usable within 30 days.
Following such directives a cleaning and disinfection protocol has been developed. Every step was performed wearing disposable protective gloves.

1. Cleaning and rinsing
    - Step 1 - Disassembly: the flowmeter turbine is separated from the spirometer body and the two spongy cushions are separated from the spring of the nose-clip and are placed in different disposable plastic cups.
    - Step 2 - Pre-soak: the different items are rinsed and soaked in tap water at $22-43\,^{\circ}C$ for few minutes, having the attention to not place the turbine under direct water flow since it may damage the rotor blades.
    - Step 3 - Clean: the items are singularly and manually handled under $22-43\,^{\circ}C$ tap water while using a neutral pH mild detergent.
    - Step 4 - Rinse: the cleaned items are rinsed with tap water for at least three times. The turbine unit, which cannot be placed under direct water flow is soaked in tap water at $22-43\,^{\circ}C$ and moved by hand while submerged to remove any residual soap.
2. High-level disinfection
   A fresh prepared 0.5% sodium hypochlorite solution is prepared previously to this stage by mixing 1 part household bleach (sodium hypochlorite 5.25%) to 9 parts water.
    - Step 5 - Disinfection: complete submersion of the item in the disinfectant solution for about 20 minutes. All the elements of the nose-clip and the turbine flowmeter unit are disinfected this way.
    - Step 6 - Rinse: the items are singularly rinsed in a cup, filled of clean water, shaking gently to remove the disinfectant.

- Step 7 - Dry: the turbine is firstly gently shaken and is then linked to the calibration syringe through the antibacterial filter used to perform some strokes at variable fluxes. The nose-clip elements are dried by tapping with clean and disposable paper cloth.

2.1.3. Software

Two softwares were used to acquire and process data:

COSMED OMNIA

This software by COSMED was firstly used for calibration and verification of the COSMED MicroQuark spirometer and secondly to record the volumes data during the various acquisitions. It comprehends also some very specific functions to perform spirometry and/or FVC tests in a guided manner. Such functions display the clinical results of the test, very interesting feature in a clinical setup, but does not allow to access to raw, unprocessed volume data from the spirometer, which are the starting point of this work. Because of this, data were acquired by using the "Control Panel" function, which allow to show, measure and save flow or volume data with a update interval ranging from 100 ms to 1000 ms, hence a 1-10 Hz sampling frequency.

PyCharm IDE

Pycharm is an Integrated Development Environment (IDE) for the programming language Python, which among its various features has also version control linked to Git, allowing pushing and pulling to/from repositories of interest.

2.2. Methods

2.2.1. Experimental setup

Data have been acquired in L.I.F.E. Italia S.r.l headquarter in Milan, via Dei Gracchi 35. The acquisition setup comprehended a long table with a foam mattress on top and a pillow used during laying down positions, a chair for the sit positions and a FASSI F12.8 AC treadmill for dynamic acquisitions. Data have been acquired using MicroQuark spirometer by COSMED, comprehensive of antibacterial filters with oval-shaped mouthpieces, holded by a custom-made tripod structure. In this way the spirometer was presented upside-down from above the subject under test so that he could perform the test with-

out the necessity to continuously hold the spirometer body. Such design was necessary because of multiple reasons. It firstly eliminated the need, by the subject or by the operator, to continuously hold the spirometer during the acquisitions, leading to more repeatable and reduced operator-dependent acquisitions, reproducing the setup of modern clinical/functional laboratories. Furthermore, in this way the acquisition resulted less biased by the position of the arms of the subject, since they are no more constantly used for holding the instrumentation. Finally a fan has been used to rapidly regulate the temperature during dynamic tests.

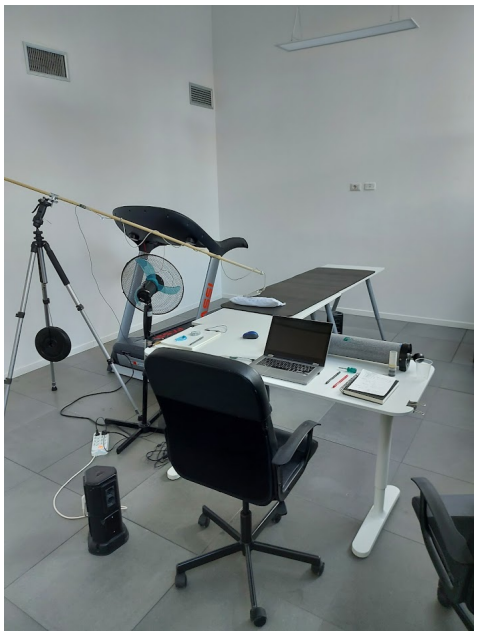

Figure 2.5: Acquisition setup

Test population

A total of 13 volunteer subjects were enrolled for the testing process. 6 of them were female, and the remaining 7 were male, with average age $31,92 \pm 5,04$ years, average height $172,85 \pm 7,08$ m, average weight $64,92 \pm 8,93$ Kg, average body mass index (BMI) $21,65 \pm 1,99$ Kg/m^2. Anagraphical and anatomical information have been listed, along to other important details, and here below:

- Subject ID
- Sex
- Age
- Height in cm

- Weight in Kg
- Body Mass Index (BMI) in Kg/m^2: rate between weight and the square of the height expressed in metres.
- Garments Size: every Healer model was available in three sizes (S, M and L) for both women and male version. The size of the garment for each subject has been chosen according to availability and fit, preferring a tighter fit to a looser one.
- Healer R1, R2, R3 fit: it ranges from 1 to 5, in which 1 stands for very tight, 3 for normal and 5 for very loose fit.

All the discussed informations are listed in detail in table 2.2.

ID	Sex	Age	Height [cm]	Weight [Kg]	BMI [Kg/m^2]	Garment size	Healer R1 fit	Healer R2 fit	Healer R3 fit
1	F	26	174	56	18.50	S	1	1	1
2	M	36	176	80	25.83	L	2	1	1
3	M	34	180	73	22.53	L	2	1	1
4	F	40	166	57	20.69	S	1	1	1
5	F	27	168	52	18.42	S	1	1	1
6	F	36	158	51	20.43	S	2	1	1
7	M	31	187	78	22.31	L	2	1	1
8	M	26	170	63	21.80	M	4	3	3
9	F	32	173	65	21.72	L	4	3	3
10	F	41	168	70	24.80	L	3	3	3
11	M	28	173	65	21.72	M	4	2	2
12	M	26	181	71	21.67	M	3	1	2
13	M	32	173	63	21.05	M	4	3	2
Count	**Count**	**Mean ± std**	**Mean ± std**	**Mean ± std**	**Mean ± std**	**Count**	**Mean**	**Mean**	**Mean**
13	F: 6; M: 7	31.92 ± 5.05	172.85 ± 7.08	64.92 ± 8.93	21.65 ± 2.00	S: 4; M: 4; L: 5	2.54	1.69	1.69

Table 2.2: Test population personal and anatomical informations

Acquisition protocol

The developed acquisition protocol involved four different types of exercises to be executed in a static or dynamic setup and in three different body positions. The four exercises were the following and can be divided in static/at rest (1, 2, 3) and dynamic (4):

1. Inspiratory Capacity (IC) and Slow Vital Capacity (SVC) maneuvers
   After two initial minutes of spontaneous breathing the subject had to perform two IC and two SVC maneuvers each spaced by 40-60 seconds of spontaneous breathing, required for the complete recovery of ventilation capabilities. Since IC and SCV maneuvers are partially forced they may lead to fatigue which may affect the following IC and SVC maneuvers, leading to underestimation of real volumes. Because of this, if the subject under test hadn't fully recovered after the inter-maneuver resting time, he had been instructed to breath spontaneously until complete recovery. An example of this exercise is shown in Figure 2.6.

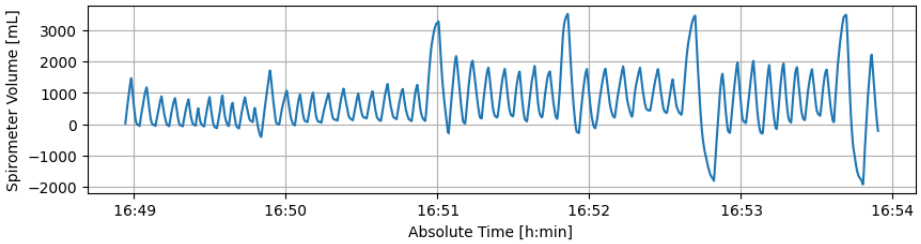

Figure 2.6: Inspiratory Capacity (IC) and Slow Vital Capacity (SVC) maneuvers

2. Breathing at modulated amplitudes
   The subject was asked to breath with three different amplitudes, each of the three for one minute. More in detail, he/she had to breath at tidal volume (TV, spontaneous breathing) for one minute, then at half tidal volume for another minute and finally at twice of the tidal volume amplitude for one minute again as can be seen in Figure 2.7.

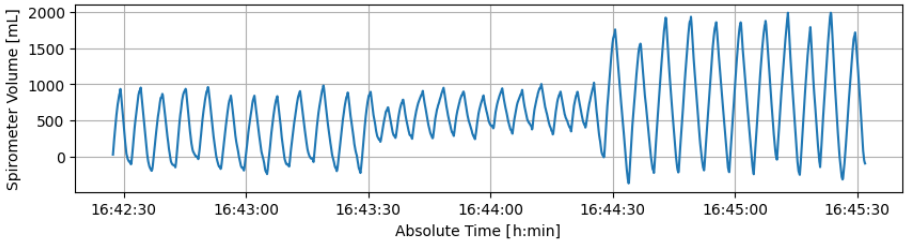

Figure 2.7: Modulated amplitudes

3. Breathing at modulated frequencies
   The subject had to firstly breath spontaneously, hence with spontaneous frequency and amplitude, then at twice such spontaneous frequency, for one minute both. A typical tracing of such exercise is reported in Figure 2.8.

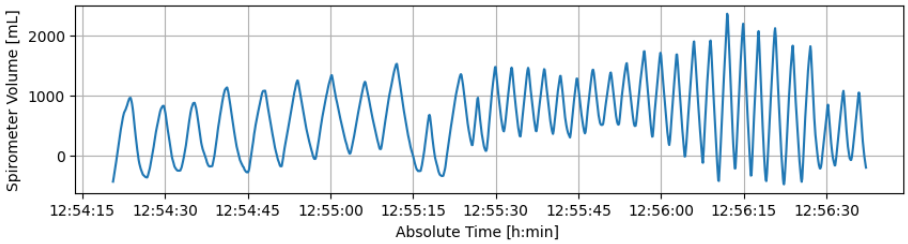

Figure 2.8: Modulated frequencies

4. Walking
   The participant had to walk on a treadmill at three different paces, each for three minutes: slow at 3.5 km/h, fast at 5 km/h and finally slow at 3.5 km/h but uphill with a 12° slope. The volume signal read at the spirometry is shown in Figure 2.9.

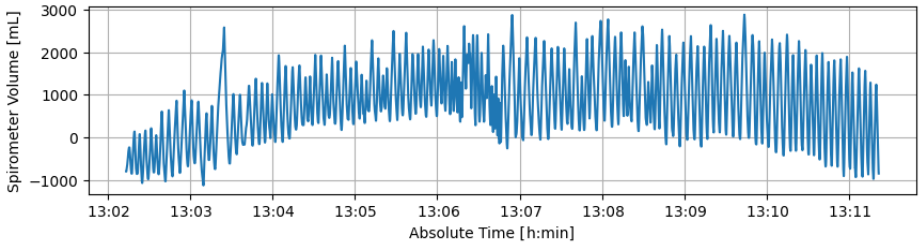

Figure 2.9: Walking on treadmill

It has to be noted that the various exercises were performed with no intra-exercise pause and with a brief inter-exercise pause. Some minutes of rest have been taken whenever the subject under test required them to assure their safety and comfort.
These four exercises have been executed in three positions, laying, sitting and standing, resulting in the following test protocol characterized by a set of static exercises (from exercises in position 1 to exercise 3.a), and a dynamic test (exercise 3.b):

1. Laying
   (a) Prone: IC and SVC maneuvers
   (b) Right side: IC and SVC maneuvers
   (c) Supine: IC and SVC maneuvers

   (d) Left side: IC and SVC maneuvers

2. Sitting
   (a) IC and SVC maneuvers
   (b) Amplitude modulations
   (c) Frequency modulations
3. Standing
   (a) IC and SVC maneuvers
   (b) Walking

This acquisition protocol has been performed wearing one Healer device (R1, R2, R3) at time while breathing in and out through the spirometer. For each device the entire exercise protocol has to be repeated. The acquisition of one single suit lasted approximately 1.15 hours, resulting in long continuous acquisition of almost 4 hours for each participant. Such a long duration of the test may have stressed the participants inducing a fatigued state, which could be visible at while acquiring the data from the third device. To prevent any bias linked to the order in which the devices have been tested linked to the fatigue induced by the prolonged duration of ventilation exercises, the order in which the Healer wearables have been acquired had been different from one patient to the other.

2.2.2. Signal processing

The recorded data of the garments have been saved within the LIFE's logger local memory in *.h5* file format. If the test for that particular suit didn't require any pause, it was saved in a single *.h5* file, which comprehended the entire test with all the exercises and phases from 1.a to 3.b. Instead the volume data measured by the MicroQuark spirometer had been saved in text file format, one for each phase, resulting in 9 different files. The healer *.h5* file contains all the data measured from each different sensor in the suit, as the three different strain gauges. The three volume signals were the only one of interest for this study and have been extracted for further processing. The main processing phases have been applied to the volume signal measured from the spirometer and to the algebraic sum of the three channels of the LIFE suit. From now on, if not specified, whenever there will be a reference to the volume of the Healer suits it will be intended as the algebraic sum of the volume signals read by the three channels.

Filtering and Oversampling

The first operation applied to the Healer signal was to filter it through a low-pass (LP) filter with a frequency of 1 Hz, in order to reduce the high-frequency components, obtaining a smoother signal with the same dynamics and morphology of the raw, unfiltered volume signal. The main drawback of this filtering approach is that it could not remove the DC component, hence the baseline value of the signal. However this is a minor problem since during the comparison between breaths it has not been evaluated absolute, but relative variations of volumes, which remained substantially unchanged with respect to the unprocessed signal. An example of the result obtained through the application of a low-pass filter with cut-off frequency set at 1 Hz is shown in the Figure 2.10.

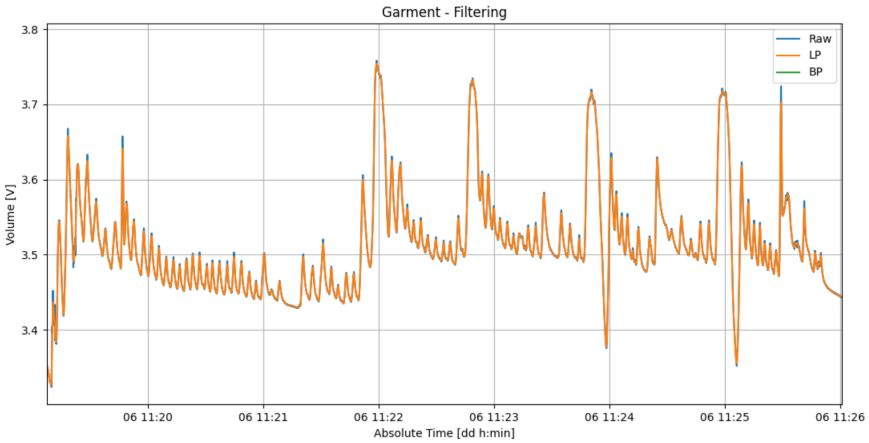

(a) Example of low-pass filtering of the volume signal of Healer R2

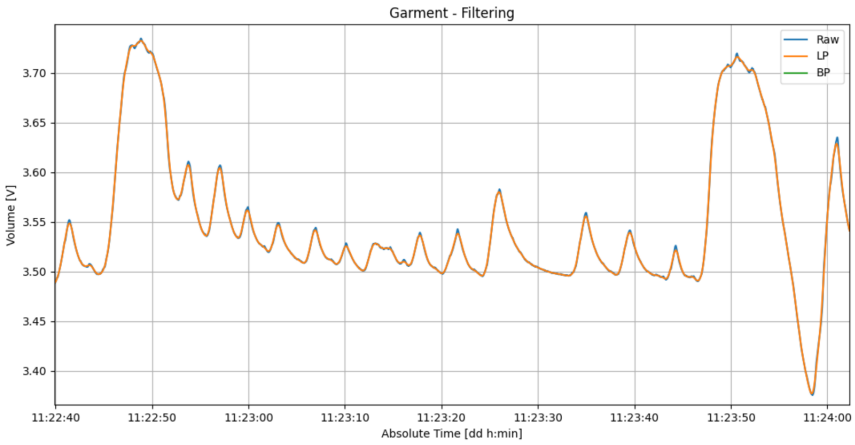

(b) Low-pass filtering focus on the central IC and SVC maneuvers

Figure 2.10: Low-pass filtering effect

The LP method was preferred to the band-pass (BP) filter between 0.045-1 Hz since it

appeared that the latter distorted abruptly the volume signal even if it compensated for the DC components. The signal filtered through such BP filter presents various deformations in amplitude and morphology, which worsen near to large volume variations, as inspiratory or expiratory maneuvers such IC and SVC. The extent of these distortions can be clearly observed in Figure 2.11a

(a) Example of band-Pass filtering of the volume signal of Healer R2

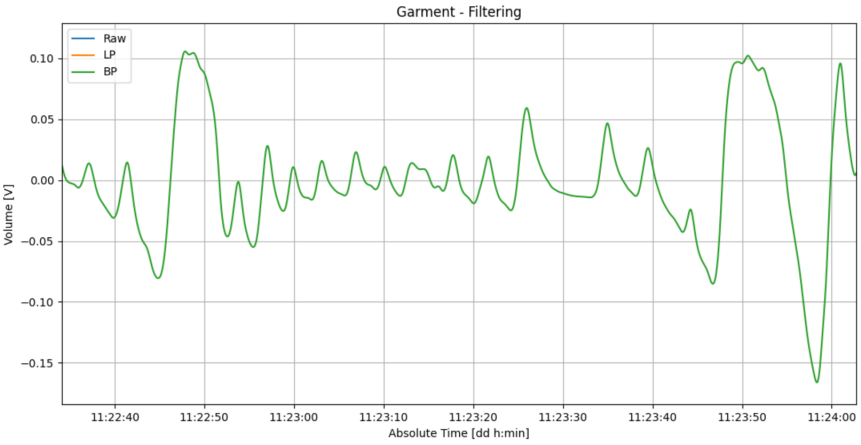

(b) Band-pass filtering focus on the central IC and SVC maneuvers

Figure 2.11: Band-pass filtering effect

Regarding the spirometer volume signal, it has been over-sampled from 10Hz to 50Hz, through linear interpolation, in order to provide the same number of samples as in the garment signal.

Healer and spirometer synchronization

The data recorded by the two sensors have to be synchronized so that the signals could be represented on the same time-base and from the same starting point in order to have the correspondent respiratory events happening at the same time in the two measurements. This has been achieved by a dedicated software solution.

To better explain and understand how this result has been accomplished, it is necessary to introduce the way the two measurement systems manage the time in the recordings. In detail, LIFE garments record data in UNIX time format, in which the Unix unit represents the number of seconds elapsed from the 1st January 1970, named the Unix epoch. The Unix time number is zero at the Unix epoch, increases by exactly 86400 per day since the epoch and is an established way to measure and represent time in Universal Central Time (UTC). On the contrary, the MicroQuark spirometer records time in a relative manner, counting the milliseconds elapsed from the beginning of the recording, proportionally to the sampling frequency. Since the spirometer acquired data at the maximum sampling frequency available of 10 Hz (hence 100 ms), volume data have been acquired starting by time zero every 100 milliseconds.

The first step in signal synchronization has been the extraction from the garment long recording of the portion of signal corresponding to the spirometer trace, which are both measurements of the same exercise. This first stage has been accomplished by saving the Unix timestamps corresponding to the start and end of each phase, resulting in a cropped garment signal as in Figure 2.12.

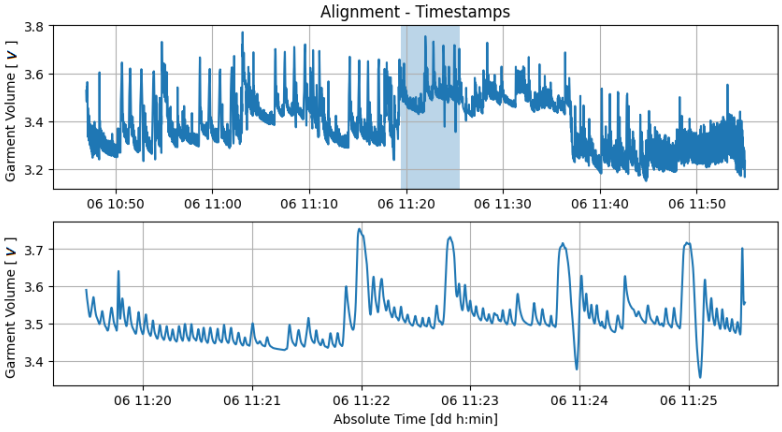

Figure 2.12: Exercise selection in Healer signal

The complete synchronization has been achieved by presenting to both measuring systems a common event which could be identified with ease and certainty within both signals. Such reference event has been a cough-stroke which the participant had to produce right

at the beginning and at the end of each exercise, and could be identified as an expiratory peak in the flow trace computed as the first derivative of the volume measurements, as it can be seen at the bottom of Figure 2.13.

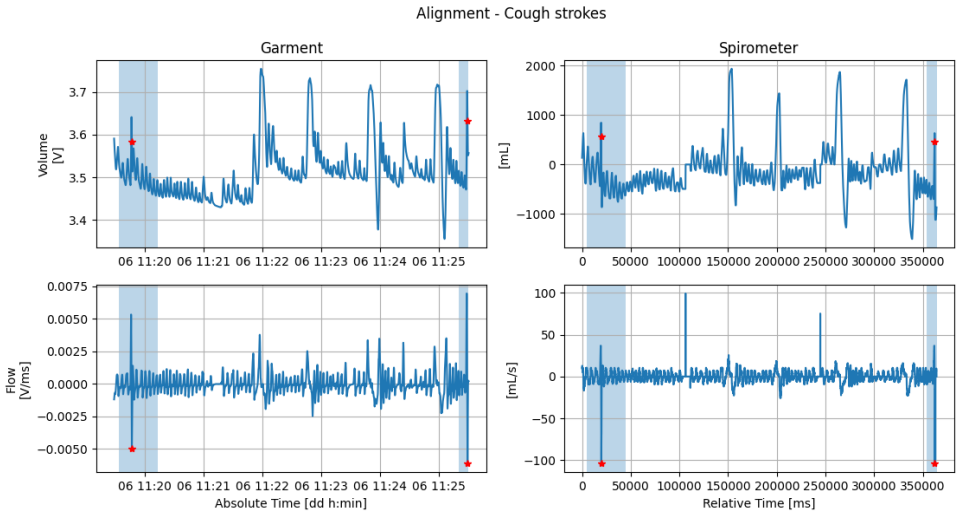

Figure 2.13: Cough strokes at the beginning and ending of Healer (left) and spirometer (right) volume (above) and flow (bottom) signals. The areas marked in blue represents the temporal windows in which the cough strokes were searched.

The desired cough stroke had to have an amplitude range in flow greater than the one during spontaneous breathing or the maneuvers, and to have an impulse-like morphology. The identification of the strokes in such ideal scenario would be non-ambiguous, minimizing temporal delays between the two signals. Some requirements were given to assure the correct identification of the cough-strokes, which had been:

1. forced and maximal: to be sure that the flux's amplitude range of the cough stroke would be far from the flux range during spontaneous expiration.

2. produced far from SVC maneuvers: in some cases such expiratory maneuver may have been wrongly delivered forcing the initial expiration. This caused an overlapping of the expiratory flux amplitude with the one of the cough-stroke, leading to ambiguous cough-stroke identification. Such event was clearly more frequent at the end of the IC and SVC maneuvers exercise, which terminates with a SVC, expiratory maneuver. A few spontaneous breaths had to be measured at the end of each exercise to prevent such ambiguous identifications.

3. produced by an instantaneous-like compression of the thorax, diaphragm and abdomen: the spirometer and healer garments measure the same physical quantity,

hence volume of air moving in and out the ventilatory system, through two different sources. The flowmeter measures the volume of air passing through the airway-opening of the participant during inspiration and expiration. On the contrary, Healer suits measure the volume of air which flows in and out the lungs by measuring the compression and extension of the ventilatory system, hence thorax and abdomen. From the very nature of measuring the same variable through two different mechanical sources may arise some problems. For example a flow of air at the mouth can be produced by a change in volume of the abdomen and/or diaphragm and with relative small movement of the thorax and rib cage, leading to an underestimation of the derived flow by Healer suits with respect to the one derived from the measured volume by the spirometer, which had been considered the gold standard. This is a simple but effective example stressing the fact that in various scenarios the flow may be underestimated in the wearable device, lading to erroneous identification of the cough-strokes. To limit those problems it had been required to produce the cough stroke by an active and very fast compression of the thorax, opposed to a passive slow expiration.

Unfortunately, the cough-stroke in various measurements did not fulfilled all three requirements leading to ambiguous and erroneous identification of the cough strokes and ultimately to failure in signals synchronization. In any situation in which at least one of the three mentioned requisites had been not respected, a manual identification of the cough strokes had been performed ensuring the correct alignment between the two signals. Moreover, in the event that the cough-stroke had been correctly identified, but the requirements 1 and 3 were not meet, delay problems between the two signals may appear. To adjust this jitter the signals have been considered starting from the beginning of the first breath after the starting cough-stroke, and terminating at the end of the last breath before the cough-stroke at the end, obtaining two synchronized signals. The synchronization final result has been illustrated in Figure 2.14.

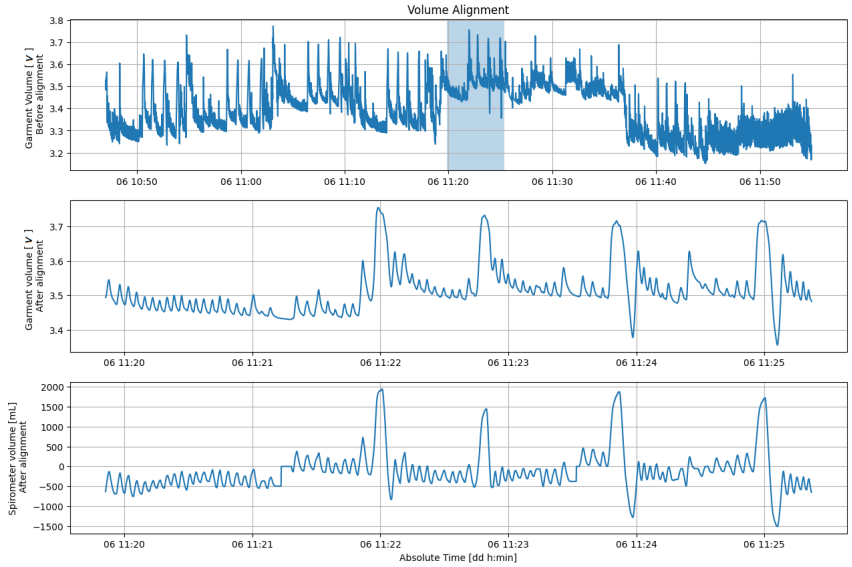

Figure 2.14: Synchronization between garment and spirometer measurements for a given exercise. The upper panel shows the complete garment recording, with the exercise under analysis highlighted in blue, which can be seen in detail in the middle panel once synchronized. The bottom plot refers to the synchronized spirometer volume signal.

Offset and Integration Drift compensation

Once the signals from the two instrument have been synchronized, it has been necessary to manage two features of the spirometer volume signal, which are the "offset error" and the integration drift.

The first one arises by the way the COSMED OMNIA software measures the volume of air flowing through the flowmeter. In detail, if at any moment the MicroQuark spirometer does not sense any volume variation, hence non-zero flow for at least three seconds, the COSMED software brings the volume value to the default one, set at $0mL$, resulting in a step change in the volume trace. This is an error introduced by the way the OMNIA software manages the flow/volume signal, resulting in a measure characterized by a discontinuity, which is far from the real volume signal. As said, this event was triggered any time there would be a constant flow for at least three seconds, which happened when the subject under test had to pause the exercise to cough (excluded the induced ones for synchronization), swallow or to adjust the test setup. Such error has been compensated by subtracting, or summing, the amplitude value before the offset step to the volume measurements after the discontinuity in volume, as shown in Figure 2.15.

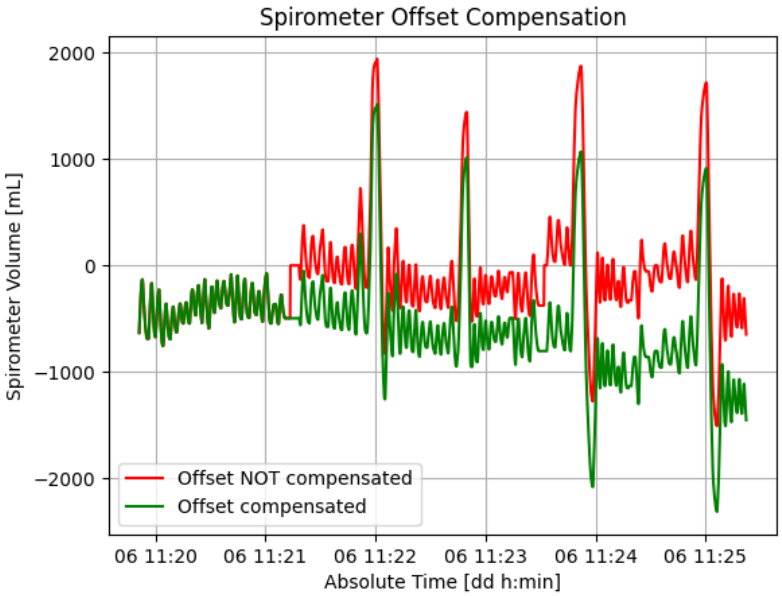

Figure 2.15: Spirometric signal affected by two offset errors (red) and corrected (green).

For what regards the integration drift, it occurs since the volume measured by the spirometer is computed by integration of the flow of air through the turbine and any constant or offset summed to the flow will lead to a linear drift in the integrated volume. The source of errors can be various, ranging from leaks at the mouthpiece or steep changes in temperature and humidity of the ambient air. It has been compensated by subtracting the linear regression line computed on the minima points, as in Figure 2.16 . Such solution have been chosen since it minimally distorts amplitude values and morphology of the signal while correcting a portion of the drift, even if some drift remained present.

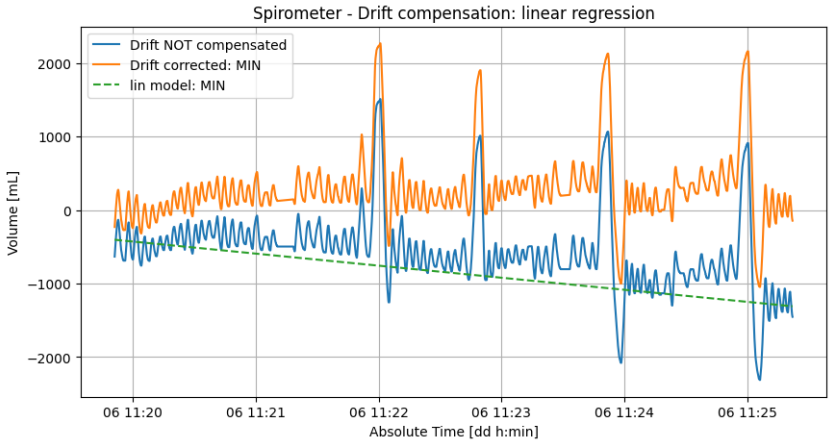

Figure 2.16: Spirometric signal affected by integration drift (blue) and corrected (orange).

All the discussed processing stages have led to the couple of signals in Figure 2.17.

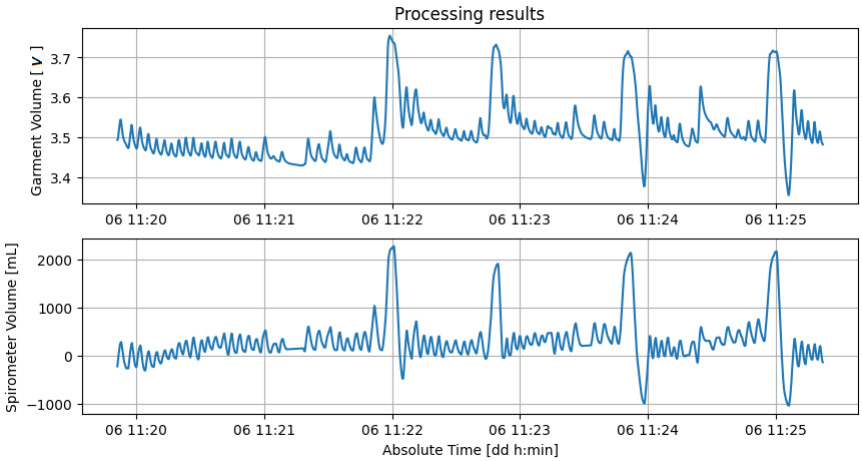

Figure 2.17: Processing result.

2.2.3. Breaths identification

Maxima and minima points of both spirometer and healer volume signals have been identified through a series of Python functions. Firstly minima and maxima points have to be found above and below the moving average (MA) value of the signal, computed through a MA filter on a variable temporal window of the signal. The alternation between a minimum and a maximum have been guaranteed, starting the identification from a minimum and terminating to a maximum. The result can be seen in Figure 2.18.

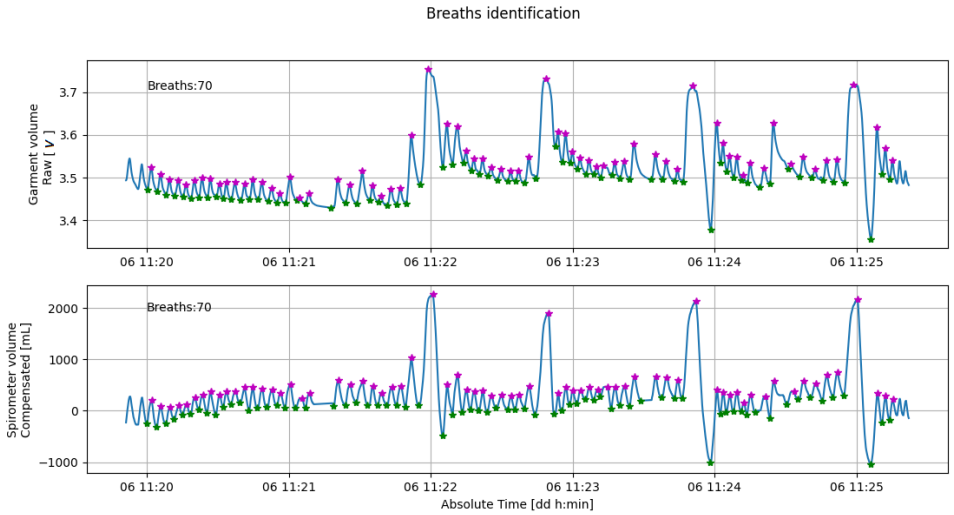

Figure 2.18: Breaths identification

In many different situations the breaths of the two signals differed in morphology, leading to a difference in the identified breaths. This behaviour could be given by several events,

for example a pause during the exercise in which the subject detaches from the spirometer to take a moment of rest, or even at the end of the inspiratory maneuvers in which multiple maximums are found in the Healer signal with respect to the correct single peak in the spirometer tracing. One example has been reported in Figure 2.19.

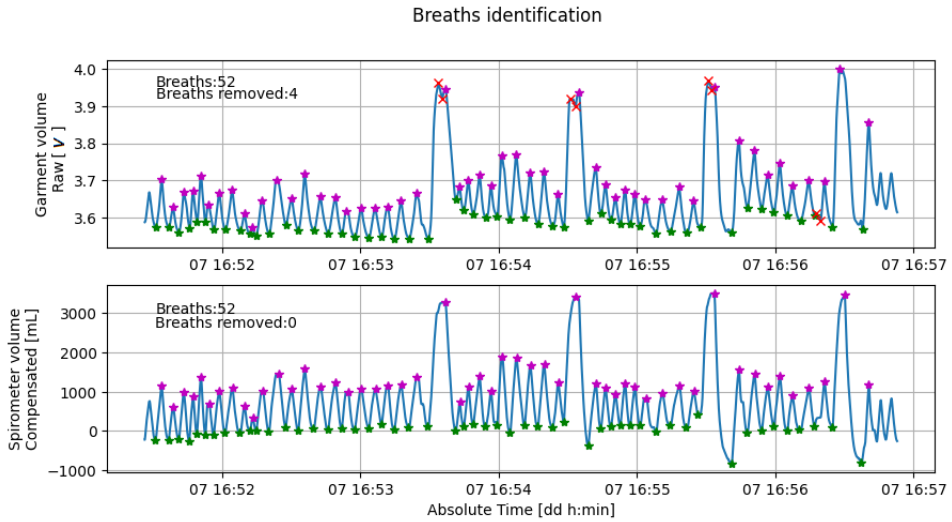

Figure 2.19: Breaths discrimination

These ambiguous cases have been solved by matching the minima (and maxima) of the healer signal to the correspondent nearest minima (or maxima) of the gold standard spirometric volume signal. This approach helped resolving the vast majority of erroneous or indecisive breath pairings. Nonetheless in very particular cases, more frequently at the end of the signals, the breaths have been manually matched.
At the end of all this processing phase the two signals have been guaranteed to be:

- synchronized, hence of the same length and with paired respiratory events
- with matched breaths, equal in number and taking place at the same time

In this way the two volume signals could be compared in a breath-by-breath fashion.

2.3. Parameters extraction

Arrived at this stage the signals have been fully processed and are guaranteed to have paired breaths, corresponding to the same respiratory events. This has been a crucial feature which allowed to compare the various parameters breath-by-breath. In detail the following metrics have been computed:

1. Primary parameters

- Breathing period $[ms]$: measured as time difference between two adjacent minima, so between the end of expiration and the beginning of inspiration
- Inspiratory time $[ms]$: measured as time difference between the maximum and minimum of the same breath, hence between the end and beginning of the inspiratory phase
- Expiratory time $[ms]$: measured as time difference between the minimum of the following breath and the maximum of the current breath, so between the end and beginning of the expiratory phase
- Inspiratory volume $[V]$ or $[mL]$: computed as the amplitude difference between the end and the beginning of the inspiratory phase of the current breath
- Expiratory volume $[V]$ or $[mL]$: computed as the amplitude difference between the end and the beginning of the expiratory phase of the current breath

2. Secondary parameters
   - Breathing rate $[bpm]$: simply computed as the inverse of the breath period multiplied by 60000, which corresponds to the number of milliseconds contained in a minute
   - Minute ventilation $[V \cdot bpm]$ or $[mL \cdot bpm]$: computed by multiplying inspiratory volume and breathing rate
   - Inspiratory flow $[V/ms]$ or $[mL/ms]$: computed as ratio between inspiratory volume and inspiratory time
   - Expiratory flow $[V/ms]$ or $[mL/ms]$: computed as ratio between expiratory volume and expiratory time
   - Duty Cycle $[0-1]$: computed as ratio between inspiratory time and breathing period

This set of parameters has been computed for both Healer and spirometer volume signals. As previously explained in Section 2.1.1 the volume variation of spontaneous breaths following a large inspiration or expiration maneuver, as IC and SVC, are underestimated in the garment signal due to a slower elastic-return dynamic with respect to the one of the anatomical structures measured by the sensors. This has found to be a systematic behaviour in the first breaths after the IC and SVC maneuvers, and for such corrupted breaths it had not been possible to compare the parameters relative to volume variations. Because of such deformation in amplitude, the breaths during the maneuvers exercise have

been classified into three different clusters: the spontaneous breaths before the first IC maneuver, the four inspiratory maneuvers (IC and SVC), and finally the inter-maneuver breaths. This classification is shown in Figure 2.20.

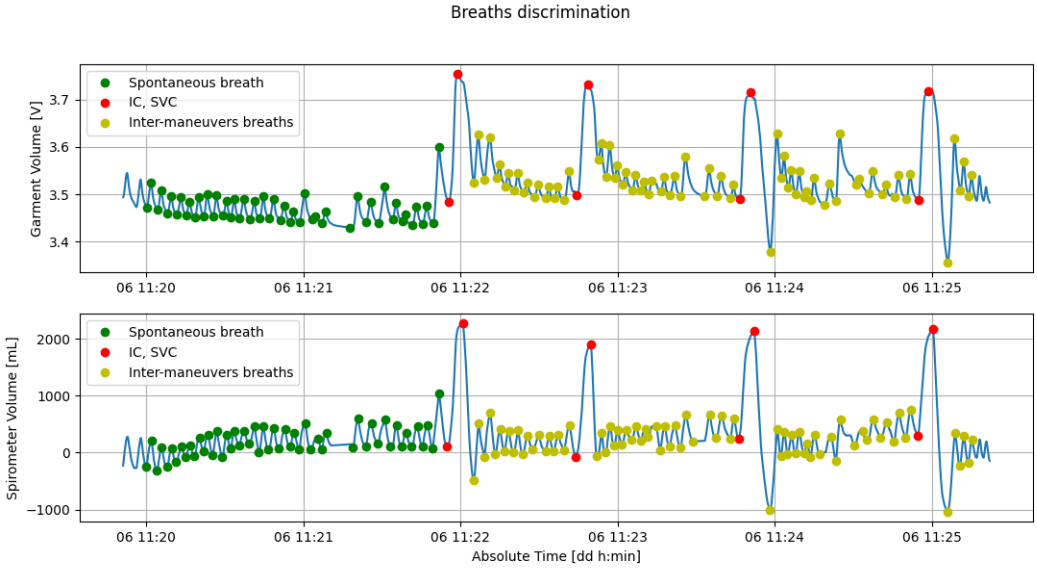

Figure 2.20: Breaths classification. Spontaneous breaths which are not influenced by the inspiratory maneuvers have been marked in green; IC and SVC maneuvers breaths have been marked in red; the remaining inter-maneuvers breaths are shown in yellow.

Regarding this critical maneuvers exercise, amplitude parameters are computed for spontaneous breaths during the first two minutes of exercise and for the maneuver breaths only; on the opposite, temporal parameters have been derived for all the breaths including the inter-maneuver ones since the not ideal mechanical coupling between strain-gauges and body affected amplitudes only. It must be stressed that the secondary parameters have been computed excluding inter-maneuver breaths too. In all the other exercises (amplitude and frequency modulation, treadmill walk) the amplitude and temporal parameters have been computed for all the breaths of the two signals, since are far lees affected by this problem, as it can be seen in Figure 2.21 which show an example of an amplitude modulation exercise.

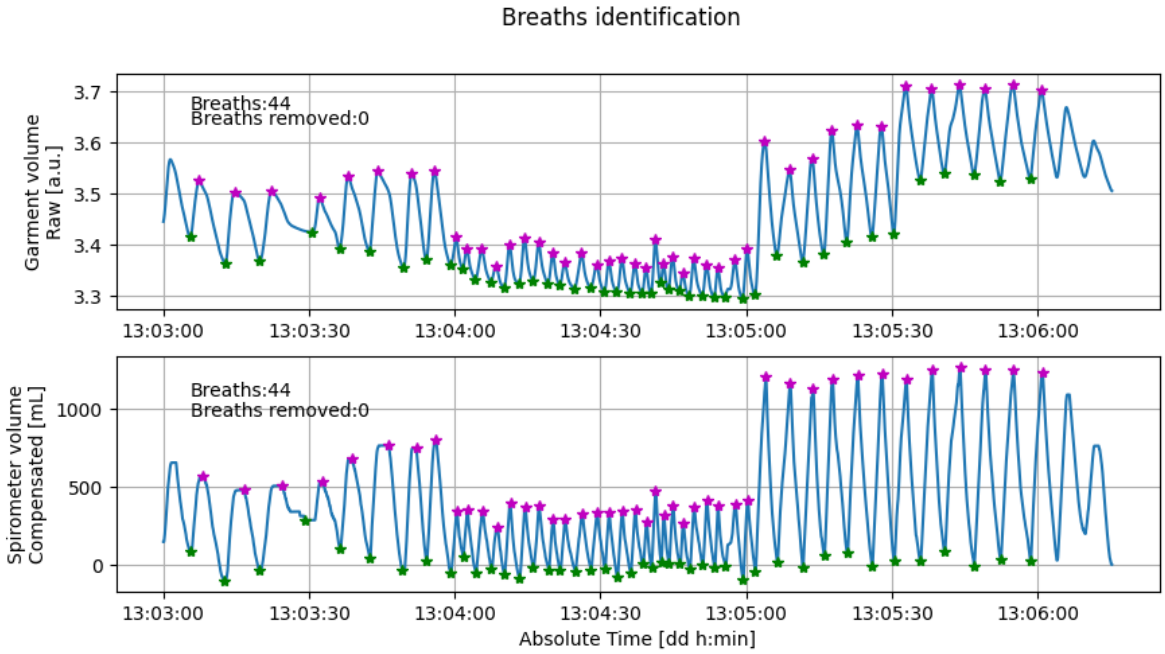

Figure 2.21: The breaths are not corrupted in amplitude, so the primary and secondary parameters are computed for every identified breath.

3 | Results

The first part of this chapter presents a typical example of comparison between a L.I.F.E. garment and the MicroQuark spirometer by COSMED. Subject 2, wearing the L.I.F.E. Healer R2 suit, has been chosen to show a typical analysis since such results are representative of the behaviour of the L.I.F.E. devices. In the second section, pooled results are analysed with the same principles applied to the single subject.

3.1. Example of comparison between L.I.F.E. Healer devices and MicroQuark spirometer

Garment and spirometer signals have been processed as explained in Chapter 2, resulting in two signals in which the different breaths have been identified and classified according to the criteria explained in the previous Section 2.2.3. As a representative example, the recording of subject 2 wearing the L.I.F.E. Healer R2 device while seating and performing the ventilatory maneuvers has been reported. The identified and classified breaths are shown in Figure 3.1, in which the sum of the signals recorded from the three strain gauges is shown in the upper panel, while the volume measurement from the gold-standard COSMED spirometer is illustrated in the bottom part.

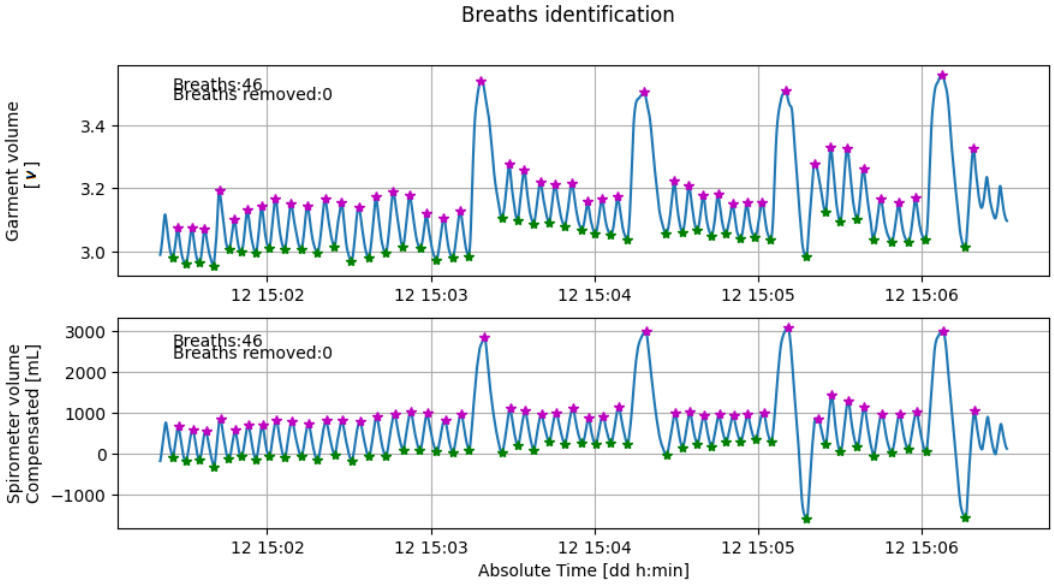

(a) Breaths coupling and identification.

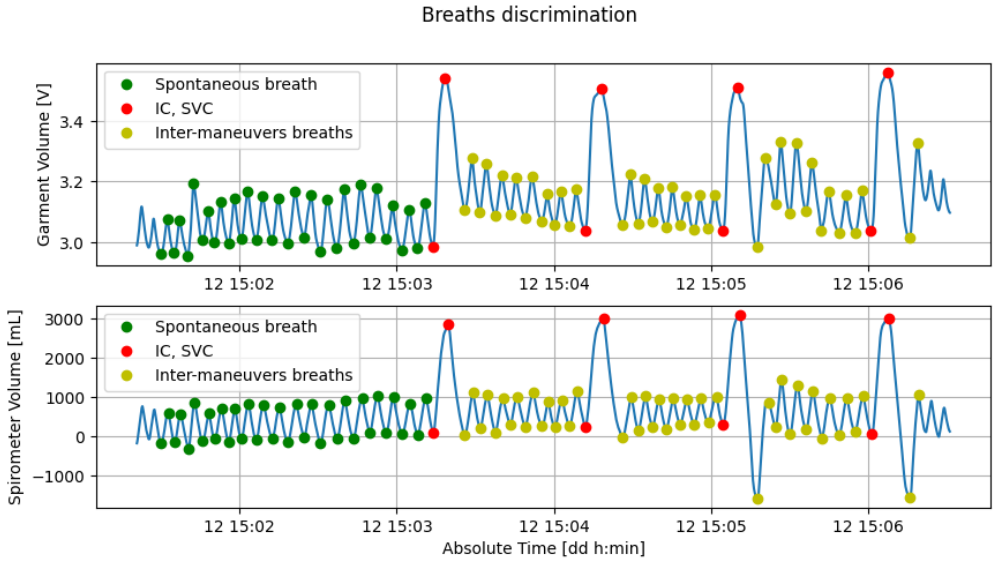

(b) Breaths coding.

Figure 3.1: Subject 2 wearing the Healer R2 garment while performing the ventilatory maneuvers protocol. Breath have been classified in spontaneous breath before the first maneuver (green); intermaneuvers breaths (yellow); IC and SVC maneuvers (red).

Having coupled and classified the breaths of the two signals, three main parameters of interest have been extracted, namely inspiratory time, inspiratory absolute volume and respiratory rate, for both signals and for each breath. Additionally, inspiratory relative volume has been computed by normalizing the inspiratory absolute volume by the average inspiratory amplitude of spontaneous breaths at rest. Such normalization is necessary to

assess the accuracy of the L.I.F.E. devices and to highlights the classification of breaths into tidal, under tidal or over tidal, in which the inspiratory relative volume is respectively around 1, less than 1 and greater than 1. The inspiratory volume normalization allows to quantitatively compare the volume amplitudes measured by the two devices, mapping them in a common relative scale. The four chosen parameters have been compared in two ways, by scatter and Bland-Altman plots. It must be noted that only reliable breaths have been included in the analysis, hence excluding inter-maneuver breaths during the maneuvers exercises, recalling the discussion in Section 2.3. Scatter plots and Bland-Altman plots representing absolute and relative inspiratory volumes, inspiratory time and respiratory rate are shown in Figure 3.2 and Figure 3.3, respectively.

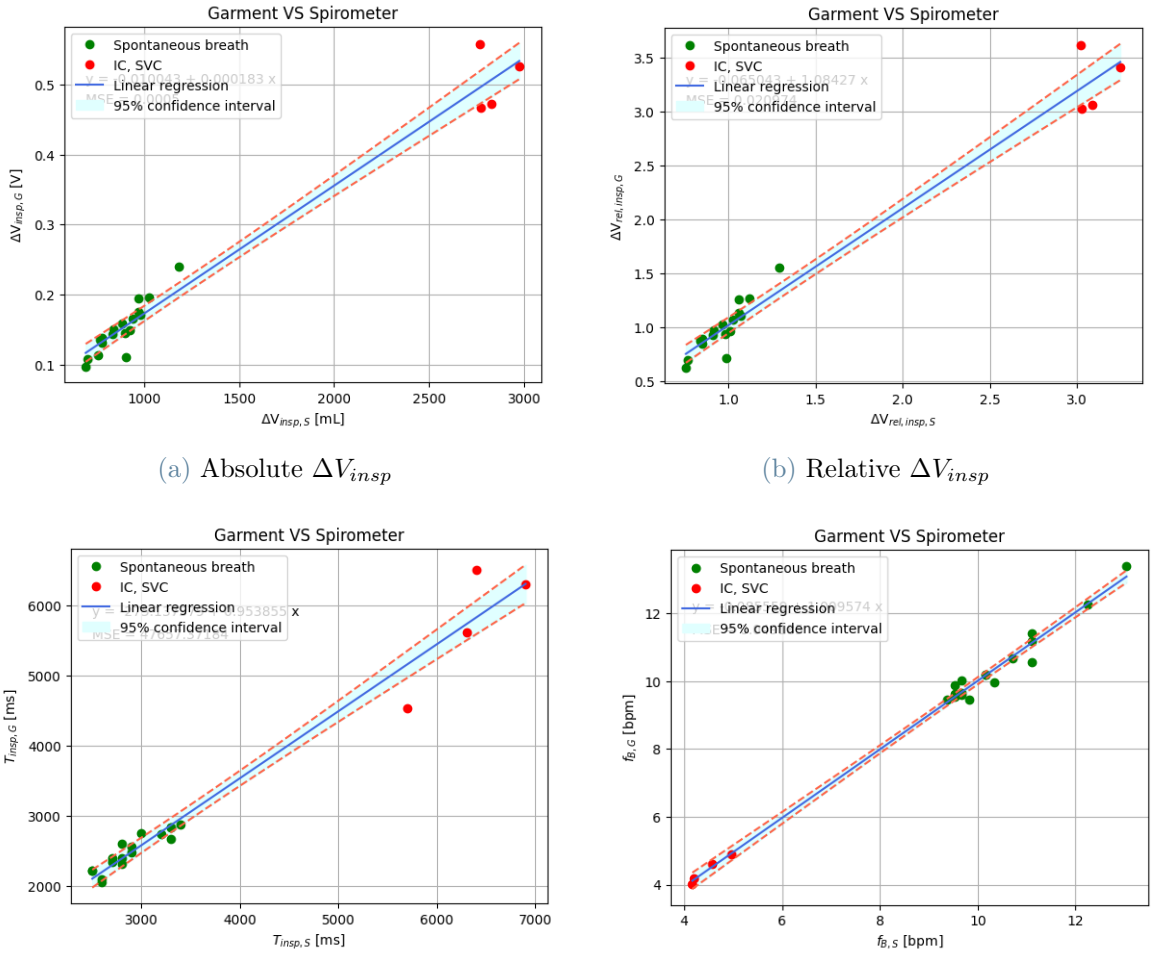

(a) Absolute ΔV_{insp}

(b) Relative ΔV_{insp}

(c) T_{insp}

(d) f_B

Figure 3.2: Scatter plots of the four parameters of interest relative to subject 2 wearing the L.I.F.E. Healer R2 garment while performing the ventilatory maneuvers protocol. Breaths classification is maintained to discriminate between spontaneous breath before the first maneuver (green) and IC and SVC maneuvers (red). Linear regression is applied as estimator of the relationship between the two devices.

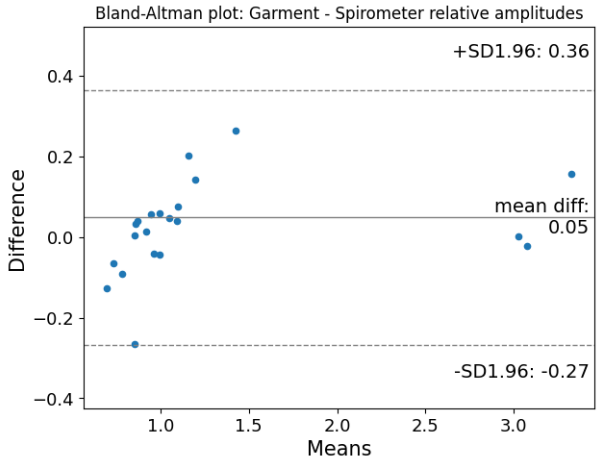

(a) Relative ΔV_{insp}

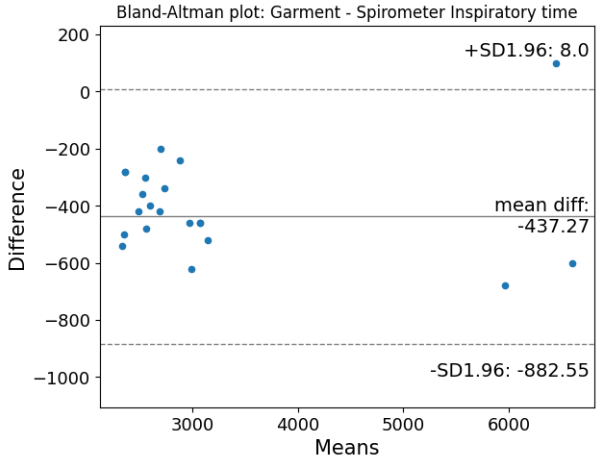

(b) T_{insp}

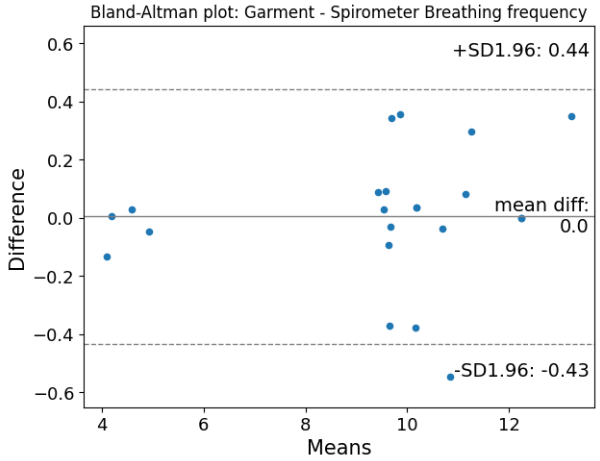

(c) f_B

Figure 3.3: Bland-Altman plots of the main parameters of interest relative to subject 2 wearing the Healer R2 garment while performing the ventilatory maneuvers protocol.

Considering the scatter plots of inspiratory volumes in Figures 3.2a and 3.2b, it is possible to qualitatively derive the inspiratory volume ranges measured by both instruments, their linear relationship, and the distribution of the breaths with respect to tidal breathing. In particular, subject 2, while seating, shows inspiratory volumes that ranges from few hundreds of milliliters to 3 liters, regarding the spirometer signal, and between 0.1-0.55V, with the vast majority of tidal breaths within the 500-1000mL and 0.1-0.2V region. This last cluster of breaths can be recognized as tidal even in Figure 3.2b, assuming relative inspiratory volume values around 1. The inspiratory maneuvers breaths are instead found in the top-right region of both absolute and relative volume plots. The relative inspiratory volume plot is particularly interesting since it shows a linear relationship, with almost unitary slope, between the measurements from the L.I.F.E. Healer R2 and the gold-standard measurement of the COSMED spirometer, suggesting a linear and accurate mapping of relative breaths amplitudes by the suit.
Regarding the inspiratory time and breathing rate in Figures 3.2c and 3.2d it is suggested that, for subject 2 in a sitting position, inspiratory times are slightly underestimated by the suit while the breathing frequencies are well represented and measured by the L.I.F.E. Healer R2.
Through the Bland-Altman analysis it is possible to determine the statistical concordance between the two instruments, highlighting any bias between measurements or the presence of outliers measures. Regarding the example analysed up to now, it is possible to confirm what hypothesized by looking at the scatter plots. In particular, in this particular scenario, the relative inspiratory volumes are measured with a slightly positive average bias by the L.I.F.E. Healer R2, and all the volume measures are concordant between the two instruments but only one dubious sample which is found in correspondence of the inferior concordance limit (0.05 ± 0.32) Moreover, it seems that the inspiratory times are underestimated by the Healer R2 with substantial bias and precision, and the concordance limits are computed as $-437.27 \pm 445.28ms$; and only one discording breath which falls outside the upper concordance limit. Finally, the respiratory rate measured by the L.I.F.E. R2 suit does not show in average any bias with respect to the one measured by the spirometer, with a $0.44bpm$ concordance interval, defining the concordance limits $0.0 \pm 0.44bpm$.
The partial results obtained on a single subject for a particular garment carried out in this section must be broadened and supported by a complete analysis on all the subjects and every L.I.F.E. Healer device, conducted in the following Section 3.2. The methods of analysis presented in this section will be applied throughout the various analysis of the pooled data.

3.2. Pooled analysis

The analysis on the data pool was conducted on the four parameters considered in the previous section: absolute inspiratory volume, normalized inspiratory volume, inspiratory time and respiratory rate.

3.2.1. Pooled analysis on the three L.I.F.E. devices and intra-subject variability

Firstly, in order to understand the best way to estimate the relationship between the garment and spirometer signals, data have been grouped by type of Healer device and subject. For each of the three L.I.F.E. garments and for every subject within each subset, a linear regression was estimated on the two temporal parameters, namely inspiratory time and breathing rate. A quadratic regression has been evaluated for absolute and relative inspiratory volumes. Coefficients of the regression curves and prediction errors, more precisely mean absolute error (MAE), mean squared error (MSE) and the coefficient of determination (R^2), have been computed for each subject wearing each garment and are reported in Table A.1 to Table A.12, listed in detail in Appendix A.1. The tables referred to the first L.I.F.E. R1 device are shown below as an example.

Subject	Slope_{Abs}	Intercept_{Abs}	Slope_{Norm}	Intercept_{Norm}	MAE	MSE	R^2
1	1.40e-04	1.27e-02	1.60e+00	-1.10e+00	4.05e-01	2.57e-01	6.27e-01
2	1.55e-04	-7.09e-02	1.60e+00	-1.10e+00	8.36e-01	1.14e+00	7.25e-01
3	1.51e-04	-7.53e-02	2.33e+00	-1.53e+00	6.71e-01	7.60e-01	8.00e-01
4	1.17e-04	-3.19e-02	5.28e-01	-6.21e-01	8.35e-01	1.16e+00	6.37e-01
5	1.21e-04	-2.25e-02	8.19e-01	-5.51e-01	5.74e-01	5.56e-01	8.73e-01
6	2.45e-04	-4.54e-02	1.43e+00	-6.39e-01	8.12e-01	1.18e+00	6.81e-01
7	7.82e-05	1.12e-02	5.27e-01	1.79e-01	4.23e-01	3.09e-01	7.45e-01
8	1.69e-04	1.88e-02	6.65e-01	1.34e-01	1.86e-01	6.44e-02	8.15e-01
9	1.06e-04	-5.83e-02	1.38e+00	-6.07e-01	4.20e-01	4.10e-01	7.33e-01
10	1.27e-04	3.61e-02	1.17e+00	2.68e-01	3.17e-01	2.36e-01	7.88e-01
11	1.69e-04	-2.31e-02	2.16e+00	-5.09e-01	7.45e-01	1.11e+00	7.34e-01
12	8.22e-05	-7.90e-03	7.13e-01	-5.31e-02	3.29e-01	1.80e-01	4.38e-01
13	1.54e-04	2.70e-02	8.93e-01	1.99e-01	1.88e-01	6.70e-02	8.43e-01
Mean	1.39e-04	-1.77e-02	1.14e+00	-3.61e-01	5.19e-01	5.72e-01	7.26e-01
Std	4.18e-05	3.61e-02	5.81e-01	5.38e-01	2.31e-01	4.24e-01	1.10e-01

Table 3.1: Healer R1: absolute and normalized inspiratory volume linear regression (order 1) coefficients and dispersion statistics for all the participants.

Subjects	**Coeff.deg.2**$_{Abs}$	**Coeff.deg.1**$_{Abs}$	**Coeff.deg.0**$_{Abs}$	**Coeff.deg.2**$_{Norm}$	**Coeff.deg.1**$_{Norm}$	**Coeff.deg.0**$_{Norm}$	**MAE**	**MSE**	**R**^{2}
1	6.54e-08	-2.15e-05	7.94e-02	1.27e-01	-9.80e-02	8.51e-01	3.09e-01	1.89e-01	7.26e-01
2	8.49e-08	-1.23e-04	1.02e-01	5.84e-01	-1.28e+00	1.59e+00	4.23e-01	3.96e-01	9.05e-01
3	6.13e-08	-5.20e-05	4.63e-02	7.21e-01	-8.04e-01	9.38e-01	3.85e-01	3.61e-01	9.05e-01
4	6.39e-08	-8.69e-05	6.89e-02	6.72e-02	-3.93e-01	1.34e+00	3.98e-01	3.28e-01	8.97e-01
5	2.33e-08	4.24e-05	1.35e-02	4.40e-02	2.88e-01	3.30e-01	4.48e-01	3.83e-01	9.13e-01
6	1.64e-07	-8.68e-05	7.21e-02	3.94e-01	-5.05e-01	1.01e+00	5.31e-01	6.90e-01	8.14e-01
7	1.97e-08	-2.24e-06	5.82e-02	5.60e-02	-1.51e-02	9.30e-01	2.96e-01	2.22e-01	8.17e-01
8	-4.30e-09	1.78e-04	1.53e-02	-9.45e-03	7.01e-01	1.09e-01	1.86e-01	6.43e-02	8.16e-01
9	1.42e-08	4.49e-05	-7.53e-03	2.34e-01	5.87e-01	-7.83e-02	3.91e-01	3.93e-01	7.43e-01
10	-1.05e-08	1.71e-04	1.64e-03	-1.21e-01	1.58e+00	1.22e-02	2.96e-01	2.29e-01	7.94e-01
11	2.48e-08	1.07e-04	6.50e-03	1.84e-01	1.37e+00	1.43e-01	7.43e-01	1.08e+00	7.42e-01
12	5.04e-08	-7.84e-05	9.07e-02	5.63e-01	-6.80e-01	6.10e-01	2.76e-01	1.45e-01	5.46e-01
13	1.01e-08	1.25e-04	4.04e-02	4.63e-02	7.28e-01	2.98e-01	1.84e-01	6.58e-02	8.46e-01
Mean	4.36e-08	1.67e-05	4.52e-02	2.22e-01	1.14e-01	6.22e-01	3.74e-01	3.49e-01	8.05e-01
Std	4.46e-08	9.91e-05	3.51e-02	2.51e-01	8.24e-01	5.11e-01	1.43e-01	2.65e-01	9.74e-02

Table 3.2: Healer R1: absolute and normalized inspiratory volume regression (order 2) coefficients and dispersion statistics for all the participants.

Subjects	Slope	Intercept	MAE	MSE	R^2
1	9.12e-01	1.69e+02	1.39e+02	6.58e+04	9.33e-01
2	9.05e-01	1.10e+02	2.19e+02	7.99e+04	9.21e-01
3	9.19e-01	8.07e+01	2.59e+02	1.92e+05	7.76e-01
4	5.41e-01	5.59e+02	1.62e+02	5.45e+04	5.81e-01
5	9.03e-01	2.21e+02	2.31e+02	1.61e+05	7.10e-01
6	1.01e+00	1.34e+02	1.21e+02	2.89e+04	9.56e-01
7	9.00e-01	9.68e+01	2.09e+02	1.01e+05	7.91e-01
8	8.38e-01	7.78e+01	1.92e+02	8.61e+04	9.59e-01
9	8.33e-01	2.44e+01	3.20e+02	1.84e+05	8.44e-01
10	5.36e-01	7.87e+02	3.65e+02	2.37e+05	5.43e-01
11	7.68e-01	2.04e+02	1.71e+02	5.36e+04	7.98e-01
12	8.51e-01	1.58e+02	2.51e+02	2.04e+05	8.42e-01
13	8.57e-01	2.33e+02	2.41e+02	1.36e+05	9.24e-01
Mean	8.28e-01	2.20e+02	2.22e+02	1.22e+05	8.14e-01
Std	1.35e-01	2.07e+02	6.64e+01	6.50e+04	1.31e-01

Table 3.3: Healer R1: inspiratory time linear regression (order 1) coefficients and dispersion statistics for all the participants.

Subject	Slope	Intercept	MAE	MSE	R^2
1	9.70e-01	7.48e-01	1.01e+00	2.93e+00	9.62e-01
2	1.01e+00	-5.23e-02	3.24e-01	2.49e-01	9.89e-01
3	1.00e+00	9.30e-03	6.69e-01	1.53e+00	9.63e-01
4	9.93e-01	1.54e-01	7.74e-01	1.28e+00	9.65e-01
5	9.51e-01	9.54e-01	1.10e+00	3.38e+00	9.30e-01
6	9.93e-01	1.56e-01	7.21e-01	1.37e+00	9.87e-01
7	9.80e-01	3.55e-01	7.32e-01	1.21e+00	9.71e-01
8	9.93e-01	1.21e-01	4.82e-01	4.85e-01	9.81e-01
9	9.53e-01	4.84e-01	5.31e-01	8.39e-01	9.51e-01
10	9.83e-01	1.89e-01	4.30e-01	7.88e-01	9.61e-01
11	1.00e+00	5.10e-02	8.33e-01	1.89e+00	9.68e-01
12	1.00e+00	5.81e-02	9.91e-01	3.77e+00	9.45e-01
13	9.83e-01	2.78e-01	6.09e-01	9.50e-01	9.75e-01
Mean	9.85e-01	2.70e-01	7.08e-01	1.59e+00	9.65e-01
Std	1.73e-02	2.87e-01	2.26e-01	1.07e+00	1.60e-02

Table 3.4: Healer R1: respiratory rate linear regression (order 1) coefficients and dispersion statistics for all the participants.

MAE, MSE and R^2 coefficients represent a valuable tool to help choosing between linear and quadratic regression to estimate the relationship between the relative volumes measured by the L.I.F.E. device and the spirometer, and to evaluate the goodness of fit by linear regression when assessing the relationship of inspiratory time and breathing rate.
In detail, L.I.F.E. Healer R1 relative inspiratory volume has been estimated by linear regression with a $MAE = 0.52 \pm 0.23$, $MSE = 0.57 \pm 0.42$, $R^2 = 0.76 \pm 0.11$, and by quadratic regression with $MAE = 0.37 \pm 0.14$, $MSE = 0.35 \pm 0.26$, $R^2 = 0.81 \pm 0.097$. Since inspiratory volume estimation by quadratic regression has shown a significant improvement, volume in L.I.F.E. Healer R1 will be estimated by a parabolic curve. Inspiratory time and respiratory rate, referred to the same suit, have been estimated with, respectively, $MAE = 222 \pm 66\ ms$, $MSE = 122000 \pm 65000\ ms^2$, $R^2 = 0.81 \pm 0.13$ and $MAE = 0.71 \pm 0.23\ bpm$, $MSE = 1.6 \pm 1.1\ bpm^2$, $R^2 = 0.97 \pm 0.016$. Time and rate in this suit appears to be linearly related to the ones measured by the spirometer, and will be accordingly be estimated by a straight line.
The same analysis has been repeated for L.I.F.E. Healer R2, for which relative inspiratory volume estimated by linear regression shows $MAE = 0.27 \pm 0.092$, $MSE =$

0.17 ± 0.11, $R^2 = 0.89 \pm 0.052$, and by quadratic regression the same errors are found to be $MAE = 0.26 \pm 0.084$, $MSE = 0.15 \pm 0.11$, $R^2 = 0.89 \pm 0.054$. This last evaluation shows no significant improvement with respect to the first one, leading to the decision to estimate the volumes of L.I.F.E. Healer R2 by linear regression. Inspiratory time and respiratory rate, referred to the same garment, have been estimated with, respectively, $MAE = 185 \pm 73$ ms, $MSE = 99200 \pm 62700$ ms^2, $R^2 = 0.85 \pm 0.12$ and $MAE = 0.82 \pm 0.44$ bpm, $MSE = 2.5 \pm 3.3$ bpm^2, $R^2 = 0.96 \pm 0.039$. This shows a pattern similar to the one found in the previous suit. Accordingly a linear regression is applied to estimate inspiratory time and respiratory rate of this suit too.
Lastly the errors for L.I.F.E. Healer R3 in linear and quadratic modeling of inspiratory volumes are respectively $MAE = 0.46 \pm 0.50$, $MSE = 0.74 \pm 1.8$, $R^2 = 0.69 \pm 0.22$, and $MAE = 0.32 \pm 0.26$, $MSE = 0.43 \pm 0.97$, $R^2 = 0.80 \pm 0.091$, leading to the choice of quadratic regression for the estimation of inspiratory volume. Regarding inspiratory time and breathing rate they are estimated by linear regression with errors $MAE = 205 \pm 96$ ms, $MSE = 154000 \pm 121000$ ms^2, $R^2 = 0.82 \pm 0.10$ and $MAE = 0.79 \pm 0.39$ bpm, $MSE = 2.4 \pm 2.0$ bpm^2, $R^2 = 0.96 \pm 0.024$, leading to the same conclusion of the previous garments.

According to these observations, the four parameters under analysis have been represented for each garment and every subject, comprehending the complete set of breaths of all static and dynamic exercises. Volume measurements may differ from one subject to the other, as suggested by the results in the various tables, and because of this such variables are shown with different colors for each subject. These plots are shown in Figures 3.4-3.7.

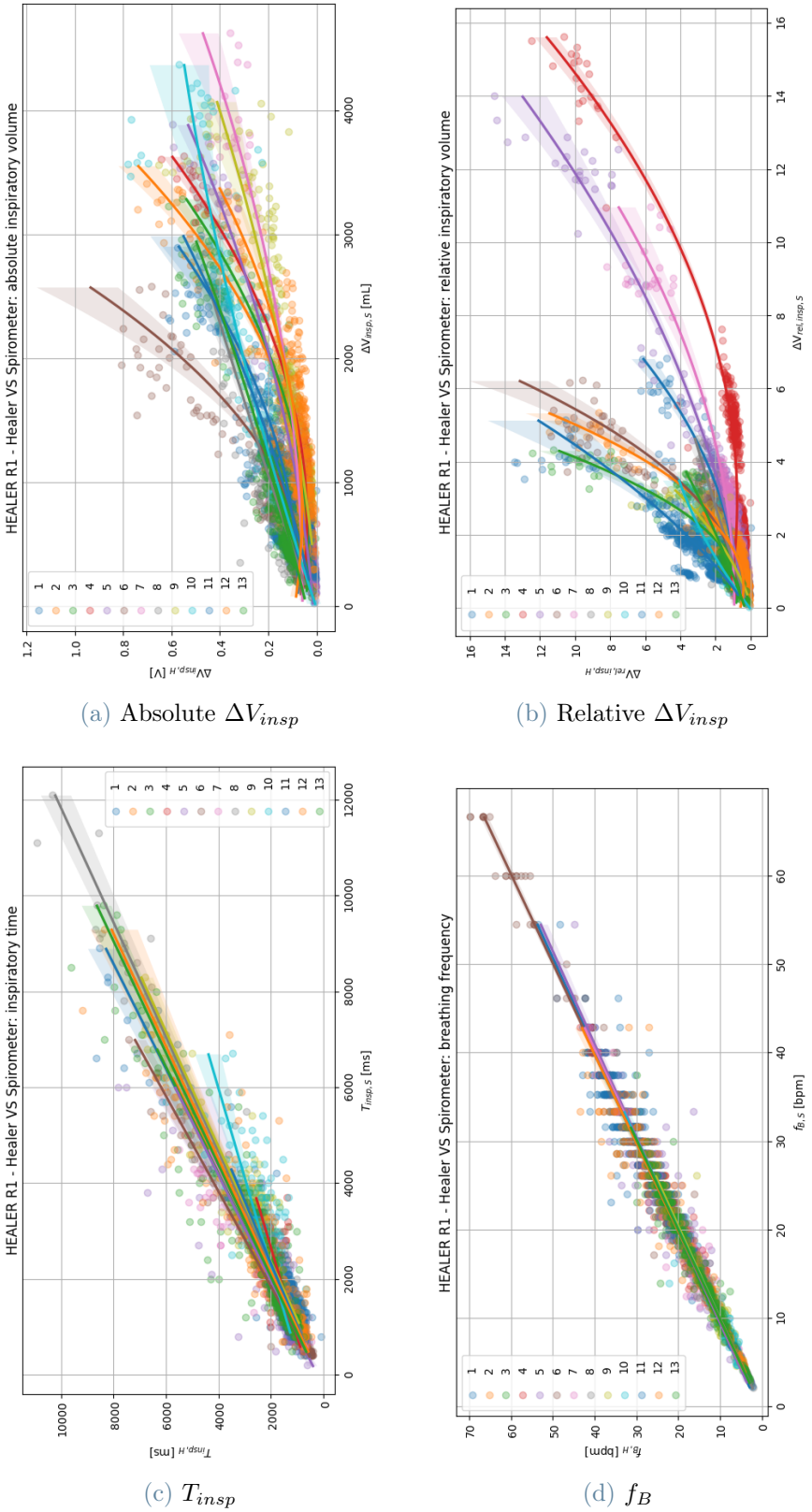

(a) Absolute ΔV_{insp} (b) Relative ΔV_{insp}

(c) T_{insp} (d) f_B

Figure 3.4: Scatter plots of the four parameters of interest relative to L.I.F.E. Healer R1 garment of all subjects.

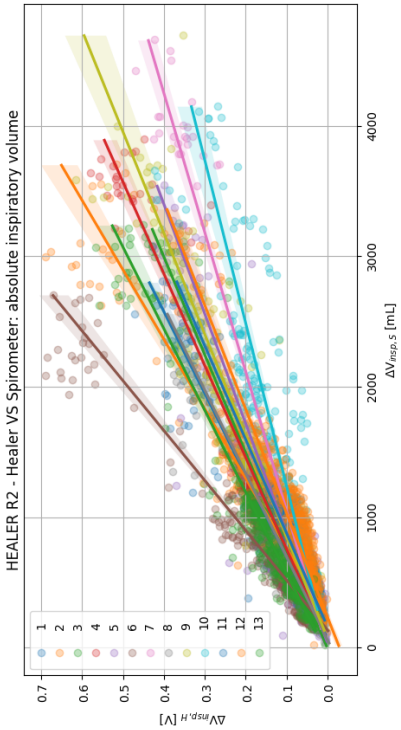

(a) Absolute ΔV_{insp}

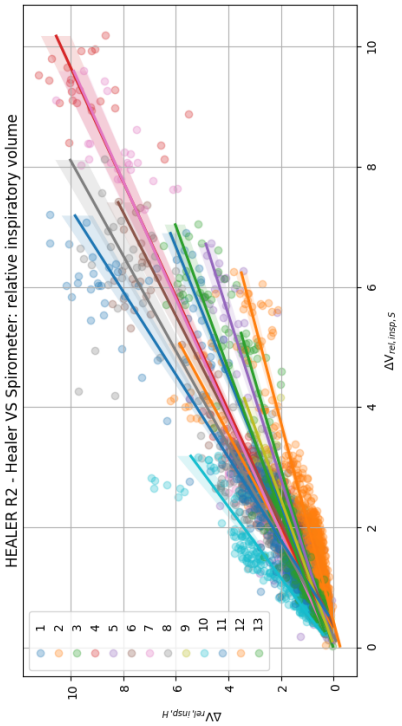

(b) Relative ΔV_{insp}

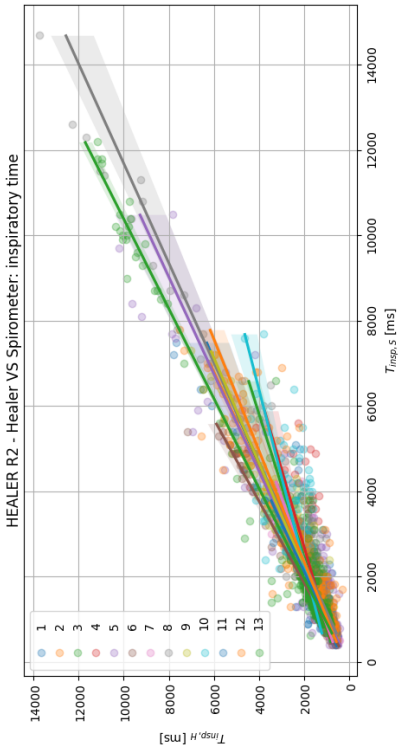

(c) T_{insp}

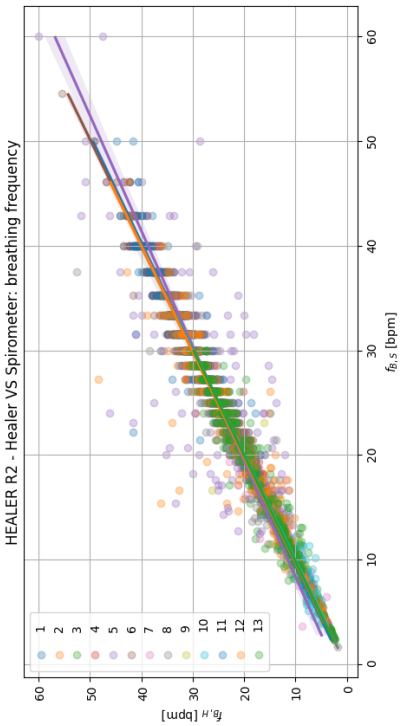

(d) f_B

Figure 3.5: Scatter plots of the four parameters of interest relative to L.I.F.E. Healer R2 garment of all subjects.

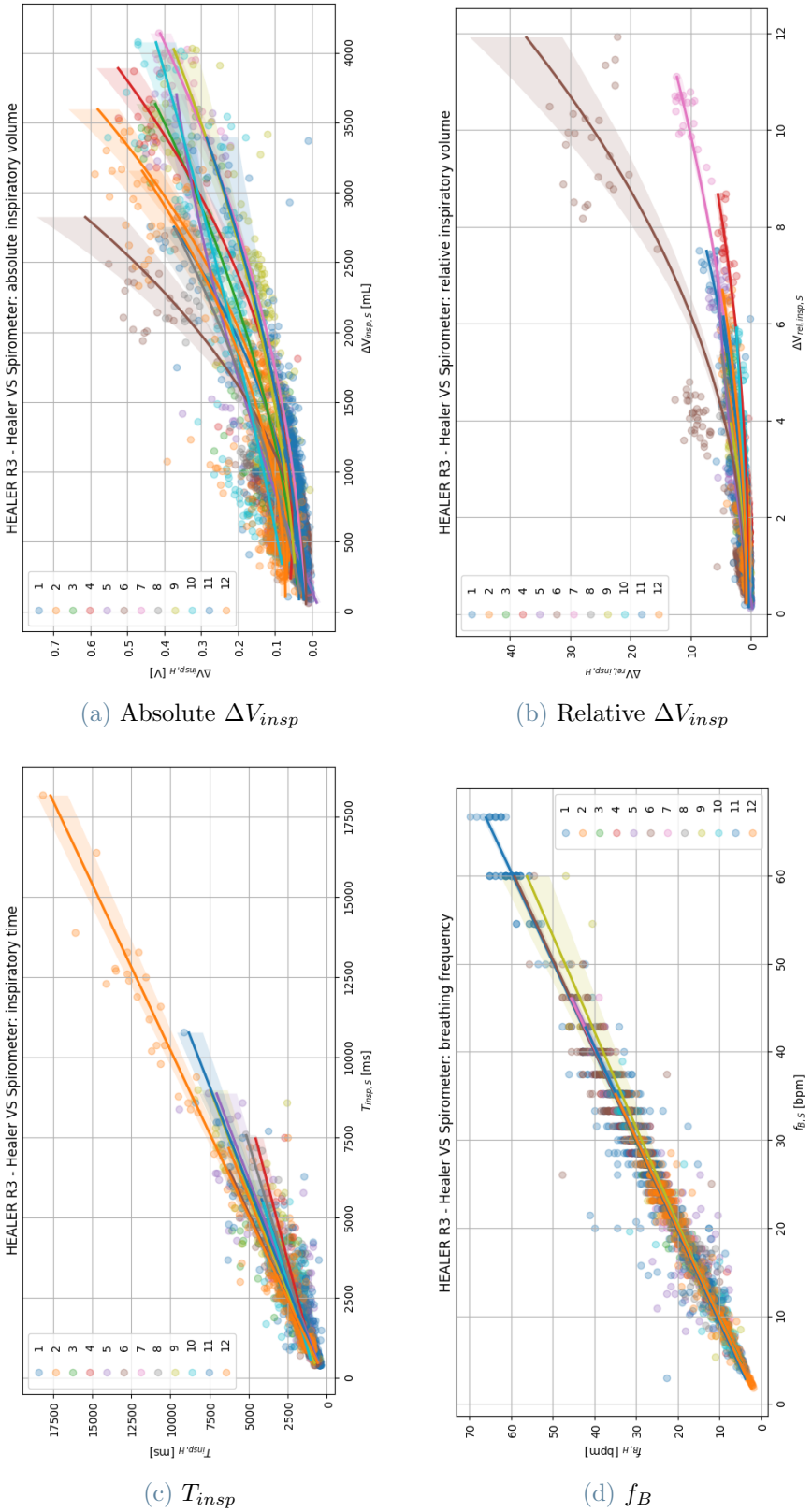

(a) Absolute ΔV_{insp} (b) Relative ΔV_{insp}

(c) T_{insp} (d) f_B

Figure 3.6: Scatter plots of the four parameters of interest relative to L.I.F.E. Healer R3 garment of all subjects.

From this qualitative (Figures 3.4 - 3.6) and quantitative (Tables A.1 - A.12) analysis, it is possible to see how a common regression curve for inspiratory volume can not be defined for all the subjects of a single L.I.F.E. garment. In fact the regression coefficients for the volume parameter have a relative large inter-subject variability, well represented graphically in Figures 3.4 - 3.6. On the contrary, inspiratory time and even more respiratory rate have small inter-subject variability, with regression lines that are, in general, adherent one to the other. In particular, breathing rate appears to have the best accuracy and repeatability among the other parameters.
Furthermore, in Figures 3.7a, 3.7b it is shown an attempt to approximate all the calibration lines of all the subject of a single garment to an average regression line.

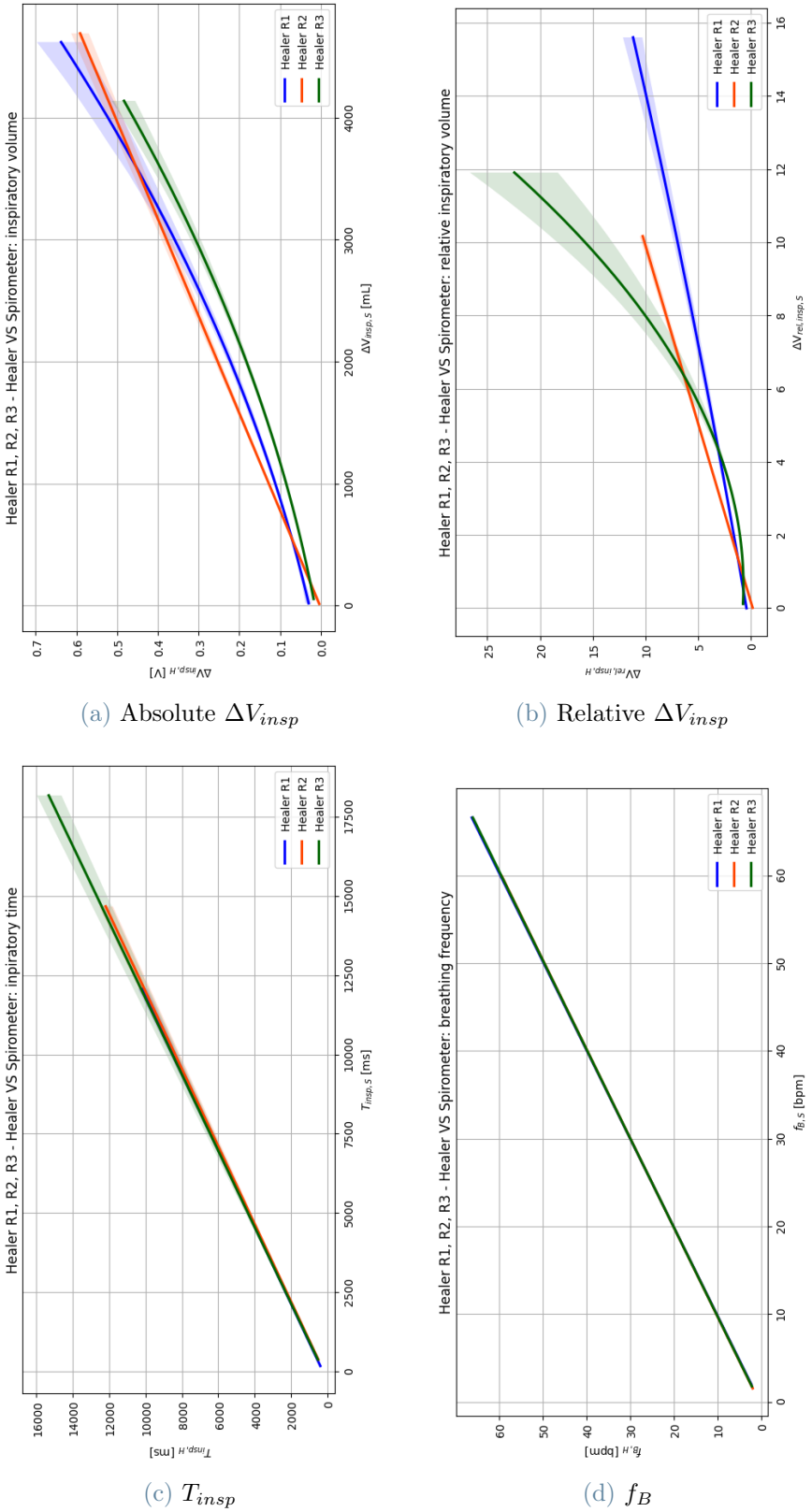

(a) Absolute ΔV_{insp} (b) Relative ΔV_{insp}

(c) T_{insp} (d) f_B

Figure 3.7: Regression plots of the four parameters of interest relative to L.I.F.E. Healer R1, R2 and R3 garment of all subjects.

The large variability of inspiratory volume behaviours within a single suit prevents the reliability of the depicted plots. On the other hand, Figures 3.7c and 3.7d appear to be reliable, due to the small inter-subject variability of temporal parameters. In fact the regression lines, computed by taking into account the entire pool of breaths of all the subjects for a single L.I.F.E. Healer garment, have been evaluated, for inspiratory time, as $T_{insp,R1} = 0.82 \cdot T_{insp,S} + 220.84\ ms$ for Healer R1, $T_{insp,R2} = 0.82 \cdot T_{insp,S} + 168.01\ ms$ for Healer R2, and $T_{insp,R3} = 0.83 \cdot T_{insp,S} + 187.10\ ms$ for Healer R3; while regarding respirator rate as $f_{B,R1} = 0.99 \cdot f_{B,S} + 0.22\ bpm$ for Healer R1, $f_{B,R2} = 0.98 \cdot f_{B,S} + 0.36\ bpm$ for Healer R2, and finally $f_{B,R3} = 0.98 \cdot f_{B,S} + 0.33\ bpm$ for R3. It is much clear how there exist a linear relationship between the two measuring systems; in particular, respiratory rate regression shows a slope very close to 1, confirming once again the goodness of this estimation.
Bland-Altman analysis has been applied to R1, R2 and R3 suits, considering the entire pool of breaths. The various Bland-Altman plots are showed in Appendix B.1. Regarding the R1 device, the relative inspiratory amplitudes, inspiratory times and respiratory rate are found within the respective concordance interval defined by -0.31 ± 2.62, $-100 \pm 824.17\ ms$ and $0.01 \pm 2.6\ bpm$. The same concordance intervals for the Healer R2 are found to be -0.16 ± 1.23, $-135.74 \pm 812.55\ ms$ and $0.0 \pm 3.29\ bpm$. Lastly, the same intervals in the case of R3 are -0.54 ± 2.83, $-109.79 \pm 933.69\ ms$ and $0.0 \pm 3.28\ bpm$. From this analysis, it can be seen more clearly how inspiratory volume and time are underestimated by the L.I.F.E. devices with an average bias while, on the other hand, breathing rate does not appear to have a statistical bias with respect to the gold standard measurement. Unfortunately, even though the vast majority of breaths are inside the concordance interval, all the parameters evaluated for each garment show a wide dispersion of data and, more importantly, the presence of various discordant breaths between the two systems. .

Because of these reasons, it is possible to conclude that each L.I.F.E. garment should be calibrated in amplitude for each different subject, for example by performing few minutes of tidal breathing in a conventional and controlled position (such as sitting on a chair) in order to accurately assess volume parameters. When measuring temporal parameters, instead, a subject-specific calibration is not required .

3.2.2. Data pooled by breathing in static or dynamic exercises

Grouping data by static or dynamic experimental conditions, it is possible to understand if the subject-sensitive calibration curve can be used for all types of breaths dynamics or if multiple curves are needed when varying exercises and pattern (for example between tidal breathing, maximal inspirations and walking). It is expected that the average calibration curves considered in the previous pooling analysis, computed on tidal breathing, forced maximal inspirations and during walking, could be improved by considering real-life conditions only, hence constraining the analysis to spontaneous breathing at rest and walking. The first approach could be applied to monitor pulmonary ventilation functions, while the second one integrating inspiratory maneuvers too could be applied in diagnostic or prognostic setups, such as performing spirometric tests wearing only the L.I.F.E. garment, thus eliminating the necessity of a standard laboratory spirometer. Both qualitative and quantitative analysis have been performed to assess these hypothesis.
Similarly to the previous analysis of pooled-data performed in Section 3.2.1, absolute and normalized inspiratory volume, inspiratory time and respiratory rate relationships between the L.I.F.E. Healer suits and the spirometers breaths have been assessed by computing the regression coefficients and estimation errors for every subject, now considering two different breathing conditions, namely breathing during static (laying down, sitting or standing) and dynamic activities (walking on treadmill). The values of the various parameters are shown in tables in Appendix A.2. Linear regression has been chosen to estimate the relationship of temporal parameters, since they clearly show a linear dependence, and of inspiratory volumes, because the improvement in residuals errors and in coefficient of determination R^2 are lower than 5% when estimating the regression through a second-order degree curve with respect to a one-order degree line. The linear regression choice is valid for both static and dynamic exercises. Scatter plots showing the linear regression for single subjects, grouped by L.I.F.E. Healer device and type of activity, are shown in Figures 3.8 - 3.13.

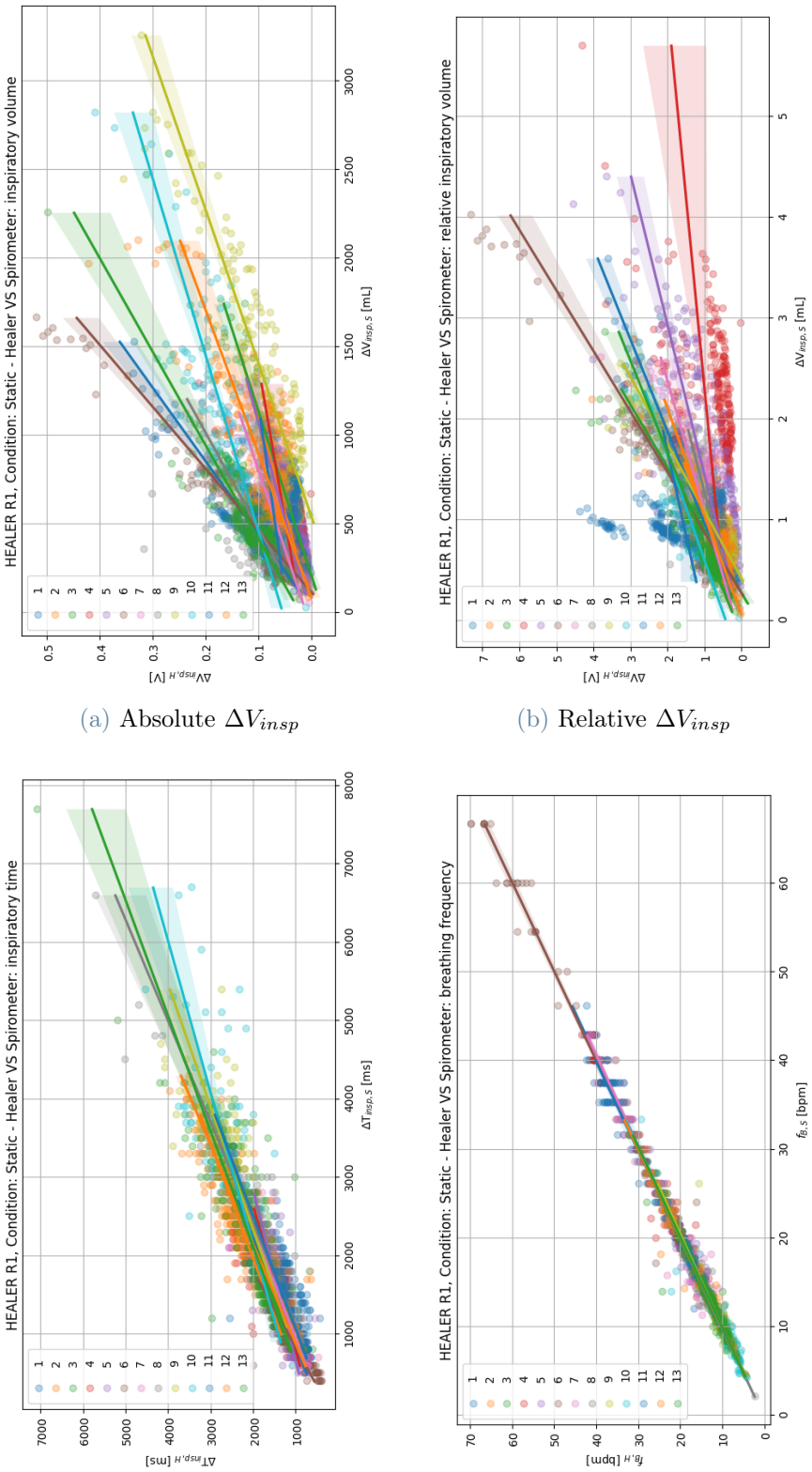

(a) Absolute ΔV_{insp}

(b) Relative ΔV_{insp}

(c) T_{insp}

(d) f_B

Figure 3.8: Regression plots of the four parameters of interest relative to L.I.F.E. Healer R1 of all subjects under static conditions.

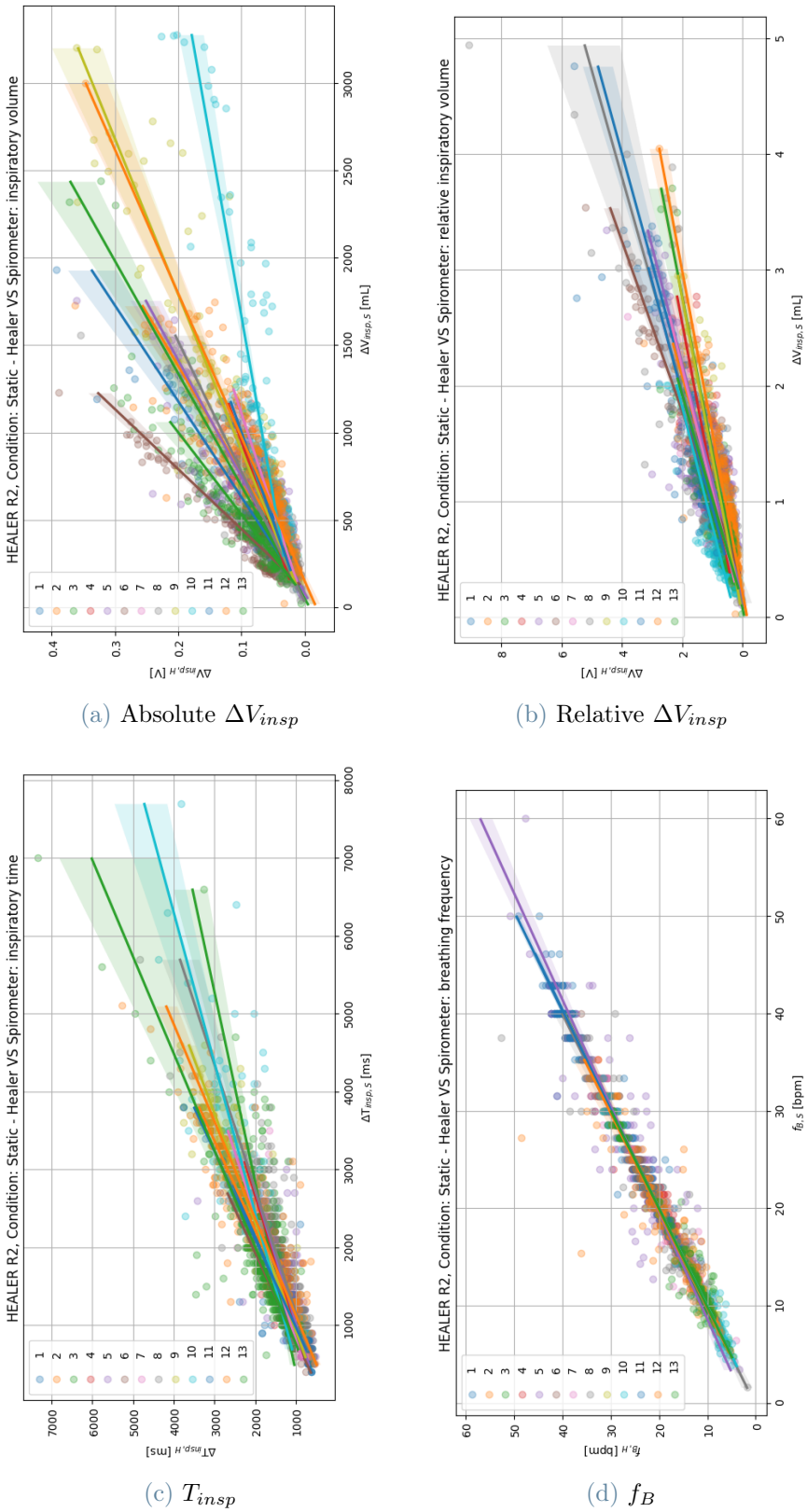

(a) Absolute ΔV_{insp} (b) Relative ΔV_{insp}

(c) T_{insp} (d) f_B

Figure 3.9: Regression plots of the four parameters of interest relative to L.I.F.E. Healer R2 of all subjects under static conditions.

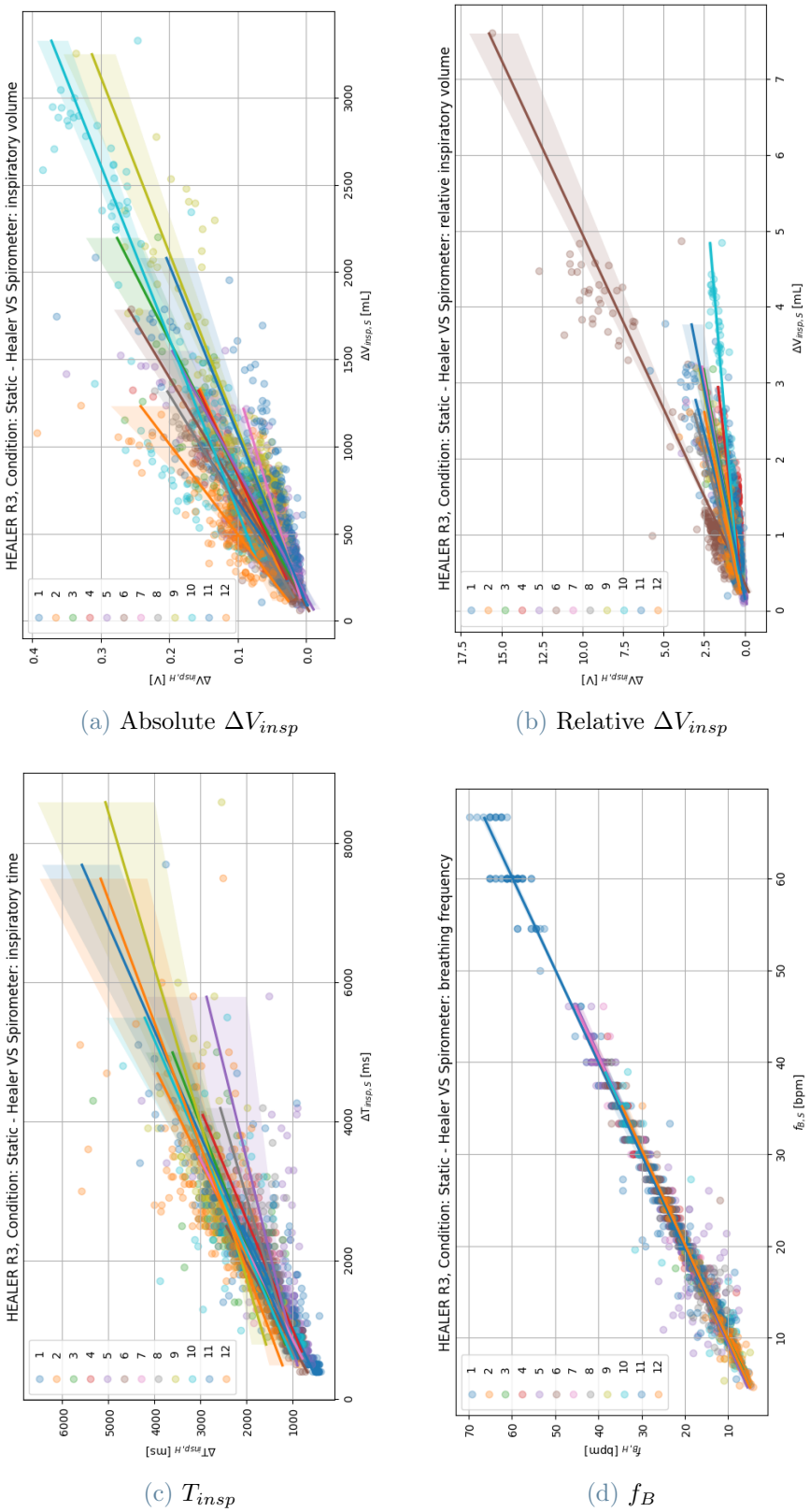

(a) Absolute ΔV_{insp} (b) Relative ΔV_{insp}

(c) T_{insp} (d) f_B

Figure 3.10: Regression plots of the four parameters of interest relative to L.I.F.E. Healer R3 of all subjects under static conditions.

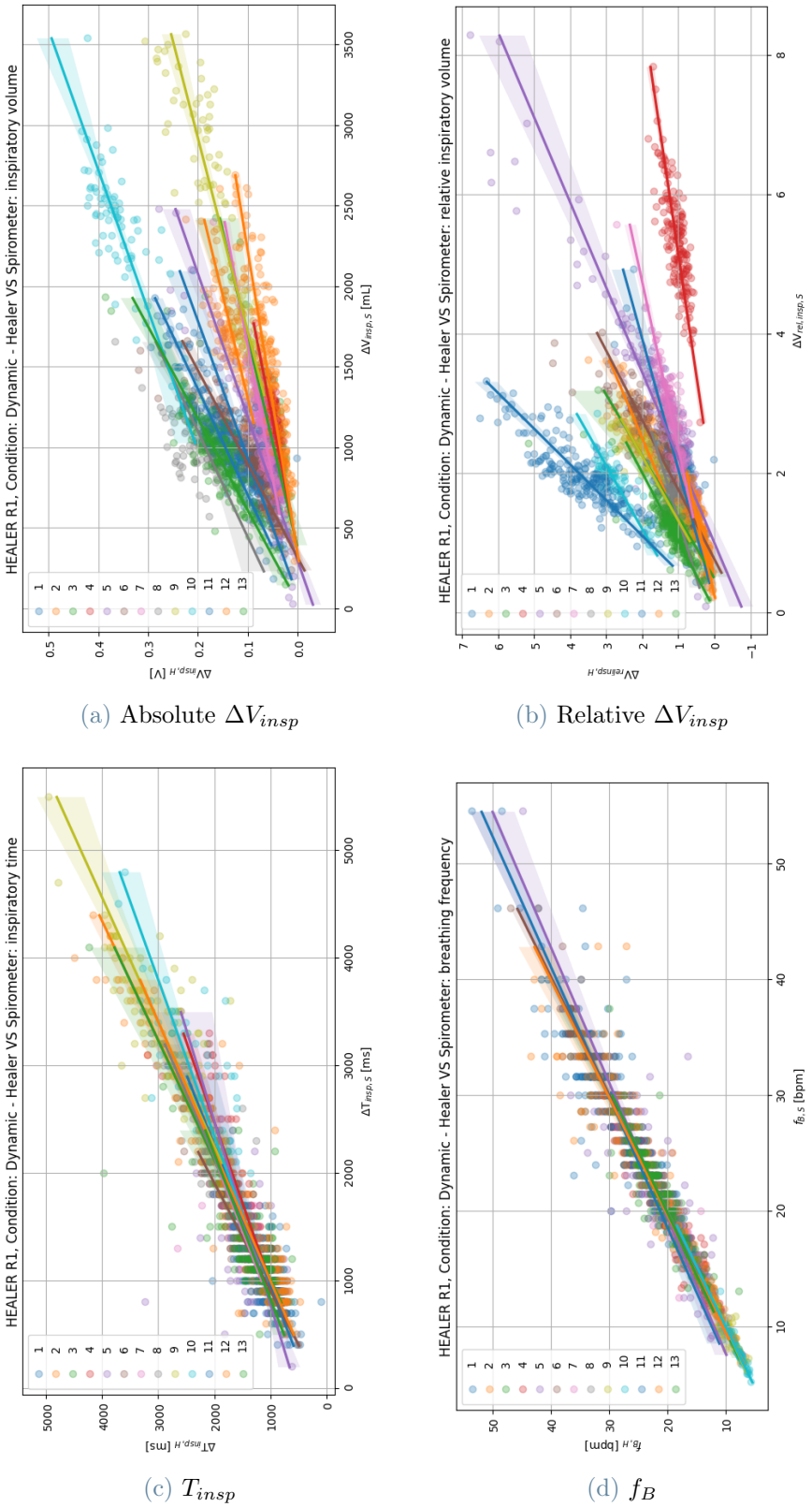

(a) Absolute ΔV_{insp} (b) Relative ΔV_{insp}

(c) T_{insp} (d) f_B

Figure 3.11: Regression plots of the four parameters of interest relative to L.I.F.E. Healer R1 of all subjects under dynamic conditions.

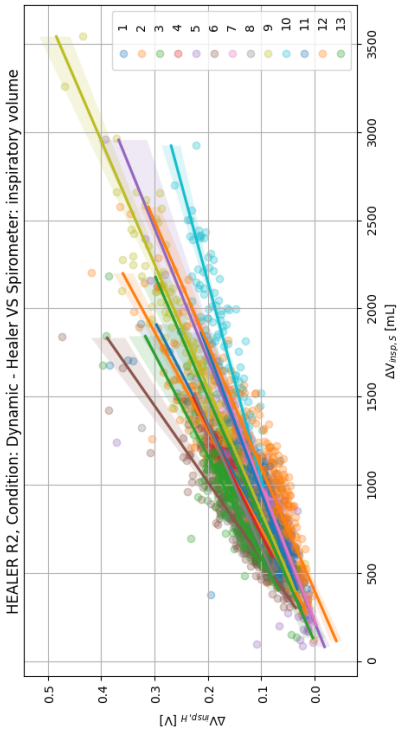

(a) Absolute ΔV_{insp}

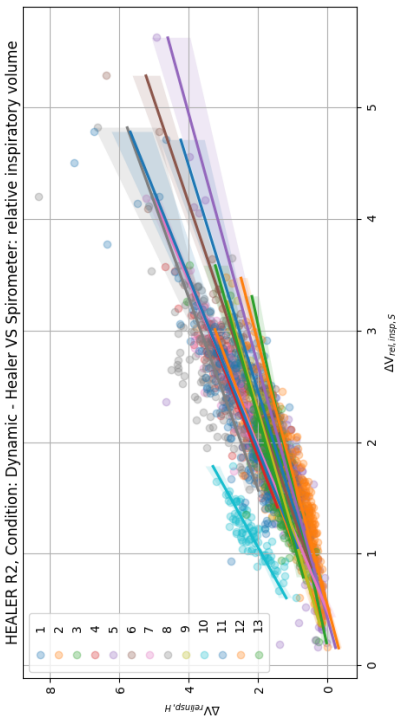

(b) Relative ΔV_{insp}

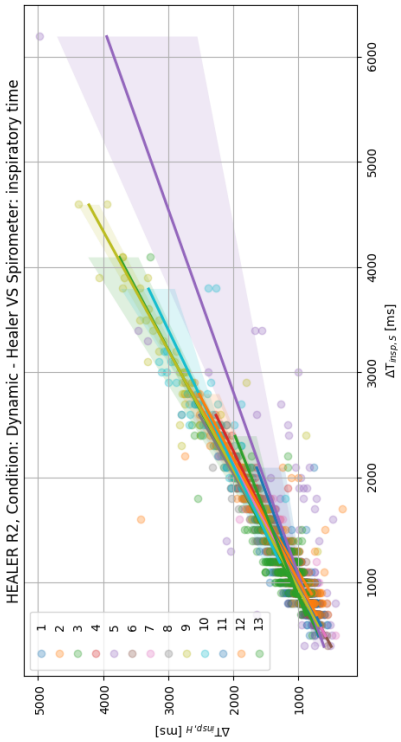

(c) T_{insp}

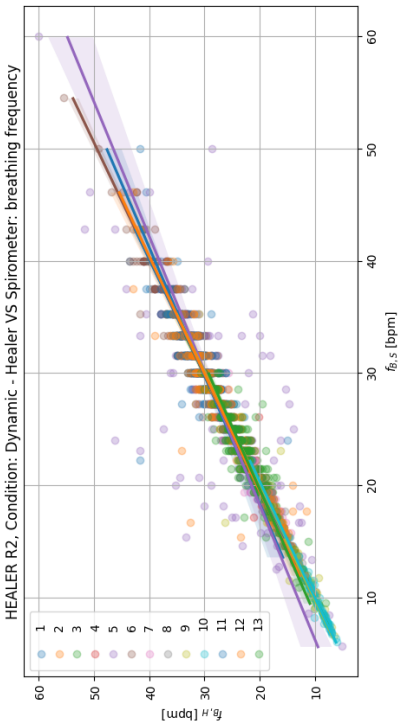

(d) f_B

Figure 3.12: Regression plots of the four parameters of interest relative to L.I.F.E. Healer R2 of all subjects under dynamic conditions.

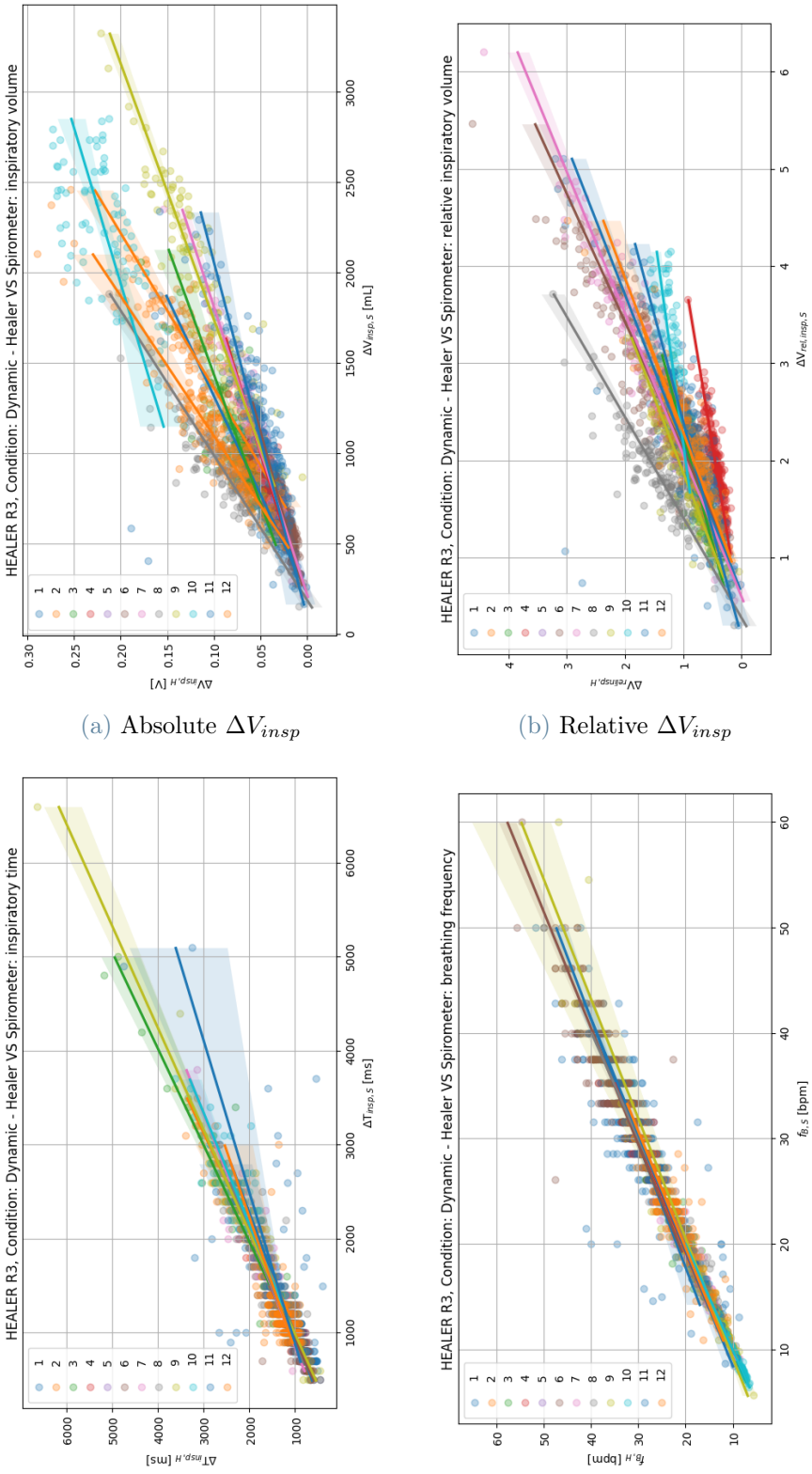

(a) Absolute ΔV_{insp}

(b) Relative ΔV_{insp}

(c) T_{insp}

(d) f_B

Figure 3.13: Regression plots of the four parameters of interest relative to L.I.F.E. Healer R3 of all subjects under dynamic conditions.

The qualitative analysis allows to confirm the sensitivity of measured volumes to different subjects for all the three L.I.F.E. Healer garments. Observing the results of this first analysis, represented in Figures 3.8 - 3.13, it is possible to reaffirm the subject-dependency of the inspiratory volume responses for the three wearable devices, in both static and dynamic scenarios. It should be easy to observe the noticeable difference in volume responses between one subject to another, within the same Healer device, in both exercise typologies. In this context, the L.I.F.E. Healer R2 suit deserves a particular mention. In fact the relative inspiratory volumes in the static and dynamic case show a common linear trend for all the tested subjects. Also for R3 garment in static condition it is possible to appreciate a linear trend, with only subject 6 showing a significant difference in response between all the other subjects.
Regarding inspiratory time and respiratory rate, it seems to exist a common trend between all the subjects suggesting, as in the previous aggregation of Section 3.2.1, that the responses of these two parameters are subject-invariant.
L.I.F.E. Healer R2 shows a better invariance to subjects when measuring relative inspiratory volumes and respiratory rate with respect to the other two suits. The reason for this difference in behaviour is due to the tighter fit of the Healer R2 device with respect to the looser and more comfortable Healer R1 and R3 devices.
These hypothesis have been assessed through the quantitative analysis, in which regression coefficients and estimation errors have been computed for each subject, each L.I.F.E. suit and in both static and dynamic conditions, and are exhibited in detail in Tables A.13 - A.30 in Appendix A.2. MAE, MSE and R^2 coefficients of the parameters estimation, averaged by participants, have been summarised for each L.I.F.E. Healer device in Tables 3.5, 3.6, 3.7, depending on the breaths included in the computation of the regression. In detail, the residual statistics have been computed considering breaths recorded in static conditions only while excluding inspiratory maneuvers breaths, during the dynamic exercise (hence the walk on the treadmill), and finally including the entire dataset (maneuvers included), as done in the aggregation above in Section 3.2.1.

In detail, the residuals measures of normalized inspiratory volume in Table 3.5 show a slightly reduced MAE and MSE during dynamic conditions for each L.I.F.E. Healer device. This may be due to the fact that the dynamic category includes only breaths recorded during the walk-on-treadmill exercise, while the other two categories comprehend breaths modulated in amplitude and frequency, in the case of the static data, or either the entire breaths dataset including the inspiratory maneuvers. This fact reflects on the variability of breaths within each category in exam, with the dynamic one having the lowest. Regarding the determination coefficient R^2 it seems to counter-intuitively worsen when

Breath selected	MAE	MSE	R^2
R1: All breaths	3.74e-01	3.49e-01	8.05e-01
R1: Static	3.24e-01	2.07e-01	5.42e-01
R1: Dynamic	2.07e-01	9.19e-02	6.67e-01
R2: All breaths	2.75e-01	1.66e-01	8.87e-01
R2: Static	2.06e-01	8.48e-02	7.11e-01
R2: Dynamic	1.98e-01	8.69e-02	7.81e-01
R3: All breaths	3.41e-01	4.66e-01	8.04e-01
R3: Static	2.62e-01	1.64e-01	6.63e-01
R3: Dynamic	1.20e-01	3.40e-02	7.36e-01

Table 3.5: Inspiratory volume regression: comparison of the dispersion statistics considering all the identified breath, during static and dynamic exercise, mediated for all participants wearing the three L.I.F.E. Healer devices.

Breath selected	MAE $[ms]$	MSE $[ms^2]$	R^2
R1: All breaths	2.22e+02	1.22e+05	8.14e-01
R1: Static	1.83e+02	6.86e+04	7.15e-01
R1: Dynamic	1.62e+02	5.77e+04	6.69e-01
R2: All breaths	1.85e+02	9.92e+04	8.50e-01
R2: Static	1.69e+02	7.07e+04	7.62e-01
R2: Dynamic	1.02e+02	2.67e+04	7.52e-01
R3: All breaths	2.22e+02	1.66e+05	8.15e-01
R3: Static	2.16e+02	1.22e+05	6.61e-01
R3: Dynamic	1.16e+02	3.56e+04	7.32e-01

Table 3.6: Inspiratory time regression: comparison of the dispersion statistics considering all the identified breath, during static and dynamic exercise, mediated for all participants wearing the three L.I.F.E. Healer devices.

Breath selected	**MAE** $[bpm]$	**MSE** $[bpm^2]$	$\mathbf{R^2}$
R1: All breaths	7.08e-01	1.59e+00	9.65e-01
R1: Static	5.03e-01	7.78e-01	9.75e-01
R1: Dynamic	1.02e+00	2.73e+00	8.92e-01
R2: All breaths	8.20e-01	2.46e+00	9.61e-01
R2: Static	7.14e-01	1.91e+00	9.58e-01
R2: Dynamic	9.70e-01	3.28e+00	9.04e-01
R3: All breaths	8.56e-01	2.55e+00	9.60e-01
R3: Static	7.03e-01	1.81e+00	9.60e-01
R3: Dynamic	9.21e-01	2.83e+00	8.87e-01

Table 3.7: Respiratory rate regression: comparison of the dispersion statistics considering all the identified breath, during static and dynamic exercise, mediated for all participants wearing the three L.I.F.E. Healer devices.

observing breaths in static or dynamic conditions, in discordance with the improvement in MAE and MSE. The reason may be found in the dependency of R^2 on the mean of the samples, which in turn depends on the width of the measurement interval since the mean is highly influenced by "extremes" samples which fall far from its value. Within this framework the three different categories of breaths have different ranges of amplitudes. In particular, the complete dataset of breaths have the widest range of amplitudes since it includes IC and SVC breaths, while the dynamic set of inspiratory volume amplitudes is characterized by a larger range of values, reaching larger volume values with respect to the static category, since it includes spontaneous breaths at rest in large portion. This is the reason behind the anomalous reduction in R^2 in static and dynamic conditions, meaning that the coefficient of determination should not be used as single indicator to determine the goodness between sets of data with different mean and range of values, but should be considered together with other dispersion measures, as MAE and MSE evaluated in this analysis.
Regarding the inspiratory time, it follows the same trend in MAE, MSE and R^2 as the inspiratory volume, showing an improvement in estimation starting from the complete breath dataset, to the static set, up to the best dynamic.
Lastly, concerning the respiratory rate, it does not show significant differences between the three L.I.F.E. devices and does not seem to exhibit any significant pattern regarding the three pools of data.

Finally, a Bland-Altman analysis have been performed to assess the concordance between

the L.I.F.E. wearable devices and the spirometer by COSMED within this second framework of pooled data. A relevant and representative example of Bland-Altman plots has been reported in Figure 3.14 which depicts the breaths recorded by L.I.F.E. Healer R2 during static exercises. The complete set of plots regarding this type of analysis on the three suits by L.I.F.E. and in both static and dynamic conditions, are listed in Appendix B.2 in Figures B.4 - B.9. Looking at the relative inspiratory volume in Figure 3.14a it can be derived the interval of concordance, specifically -0.13 ± 0.68. The L.I.F.E. Healer R2 garment appears to slightly under-estimate the normalized inspired volume with an average negative bias of 13% of the mean tidal volume under static conditions, with a standard deviation 0.34. Such width of the concordance limits is coupled by a linear descending trend between the differences and the means of the two inspiratory volumes, meaning that as the measured relative volume increases the error committed by the wearable device increases accordingly. This can be attributed to the prolonged elastic-return dynamic of the strain gauges occurring with larger amplitude at larger inspired volumes. Nonetheless, it appears that the breaths taken in analysis falls, for the most part, within the concordance limits.
The same considerations are applicable to the concordance analysis of the inspiratory time, shown in Figure 3.14b. Regarding this parameter the value measured by the L.I.F.E. Healer R2 falls within the concordance limits, defined by $-168.85 \pm 787,03\ ms$, revealing a mean underestimation of the inspiratory time by 168.8 ms, and a relatively large standard deviation measuring 401.55 ms.
Lastly, through Bland-Altman analysis of the respiratory rate, shown in Figure 3.14c, it is found that L.I.F.E. suits does not have any bias in measuring breathing frequency, and has a small standard deviation of $1.44 bpm$. This appreciable result is coupled with a strange behaviour since it appears to exist a dependency between the difference and mean of the measurements above a measured rate value. This behaviour may be due to the method used to oversample the spirometer signal from 10 Hz to 50 Hz, which may poorly interpolate the undersampled volume signal during occurring breathing pattern with small breathing time, and hence large breathing frequency. In such cases it may be possible that such patterns or signal's artifacts influence the computation of the breathing rate, resulting in a peculiar behaviour in the Bland-Altman plot. This phenomenon should be further investigated in detail in a future work.

In conclusion, within this second pooling of breaths discriminating between static and dynamic breathing conditions, it has been demonstrated the necessity of a dedicated calibration for each subject when measuring volume or time inspiratory parameters. Meanwhile,

if the only variable of interest is the breathing rate, a common calibration computed on the mean response of several subjects can be employed with accurate results. No significant difference exists in the responses in static or walking conditions, anyway if forced maximal breathing maneuvers are required, as during a spirometric test, the volumes measured by the L.I.F.E. Healer devices resulted inaccurate and non reliable while the respiratory rate is accurately measured.

Fit was found to be a determinant factor into reducing the variance of the ventilatory variables measures depending on the subject wearing the garment. Since L.I.F.E. Healer R2 device has been designed to be worn with a tighter fit, it shows a decreased user-variant response.

Finally, from the Bland-Altman analysis it was possible to understand that the measured inspiratory volumes and times are underestimated by the L.I.F.E. devices with a relatively large standard deviation, both in static and dynamic conditions. Furthermore, the bias shows a positive linear dependency from the amplitude of the measured volume or time value. On the contrary, respiratory rate is measured by the garments with no bias and with small standard deviation, but shows a dependency yet to be clarified and explained.

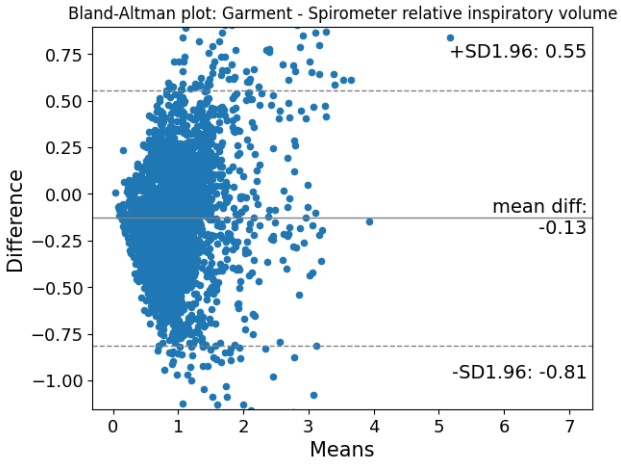

(a) Relative ΔV_{insp}

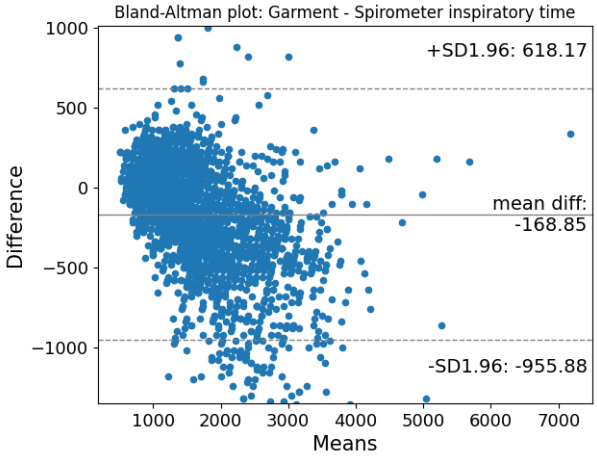

(b) T_{insp}

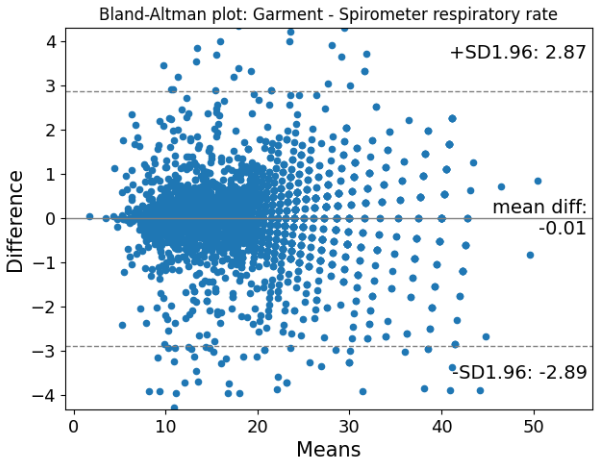

(c) f_B

Figure 3.14: Bland-Altman plots of the parameters of interest relative to L.I.F.E. Healer R2 garment and to all subjects under static exercises conditions, excluding inspiratory and expiratory maneuvers-related breaths.

4 | Conclusions

In this work of thesis the validation of L.I.F.E. Healer R1, R2 and R3 have been discussed. Ventilatory variables are measured by means of three strain-gauges placed at three different locations on the surface of the chest-wall and mounted within the suit's fabric. Such sensors change their electrical resistance when stretched or compressed, allowing the measurement of ventilatory variables based on the expansion and compression of the chest wall while breathing. These variables have been validated by comparison with a gold standard system, the MicroQuark spirometer by COSMED.

A validation protocol have been executed by 13 participants performing both static and dynamic exercises while wearing one L.I.F.E. Healer suit at time and breathing through the spirometer simultaneously. Static exercises included spontaneous, unforced breathing, forced inspiratory and expiratory maneuvers and breathing modulation in amplitude and frequency. At the end of the acquisition with each garment, a dynamic test has been performed by walking on a treadmill at different velocities and slopes. The measured volume signals have been processed in order to be compared in a breath-by-breath fashion. During this phase, the signals of the two measurement devices have been filtered, synchronized, compensated by errors and artifacts, and matching breaths have been identified in order to compute the ventilatory parameters of interest. In particular, the parameters used to validate the L.I.F.E. garments have been inspiratory volume (both absolute and normalized), inspiratory time and breathing rate.

Scatter plots have been used to qualitatively assess the relationships of the ventilatory parameters between L.I.F.E. Healer devices and spirometer. Mean absolute errors (MAE), mean squared errors (MSE) and the coefficient of determination R^2 have been computed and Bland-Altman analysis has been performed to assess the statistical concordance between the devices to validate and the gold standard. These analysis have been performed for each L.I.F.E. wearable device, for each tester, considering three sets of pooled data. Through scatter plots and estimation error analysis on MAE, MSE and R^2, it has been possible to show the necessity of a dedicated calibration for each subject when measuring volume or time inspiratory parameters, since those parameters have appeared to be subject-sensitive. On the other hand, respiratory rate measured by L.I.F.E. did not

result subject-dependent, and can be calibrated by a common regression curve. Furthermore, scatter and Bland-Altman plots have underlined a tendency to underestimate inspiratory volumes and times in L.I.F.E. Healer devices when compared to the COSMED gold standard. Such negative bias is also proportional to the amplitude of the parameter. Even in this case, the respiratory rate has been the one having the best estimate, with almost one-to-one correspondence with the gold standard and not showing any bias. These results have been found to be valid in both static and dynamic conditions, but not when inspiratory and expiratory maneuvers are included in the analysis. In fact at maximal inspiratory and expiratory volumes, or during extreme variations of volume, the strain-gauges show an elastic-return dynamic much slower than the anatomical dynamic of expansion/compression of the chest wall. Furthermore, the strain-gauge dynamic of elastic return appeared to be inversely proportional to the amplitude of volume variation. This structural characteristic of these piezo-resistive sensors worsen the measurement of temporal and volume parameters. Inspiratory volumes measured by the L.I.F.E. Healer devices can not be considered in complete agreement with the gold standard, due to the large dispersion of values. On the contrary, inspiratory time and respiratory rate can be considered concordant with the one measured by the gold standard, in both static and dynamic settings.

It also appeared how the slim-fit of the L.I.F.E. Healer R2 garment, tighter than two other suits, has been determinant for the good behaviour of the sensors, which reflected in a more subject-insensitive regression curve for both relative inspiratory volumes and inspiratory time when compared to the same behaviour of the other models.

Bibliography

[1] Kimio Konno and Jere Mead. Measurement of the separate volume changes of rib cage and abdomen during breathing. *Journal of applied physiology*, 22(3):407–422, 1967.

[2] John F Fieselmann, Michael S Hendryx, Charles M Helms, and Douglas S Wakefield. Respiratory rate predicts cardiopulmonary arrest for internal medicine inpatients. *Journal of general internal medicine*, 8(7):354–360, 1993.

[3] Michelle A Cretikos, Rinaldo Bellomo, Ken Hillman, Jack Chen, Simon Finfer, and Arthas Flabouris. Respiratory rate: the neglected vital sign. *Medical Journal of Australia*, 188(11):657–659, 2008.

[4] Richard Strauß, Santiago Ewig, Klaus Richter, Thomas König, Günther Heller, and Torsten T Bauer. The prognostic significance of respiratory rate in patients with pneumonia: a retrospective analysis of data from 705 928 hospitalized patients in germany from 2010–2012. *Deutsches Ärzteblatt International*, 111(29-30):503, 2014.

[5] Matthew M Churpek, Trevor C Yuen, Seo Young Park, David O Meltzer, Jesse B Hall, and Dana P Edelson. Derivation of a cardiac arrest prediction model using ward vital signs. *Critical care medicine*, 40(7):2102, 2012.

[6] Andrea Aliverti. Wearable technology: role in respiratory health and disease. *Breathe*, 13(2):e27–e36, 2017.

[7] Irene Steenbruggen et al. Brian L. Graham. Standardization of spirometry 2019 update. *American Journal of Respiratory and Critical Care Medicine*, 200(8), 10 2019.

[8] Warren M. Gold Murray, Nadel and Laura L. Koth. *Textbook of Respiratory Medicine, Pulmonary Function Testing.* 2016.

[9] V. Brusasco et al. M.R. Miller, J. Hankinson. Ats/ers task force: Standardisation of lung function testing. *American Journal of Respiratory and Critical Care Medicine*, 26(2), 2005.

[10] Julia AE Walters, Richard WOOD-BAKER, Justin Walls, and David P Johns. Stability of the easyone ultrasonic spirometer for use in general practice. *Respirology*, 11(3):306–310, 2006.

[11] Christian Buess, Peter Pietsch, Walter Guggenbuhl, and Erwin A Koller. Design and construction of a pulsed ultrasonic air flowmeter. *IEEE transactions on biomedical engineering*, (8):768–774, 1986.

[12] C Duvivier, R Peslin, and C Gallina. An incremental method to assess the linearity of gas flowmeters: application to fleisch pneumotachographs. *European Respiratory Journal*, 1(7):661–665, 1988.

[13] MR Miller and T Sigsgaard. Prevention of thermal and condensation errors in pneumotachographic recordings of the maximal forced expiratory manoeuvre. *European Respiratory Journal*, 7(1):198–201, 1994.

[14] COSMED. *Omnia Software User manual*. COSMED Srl, 7 edition, 2 2017.

[15] YI Sokol, RS Tomashevsky, and KV Kolisnyk. Turbine spirometers metrological support. *2016 International Conference on Electronics and Information Technology (EIT)*, pages 1–4, 2016.

[16] Jacob Fraden. Handbook of modern sensors: physics, designs, and applications, 1998.

[17] Ja-Woong Yoon, Yeon-Sik Noh, Yi-Suk Kwon, Won-Ki Kim, and Hyung-Ro Yoon. Improvement of dynamic respiration monitoring through sensor fusion of accelerometer and gyro-sensor. *Journal of Electrical Engineering and Technology*, 9(1):334–343, 2014.

[18] Henrik Gollee and Wei Chen. Real-time detection of respiratory activity using an inertial measurement unit. In *2007 29th Annual International Conference of the IEEE Engineering in Medicine and Biology Society*, pages 2230–2233. IEEE, 2007.

[19] J Dall'Ava-Santucci and A Armanganidis. Respiratory inductive plethysmography. In *Pulmonary Function in Mechanically Ventilated Patients*, pages 121–142. Springer, 1991.

[20] Leo Pekka Malmberg, Ville-Pekka Seppä, Anne Kotaniemi-Syrjänen, Kristiina Malmström, Merja Kajosaari, Anna S Pelkonen, Jari Viik, and Mika J Mäkelä. Measurement of tidal breathing flows in infants using impedance pneumography. *European Respiratory Journal*, 49(2), 2017.

[21] Jonathan D Sackner, Asa J Nixon, Brian Davis, Neal Atkins, and Marvin A Sackner.

Non-invasive measurement of ventilation during exercise using a respiratory inductive plethysmograph. i. *American Review of Respiratory Disease*, 122(6):867–871, 1980.

[22] Yinming Zhao, Yang Liu, Yongqian Li, and Qun Hao. Development and application of resistance strain force sensors. *Sensors*, 20(20):5826, 2020.

A | Appendix A: Tables of Pooled data

A.1. Pooled analysis on the three L.I.F.E. devices and intra-subject variability.

Subject	**Slope**$_{Abs}$	**Intercept**$_{Abs}$	**Slope**$_{Norm}$	**Intercept**$_{Norm}$	**MAE**	**MSE**	**R**^{2}
1	1.40e-04	1.27e-02	1.60e+00	-1.10e+00	4.05e-01	2.57e-01	6.27e-01
2	1.55e-04	-7.09e-02	1.60e+00	-1.10e+00	8.36e-01	1.14e+00	7.25e-01
3	1.51e-04	-7.53e-02	2.33e+00	-1.53e+00	6.71e-01	7.60e-01	8.00e-01
4	1.17e-04	-3.19e-02	5.28e-01	-6.21e-01	8.35e-01	1.16e+00	6.37e-01
5	1.21e-04	-2.25e-02	8.19e-01	-5.51e-01	5.74e-01	5.56e-01	8.73e-01
6	2.45e-04	-4.54e-02	1.43e+00	-6.39e-01	8.12e-01	1.18e+00	6.81e-01
7	7.82e-05	1.12e-02	5.27e-01	1.79e-01	4.23e-01	3.09e-01	7.45e-01
8	1.69e-04	1.88e-02	6.65e-01	1.34e-01	1.86e-01	6.44e-02	8.15e-01
9	1.06e-04	-5.83e-02	1.38e+00	-6.07e-01	4.20e-01	4.10e-01	7.33e-01
10	1.27e-04	3.61e-02	1.17e+00	2.68e-01	3.17e-01	2.36e-01	7.88e-01
11	1.69e-04	-2.31e-02	2.16e+00	-5.09e-01	7.45e-01	1.11e+00	7.34e-01
12	8.22e-05	-7.90e-03	7.13e-01	-5.31e-02	3.29e-01	1.80e-01	4.38e-01
13	1.54e-04	2.70e-02	8.93e-01	1.99e-01	1.88e-01	6.70e-02	8.43e-01
Mean	1.39e-04	-1.77e-02	1.14e+00	-3.61e-01	5.19e-01	5.72e-01	7.26e-01
Std	4.18e-05	3.61e-02	5.81e-01	5.38e-01	2.31e-01	4.24e-01	1.10e-01

Table A.1: Healer R1; inspiratory volume linear regression (order 1) coefficients and dispersion statistics for all the participants.

Subjects	Coeff.deg.2$_{Abs}$	Coeff.deg.1$_{Abs}$	Coeff.deg.0$_{Abs}$	Coeff.deg.2$_{Norm}$	Coeff.deg.1$_{Norm}$	Coeff.deg.0$_{Norm}$	MAE	MSE	R^2
1	6.54e-08	-2.15e-05	7.94e-02	1.27e-01	-9.80e-02	8.51e-01	3.09e-01	1.89e-01	7.26e-01
2	8.49e-08	-1.23e-04	1.02e-01	5.84e-01	-1.28e+00	1.59e+00	4.23e-01	3.96e-01	9.05e-01
3	6.13e-08	-5.20e-05	4.63e-02	7.21e-01	-8.04e-01	9.38e-01	3.85e-01	3.61e-01	9.05e-01
4	6.39e-08	-8.69e-05	6.89e-02	6.72e-02	-3.93e-01	1.34e+00	3.98e-01	3.28e-01	8.97e-01
5	2.33e-08	4.24e-05	1.35e-02	4.40e-02	2.88e-01	3.30e-01	4.48e-01	3.83e-01	9.13e-01
6	1.64e-07	-8.68e-05	7.21e-02	3.94e-01	-5.05e-01	1.01e+00	5.31e-01	6.90e-01	8.14e-01
7	1.97e-08	-2.24e-06	5.82e-02	5.60e-02	-1.51e-02	9.30e-01	2.96e-01	2.22e-01	8.17e-01
8	-4.30e-09	1.78e-04	1.53e-02	-9.45e-03	7.01e-01	1.09e-01	1.86e-01	6.43e-02	8.16e-01
9	1.42e-08	4.49e-05	-7.53e-03	2.34e-01	5.87e-01	-7.83e-02	3.91e-01	3.93e-01	7.43e-01
10	-1.05e-08	1.71e-04	1.64e-03	-1.21e-01	1.58e+00	1.22e-02	2.96e-01	2.29e-01	7.94e-01
11	2.48e-08	1.07e-04	6.50e-03	1.84e-01	1.37e+00	1.43e-01	7.43e-01	1.08e+00	7.42e-01
12	5.04e-08	-7.84e-05	9.07e-02	5.63e-01	-6.80e-01	6.10e-01	2.76e-01	1.45e-01	5.46e-01
13	1.01e-08	1.25e-04	4.04e-02	4.63e-02	7.28e-01	2.98e-01	1.84e-01	6.58e-02	8.46e-01
Mean	4.36e-08	1.67e-05	4.52e-02	2.22e-01	1.14e-01	6.22e-01	3.74e-01	3.49e-01	8.05e-01
Std	4.46e-08	9.91e-05	3.51e-02	2.51e-01	8.24e-01	5.11e-01	1.43e-01	2.65e-01	9.74e-02

Table A.2: Healer R1; inspiratory volume regression (order 2) coefficients and dispersion statistics for all the participants.

Subjects	Slope	Intercept	MAE	MSE	R^2
1	9.12e-01	1.69e+02	1.39e+02	6.58e+04	9.33e-01
2	9.05e-01	1.10e+02	2.19e+02	7.99e+04	9.21e-01
3	9.19e-01	8.07e+01	2.59e+02	1.92e+05	7.76e-01
4	5.41e-01	5.59e+02	1.62e+02	5.45e+04	5.81e-01
5	9.03e-01	2.21e+02	2.31e+02	1.61e+05	7.10e-01
6	1.01e+00	1.34e+02	1.21e+02	2.89e+04	9.56e-01
7	9.00e-01	9.68e+01	2.09e+02	1.01e+05	7.91e-01
8	8.38e-01	7.78e+01	1.92e+02	8.61e+04	9.59e-01
9	8.33e-01	2.44e+01	3.20e+02	1.84e+05	8.44e-01
10	5.36e-01	7.87e+02	3.65e+02	2.37e+05	5.43e-01
11	7.68e-01	2.04e+02	1.71e+02	5.36e+04	7.98e-01
12	8.51e-01	1.58e+02	2.51e+02	2.04e+05	8.42e-01
13	8.57e-01	2.33e+02	2.41e+02	1.36e+05	9.24e-01
Mean	8.28e-01	2.20e+02	2.22e+02	1.22e+05	8.14e-01
Std	1.35e-01	2.07e+02	6.64e+01	6.50e+04	1.31e-01

Table A.3: Healer R1; inspiratory time linear regression (order 1) coefficients and dispersion statistics for all the participants.

Subject	Slope	Intercept	MAE	MSE	R^2
1	9.70e-01	7.48e-01	1.01e+00	2.93e+00	9.62e-01
2	1.01e+00	-5.23e-02	3.24e-01	2.49e-01	9.89e-01
3	1.00e+00	9.30e-03	6.69e-01	1.53e+00	9.63e-01
4	9.93e-01	1.54e-01	7.74e-01	1.28e+00	9.65e-01
5	9.51e-01	9.54e-01	1.10e+00	3.38e+00	9.30e-01
6	9.93e-01	1.56e-01	7.21e-01	1.37e+00	9.87e-01
7	9.80e-01	3.55e-01	7.32e-01	1.21e+00	9.71e-01
8	9.93e-01	1.21e-01	4.82e-01	4.85e-01	9.81e-01
9	9.53e-01	4.84e-01	5.31e-01	8.39e-01	9.51e-01
10	9.83e-01	1.89e-01	4.30e-01	7.88e-01	9.61e-01
11	1.00e+00	5.10e-02	8.33e-01	1.89e+00	9.68e-01
12	1.00e+00	5.81e-02	9.91e-01	3.77e+00	9.45e-01
13	9.83e-01	2.78e-01	6.09e-01	9.50e-01	9.75e-01
Mean	9.85e-01	2.70e-01	7.08e-01	1.59e+00	9.65e-01
Std	1.73e-02	2.87e-01	2.26e-01	1.07e+00	1.60e-02

Table A.4: Healer R1; respiratory rate linear regression (order 1) coefficients and dispersion statistics for all the participants.

Subject	**Slope**$_{Abs}$	**Intercept**$_{Abs}$	**Slope**$_{Norm}$	**Intercept**$_{Norm}$	**MAE**	**MSE**	**R**^{2}
1	1.60e-04	-1.20e-02	9.23e-01	-1.71e-01	2.14e-01	9.60e-02	8.98e-01
2	1.88e-04	-4.48e-02	1.23e+00	-4.04e-01	2.15e-01	9.59e-02	9.20e-01
3	1.33e-04	-2.39e-04	6.70e-01	-1.96e-03	1.71e-01	6.29e-02	8.76e-01
4	1.42e-04	-8.27e-03	1.05e+00	-1.60e-01	3.30e-01	2.00e-01	9.45e-01
5	1.19e-04	-5.19e-03	7.30e-01	-6.06e-02	2.96e-01	1.63e-01	7.89e-01
6	2.62e-04	-3.70e-02	1.17e+00	-4.52e-01	3.02e-01	1.59e-01	9.24e-01
7	9.37e-05	1.06e-03	1.03e+00	2.40e-02	2.43e-01	1.24e-01	9.55e-01
8	1.57e-04	-1.03e-02	1.27e+00	-2.65e-01	4.41e-01	3.99e-01	8.85e-01
9	1.29e-04	-1.02e-02	8.29e-01	-5.81e-02	1.66e-01	5.72e-02	8.54e-01
10	8.00e-05	4.11e-04	1.69e+00	6.72e-03	4.50e-01	3.94e-01	7.89e-01
11	1.39e-04	-2.30e-02	1.45e+00	-6.14e-01	3.51e-01	2.29e-01	9.19e-01
12	1.25e-04	-3.02e-02	6.04e-01	-2.70e-01	1.93e-01	8.41e-02	8.53e-01
13	1.60e-04	8.30e-03	8.40e-01	9.50e-02	2.06e-01	9.36e-02	9.24e-01
Mean	1.45e-04	-1.32e-02	1.04e+00	-1.79e-01	2.75e-01	1.66e-01	8.87e-01
Std	4.33e-05	1.54e-02	3.07e-01	2.04e-01	9.24e-02	1.10e-01	5.17e-02

Table A.5: Healer R2; inspiratory volume linear regression (order 1) coefficients and dispersion statistics for all the participants.

Subjects	Coeff.deg.2$_{Abs}$	Coeff.deg.1$_{Abs}$	Coeff.deg.0$_{Abs}$	Coeff.deg.2$_{Norm}$	Coeff.deg.1$_{Norm}$	Coeff.deg.0$_{Norm}$	MAE	MSE	R^2
1	1.61e-08	1.22e-04	2.88e-03	3.77e-02	7.07e-01	4.11e-02	1.98e-01	9.09e-02	9.03e-01
2	-9.00e-10	1.91e-04	-4.68e-02	-4.08e-03	1.25e+00	-4.21e-01	2.16e-01	9.59e-02	9.20e-01
3	0.00e+00	1.33e-04	-1.96e-04	7.15e-05	6.70e-01	-1.61e-03	1.71e-01	6.29e-02	8.76e-01
4	-8.90e-09	1.75e-04	-2.55e-02	-2.53e-02	1.29e+00	-4.94e-01	3.04e-01	1.82e-01	9.50e-01
5	-2.20e-09	1.26e-04	-8.43e-03	-7.08e-03	7.73e-01	-9.83e-02	2.96e-01	1.63e-01	7.89e-01
6	3.75e-08	1.74e-04	-4.56e-03	6.09e-02	7.77e-01	-5.57e-02	2.52e-01	1.33e-01	9.37e-01
7	-6.90e-09	1.23e-04	-1.62e-02	-3.67e-02	1.35e+00	-3.67e-01	2.24e-01	1.04e-01	9.63e-01
8	-3.50e-09	1.64e-04	-1.27e-02	-8.81e-03	1.32e+00	-3.26e-01	4.40e-01	3.98e-01	8.85e-01
9	-1.34e-08	1.83e-04	-5.38e-02	-9.75e-02	1.18e+00	-3.07e-01	1.57e-01	5.27e-02	8.66e-01
10	-7.10e-09	1.08e-04	-2.01e-02	-1.94e-01	2.29e+00	-3.29e-01	4.09e-01	3.80e-01	7.96e-01
11	3.00e-08	6.39e-05	9.26e-03	1.22e-01	6.66e-01	2.47e-01	2.65e-01	1.59e-01	9.43e-01
12	6.80e-09	1.05e-04	-1.87e-02	1.76e-02	5.03e-01	-1.68e-01	1.85e-01	8.28e-02	8.55e-01
13	-8.40e-09	1.84e-04	-2.90e-03	-2.02e-02	9.69e-01	-3.32e-02	2.07e-01	9.09e-02	9.26e-01
Mean	3.00e-09	1.42e-04	-1.52e-02	-1.20e-02	1.06e+00	-1.78e-01	2.56e-01	1.53e-01	8.93e-01
Std	1.50e-08	3.73e-05	1.78e-02	7.25e-02	4.54e-01	2.07e-01	8.41e-02	1.07e-01	5.35e-02

Table A.6: Healer R2; inspiratory volume regression (order 2) coefficients and dispersion statistics for all the participants.

Subject	Slope	Intercept	MAE	MSE	R^2
1	8.11e-01	2.34e+02	1.21e+02	6.98e+04	8.66e-01
2	8.69e-01	7.55e+01	1.29e+02	3.95e+04	9.59e-01
3	5.95e-01	5.27e+02	2.44e+02	1.45e+05	6.77e-01
4	5.49e-01	5.09e+02	1.53e+02	7.76e+04	6.77e-01
5	8.78e-01	5.27e+01	2.10e+02	1.50e+05	8.73e-01
6	1.04e+00	4.60e+01	1.04e+02	2.12e+04	9.60e-01
7	6.72e-01	3.99e+02	1.18e+02	3.09e+04	8.60e-01
8	8.56e-01	-2.79e+01	2.64e+02	1.56e+05	9.36e-01
9	8.12e-01	1.95e+02	1.97e+02	9.09e+04	9.23e-01
10	4.87e-01	8.79e+02	3.54e+02	2.31e+05	5.79e-01
11	8.81e-01	1.14e+02	8.71e+01	1.43e+04	9.18e-01
12	7.66e-01	1.92e+02	2.13e+02	1.52e+05	8.50e-01
13	9.50e-01	1.11e+02	2.06e+02	1.11e+05	9.73e-01
Mean	7.82e-01	2.54e+02	1.85e+02	9.92e+04	8.50e-01
Std	1.56e-01	2.47e+02	7.30e+01	6.27e+04	1.21e-01

Table A.7: Healer R2; inspiratory time linear regression (order 1) coefficients and dispersion statistics for all the participants.

Subject	Slope	Intercept	MAE	MSE	R^2
1	9.74e-01	6.87e-01	9.09e-01	2.38e+00	9.67e-01
2	1.00e+00	-3.98e-02	2.46e-01	1.67e-01	9.93e-01
3	9.96e-01	8.50e-02	6.12e-01	9.46e-01	9.79e-01
4	9.85e-01	2.68e-01	5.63e-01	7.17e-01	9.74e-01
5	9.08e-01	2.32e+00	2.11e+00	1.28e+01	8.37e-01
6	9.90e-01	2.41e-01	7.80e-01	1.33e+00	9.80e-01
7	9.90e-01	2.09e-01	6.77e-01	9.91e-01	9.76e-01
8	9.95e-01	1.06e-01	8.48e-01	2.40e+00	9.51e-01
9	9.92e-01	1.16e-01	5.26e-01	1.01e+00	9.76e-01
10	9.91e-01	5.54e-02	5.39e-01	7.18e-01	9.85e-01
11	9.88e-01	2.81e-01	8.04e-01	1.41e+00	9.76e-01
12	9.89e-01	3.61e-01	1.21e+00	5.35e+00	9.26e-01
13	9.82e-01	3.00e-01	8.33e-01	1.70e+00	9.68e-01
Mean	9.83e-01	3.84e-01	8.20e-01	2.46e+00	9.61e-01
Std	2.28e-02	5.85e-01	4.35e-01	3.25e+00	3.92e-02

Table A.8: Healer R2; respiratory rate linear regression (order 1) coefficients and dispersion statistics for all the participants.

Subject	**Slope**$_{Abs}$	**Intercept**$_{Abs}$	**Slope**$_{Norm}$	**Intercept**$_{Norm}$	**MAE**	**MSE**	**R**^{2}
1	1.04e-04	-6.17e-03	7.49e-01	-1.21e-01	3.98e-01	2.69e-01	7.30e-01
2	1.24e-04	-2.28e-02	6.74e-01	-1.69e-01	3.09e-01	1.52e-01	7.52e-01
3	1.07e-04	-1.45e-02	6.64e-01	-1.33e-01	2.41e-01	1.03e-01	8.02e-01
4	1.10e-04	-2.04e-02	5.16e-01	-2.13e-01	3.49e-01	1.69e-01	7.10e-01
5	1.07e-04	-4.10e-03	8.42e-01	-6.42e-02	3.94e-01	3.00e-01	8.55e-01
6	1.60e-04	-4.32e-02	2.31e+00	-2.62e+00	2.11e+00	6.97e+00	7.09e-01
7	8.65e-05	-1.91e-02	9.64e-01	-5.70e-01	5.70e-01	5.13e-01	8.93e-01
8	1.14e-04	3.56e-03	7.68e-01	4.68e-02	2.36e-01	1.22e-01	8.19e-01
9	8.05e-05	-7.84e-03	7.30e-01	-6.98e-02	2.99e-01	1.54e-01	7.04e-01
10	8.78e-05	4.34e-02	3.47e-01	2.49e-01	2.00e-01	7.26e-02	7.69e-01
11	-	-	-	-	-	-	-
12	7.11e-05	-4.97e-03	6.30e-01	-7.96e-02	4.63e-01	4.31e-01	5.50e-01
13	1.17e-04	5.80e-03	5.65e-01	5.97e-02	4.22e-01	2.92e-01	6.27e-01
Mean	9.76e-05	-6.94e-03	8.13e-01	-3.07e-01	4.99e-01	7.96e-01	7.43e-01
Std	3.55e-05	1.92e-02	4.77e-01	7.22e-01	4.97e-01	1.87e+00	9.12e-02

Table A.9: Healer R3; inspiratory volume linear regression (order 1) coefficients and dispersion statistics for all the participants.

Subjects	Coeff.deg.2$_{Abs}$	Coeff.deg.1$_{Abs}$	Coeff.deg.0$_{Abs}$	Coeff.deg.2$_{Norm}$	Coeff.deg.1$_{Norm}$	Coeff.deg.0$_{Norm}$	MAE	MSE	R^2
1	4.80e-08	-9.91e-06	3.49e-02	1.27e-01	-7.16e-02	6.88e-01	2.74e-01	1.61e-01	8.38e-01
2	5.05e-08	-4.18e-05	7.50e-02	2.01e-01	-2.27e-01	5.57e-01	2.02e-01	7.89e-02	8.71e-01
3	2.15e-08	2.92e-05	3.29e-02	8.99e-02	1.80e-01	3.01e-01	2.07e-01	8.69e-02	8.33e-01
4	4.23e-08	-4.72e-05	6.62e-02	8.89e-02	-2.21e-01	6.92e-01	2.50e-01	1.07e-01	8.16e-01
5	-1.35e-08	1.55e-04	-2.41e-02	-5.34e-02	1.22e+00	-3.77e-01	3.83e-01	2.80e-01	8.65e-01
6	8.11e-08	-1.85e-05	1.66e-02	2.77e-01	-2.67e-01	1.01e+00	1.14e+00	3.78e+00	8.42e-01
7	2.03e-08	9.79e-06	2.04e-02	8.45e-02	1.09e-01	6.11e-01	2.20e-01	1.35e-01	9.72e-01
8	2.38e-08	6.14e-05	2.28e-02	8.19e-02	4.13e-01	2.99e-01	2.00e-01	1.09e-01	8.39e-01
9	1.63e-08	1.76e-05	3.84e-02	1.50e-01	1.60e-01	3.42e-01	2.85e-01	1.40e-01	7.31e-01
10	5.30e-09	6.77e-05	5.67e-02	1.45e-02	2.67e-01	3.26e-01	1.99e-01	7.18e-02	7.72e-01
11	-	-	-	-	-	-	-	-	-
12	1.55e-08	2.56e-05	1.90e-02	7.58e-02	2.27e-01	3.05e-01	4.11e-01	4.08e-01	5.74e-01
13	4.14e-08	-8.38e-06	7.19e-02	9.45e-02	-4.06e-02	7.39e-01	3.30e-01	2.41e-01	6.93e-01
Mean	2.71e-08	1.85e-05	3.31e-02	1.03e-01	1.46e-01	4.58e-01	3.41e-01	4.66e-01	8.04e-01
Std	2.41e-08	5.15e-05	2.78e-02	8.01e-02	3.85e-01	3.32e-01	2.50e-01	1.00e+00	9.71e-02

Table A.10: Healer R3; inspiratory volume regression (order 2) coefficients and dispersion statistics for all the participants.

Subject	Slope	Intercept	MAE	MSE	R^2
1	6.90e-01	2.94e+02	1.17e+02	4.59e+04	8.29e-01
2	8.38e-01	2.33e+02	2.14e+02	1.02e+05	9.07e-01
3	7.41e-01	3.79e+02	2.61e+02	2.04e+05	7.14e-01
4	5.36e-01	5.19e+02	1.26e+02	4.26e+04	8.25e-01
5	7.73e-01	1.59e+02	3.04e+02	3.45e+05	7.74e-01
6	9.27e-01	1.91e+02	1.13e+02	2.94e+04	9.15e-01
7	8.24e-01	2.58e+02	1.30e+02	3.38e+04	8.98e-01
8	6.14e-01	4.82e+02	2.10e+02	1.18e+05	7.80e-01
9	7.82e-01	3.86e+02	2.77e+02	2.38e+05	8.27e-01
10	6.20e-01	6.56e+02	3.09e+02	1.95e+05	5.48e-01
11	-	-	-	-	-
12	7.95e-01	2.25e+02	2.81e+02	2.71e+05	8.19e-01
13	9.64e-01	1.01e+02	3.27e+02	3.71e+05	9.48e-01
Mean	7.59e-01	3.24e+02	2.22e+02	1.66e+05	8.15e-01
Std	1.22e-01	1.58e+02	7.87e+01	1.17e+05	1.03e-01

Table A.11: Healer R3; inspiratory time linear regression (order 1) coefficients and dispersion statistics for all the participants.

Subject	Slope	Intercept	MAE	MSE	R^2
1	9.81e-01	5.76e-01	1.29e+00	4.44e+00	9.66e-01
2	1.00e+00	1.74e-02	3.44e-01	2.41e-01	9.89e-01
3	9.99e-01	4.69e-02	4.80e-01	6.17e-01	9.86e-01
4	9.87e-01	2.53e-01	7.85e-01	1.19e+00	9.78e-01
5	9.62e-01	7.70e-01	1.35e+00	5.93e+00	9.33e-01
6	9.73e-01	7.11e-01	1.14e+00	3.84e+00	9.48e-01
7	9.80e-01	2.98e-01	5.77e-01	8.92e-01	9.80e-01
8	9.80e-01	3.34e-01	8.05e-01	1.61e+00	9.58e-01
9	9.18e-01	1.06e+00	6.66e-01	1.61e+00	9.53e-01
10	9.78e-01	2.62e-01	5.95e-01	1.87e+00	9.70e-01
11	-	-	-	-	-
12	9.61e-01	8.82e-01	1.29e+00	6.30e+00	8.93e-01
13	9.76e-01	3.97e-01	9.37e-01	2.11e+00	9.67e-01
Mean	9.75e-01	4.67e-01	8.56e-01	2.55e+00	9.60e-01
Std	2.06e-02	3.16e-01	3.31e-01	1.98e+00	2.55e-02

Table A.12: Healer R3; respiratory rate linear regression (order 1) coefficients and dispersion statistics for all the participants.

A.2. Data pooled by breathing in static or dynamic exercises

Subject	Slope_{Abs}	Intercept_{Abs}	Slope_{Norm}	Intercept_{Norm}	MAE	MSE	R^2
1	2.41e-04	-6.53e-03	1.10e+00	-6.99e-02	2.06e-01	7.11e-02	7.75e-01
2	9.38e-05	-3.23e-03	9.71e-01	-5.02e-02	3.32e-01	1.87e-01	3.59e-01
3	1.08e-04	-2.31e-02	1.61e+00	-4.52e-01	2.74e-01	1.18e-01	7.84e-01
4	5.78e-05	1.93e-02	2.63e-01	3.88e-01	5.80e-01	4.37e-01	6.57e-02
5	9.21e-05	1.03e-03	6.71e-01	2.49e-02	4.56e-01	3.22e-01	4.57e-01
6	2.87e-04	-3.32e-02	1.67e+00	-4.67e-01	3.42e-01	1.84e-01	8.64e-01
7	1.12e-04	9.49e-03	7.75e-01	1.52e-01	2.81e-01	1.32e-01	3.87e-01
8	1.85e-04	1.22e-02	7.20e-01	7.48e-02	1.37e-01	4.09e-02	4.61e-01
9	1.16e-04	-6.30e-02	1.50e+00	-6.41e-01	2.50e-01	9.98e-02	8.37e-01
10	1.00e-04	5.39e-02	9.60e-01	4.16e-01	2.25e-01	7.78e-02	6.69e-01
11	4.69e-05	4.46e-02	6.01e-01	9.84e-01	8.05e-01	9.34e-01	2.16e-02
12	1.23e-04	-1.09e-02	1.02e+00	-6.76e-02	1.75e-01	5.34e-02	6.19e-01
13	1.90e-04	2.07e-02	1.10e+00	1.52e-01	1.51e-01	3.79e-02	7.43e-01
Mean	1.35e-04	1.63e-03	9.97e-01	3.42e-02	3.24e-01	2.07e-01	5.42e-01
Std	6.79e-05	3.00e-02	3.95e-01	4.09e-01	1.83e-01	2.38e-01	2.68e-01

Table A.13: Healer R1; inspiratory volume linear regression (order 1) coefficients and dispersion statistics for all the participants in static conditions.

Subject	Slope	Intercept	MAE	MSE	R^2
1	7.29e-01	3.78e+02	1.07e+02	2.29e+04	6.93e-01
2	6.79e-01	6.61e+02	1.98e+02	5.55e+04	8.16e-01
3	5.77e-01	6.52e+02	1.85e+02	7.53e+04	6.58e-01
4	5.40e-01	5.77e+02	1.62e+02	4.78e+04	4.21e-01
5	4.59e-01	6.95e+02	1.37e+02	3.36e+04	5.16e-01
6	1.02e+00	1.51e+02	1.04e+02	1.93e+04	7.72e-01
7	7.04e-01	3.35e+02	1.19e+02	3.12e+04	8.56e-01
8	7.74e-01	1.27e+02	1.59e+02	5.18e+04	8.61e-01
9	6.39e-01	5.02e+02	2.47e+02	1.15e+05	7.62e-01
10	5.16e-01	8.92e+02	3.49e+02	2.02e+05	6.22e-01
11	6.93e-01	2.59e+02	1.82e+02	5.91e+04	6.62e-01
12	7.89e-01	3.02e+02	1.95e+02	7.84e+04	8.38e-01
13	6.78e-01	5.62e+02	2.30e+02	9.97e+04	8.13e-01
Mean	6.76e-01	4.69e+02	1.83e+02	6.86e+04	7.15e-01
Std	1.37e-01	2.21e+02	6.40e+01	4.74e+04	1.31e-01

Table A.14: Healer R1; inspiratory time linear regression (order 1) coefficients and dispersion statistics for all the participants in static conditions.

Subject	Slope	Intercept	MAE	MSE	R^2
1	9.80e-01	4.35e-01	5.61e-01	6.89e-01	9.88e-01
2	9.93e-01	8.55e-02	2.26e-01	8.90e-02	9.94e-01
3	1.01e+00	-1.15e-01	2.54e-01	2.22e-01	9.87e-01
4	9.84e-01	3.20e-01	5.60e-01	7.58e-01	9.76e-01
5	9.72e-01	5.10e-01	6.11e-01	7.86e-01	9.80e-01
6	9.95e-01	9.27e-02	5.77e-01	1.14e+00	9.91e-01
7	9.68e-01	5.66e-01	6.68e-01	1.19e+00	9.76e-01
8	9.88e-01	1.97e-01	4.86e-01	5.10e-01	9.77e-01
9	9.47e-01	5.89e-01	5.57e-01	1.02e+00	9.49e-01
10	9.84e-01	2.09e-01	5.60e-01	1.23e+00	9.56e-01
11	1.00e+00	-1.28e-02	5.31e-01	7.69e-01	9.86e-01
12	9.96e-01	7.66e-02	4.50e-01	7.37e-01	9.80e-01
13	9.79e-01	2.79e-01	4.93e-01	9.74e-01	9.37e-01
Mean	9.85e-01	2.49e-01	5.03e-01	7.78e-01	9.75e-01
Std	1.58e-02	2.17e-01	1.24e-01	3.36e-01	1.66e-02

Table A.15: Healer R1; breathing rate linear regression (order 1) coefficients and dispersion statistics for all the participants in static conditions.

Subject	Slope_{Abs}	Intercept_{Abs}	Slope_{Norm}	Intercept_{Norm}	MAE	MSE	R^2
1	1.82e-04	-1.60e-02	1.05e+00	-2.27e-01	1.72e-01	6.09e-02	8.28e-01
2	1.64e-04	-2.77e-02	1.08e+00	-2.49e-01	1.85e-01	6.34e-02	7.07e-01
3	1.55e-04	-8.53e-03	7.44e-01	-6.20e-02	1.91e-01	5.98e-02	7.07e-01
4	9.61e-05	7.97e-03	7.30e-01	1.44e-01	2.42e-01	8.08e-02	4.80e-01
5	1.50e-04	-1.30e-02	9.87e-01	-1.62e-01	3.26e-01	1.75e-01	6.06e-01
6	2.91e-04	-3.16e-02	1.36e+00	-4.24e-01	2.11e-01	7.55e-02	8.83e-01
7	9.09e-05	-1.46e-03	9.42e-01	-3.14e-02	1.65e-01	4.70e-02	6.22e-01
8	1.34e-04	-5.14e-03	1.08e+00	-1.32e-01	3.71e-01	2.75e-01	6.83e-01
9	1.12e-04	-1.70e-03	7.29e-01	-1.02e-02	1.78e-01	5.40e-02	7.73e-01
10	4.88e-05	1.83e-02	9.76e-01	2.24e-01	1.92e-01	6.14e-02	7.40e-01
11	9.81e-05	1.07e-03	1.02e+00	2.85e-02	1.74e-01	7.61e-02	6.74e-01
12	1.22e-04	-1.90e-02	7.19e-01	-1.51e-01	1.18e-01	3.54e-02	7.77e-01
13	2.13e-04	-1.39e-02	1.11e+00	-1.41e-01	1.54e-01	3.79e-02	7.63e-01
Mean	1.43e-04	-8.50e-03	9.64e-01	-9.18e-02	2.06e-01	8.48e-02	7.11e-01
Std	5.97e-05	1.33e-02	1.83e-01	1.63e-01	6.72e-02	6.43e-02	9.98e-02

Table A.16: Healer R2; inspiratory volume linear regression (order 1) coefficients and dispersion statistics for all the participants in static conditions.

Subject	Slope	Intercept	MAE	MSE	R^2
1	8.04e-01	2.73e+02	9.43e+01	2.66e+04	7.45e-01
2	8.72e-01	5.40e+01	1.33e+02	3.50e+04	8.95e-01
3	4.10e-01	8.31e+02	2.58e+02	1.12e+05	5.25e-01
4	5.97e-01	4.00e+02	9.82e+01	1.74e+04	7.84e-01
5	5.87e-01	3.88e+02	1.38e+02	4.61e+04	5.44e-01
6	8.90e-01	2.72e+02	7.74e+01	9.18e+03	8.40e-01
7	6.23e-01	4.84e+02	1.23e+02	3.01e+04	8.37e-01
8	6.27e-01	2.67e+02	2.06e+02	9.29e+04	7.38e-01
9	7.15e-01	3.32e+02	2.00e+02	8.32e+04	8.42e-01
10	5.19e-01	7.27e+02	3.34e+02	1.94e+05	6.90e-01
11	8.86e-01	1.25e+02	7.42e+01	9.32e+03	9.37e-01
12	8.02e-01	8.85e+01	2.04e+02	1.00e+05	8.20e-01
13	8.05e-01	3.78e+02	2.52e+02	1.63e+05	7.10e-01
Mean	7.03e-01	3.55e+02	1.69e+02	7.07e+04	7.62e-01
Std	1.48e-01	2.19e+02	7.75e+01	5.74e+04	1.19e-01

Table A.17: Healer R2; inspiratory time linear regression (order 1) coefficients and dispersion statistics for all the participants in static conditions.

Subject	Slope	Intercept	MAE	MSE	R^2
1	9.77e-01	5.40e-01	7.65e-01	1.57e+00	9.77e-01
2	9.87e-01	1.47e-01	2.30e-01	2.01e-01	9.87e-01
3	9.75e-01	3.68e-01	4.64e-01	8.08e-01	9.72e-01
4	9.83e-01	3.14e-01	5.73e-01	7.41e-01	9.65e-01
5	9.14e-01	2.01e+00	1.54e+00	6.31e+00	8.93e-01
6	9.76e-01	4.81e-01	4.19e-01	3.20e-01	9.85e-01
7	9.77e-01	3.78e-01	5.84e-01	9.16e-01	9.75e-01
8	9.95e-01	1.31e-01	1.16e+00	3.82e+00	9.35e-01
9	9.94e-01	9.61e-02	4.61e-01	4.67e-01	9.84e-01
10	9.94e-01	2.38e-02	7.22e-01	1.10e+00	9.85e-01
11	9.77e-01	4.45e-01	5.42e-01	7.00e-01	9.86e-01
12	9.97e-01	2.31e-01	1.21e+00	6.80e+00	8.35e-01
13	9.90e-01	1.39e-01	6.04e-01	1.09e+00	9.71e-01
Mean	9.80e-01	4.08e-01	7.14e-01	1.91e+00	9.58e-01
Std	2.04e-02	4.89e-01	3.57e-01	2.17e+00	4.36e-02

Table A.18: Healer R2; breathing rate linear regression (order 1) coefficients and dispersion statistics for all the participants in static conditions.

Subject	Slope_{Abs}	Intercept_{Abs}	Slope_{Norm}	Intercept_{Norm}	MAE	MSE	R^2
1	1.71e-04	-1.81e-02	1.21e+00	-3.50e-01	2.10e-01	7.06e-02	6.94e-01
2	1.12e-04	6.18e-03	6.07e-01	4.58e-02	1.72e-01	4.62e-02	4.16e-01
3	1.30e-04	-9.80e-03	8.21e-01	-8.98e-02	1.62e-01	5.02e-02	7.03e-01
4	1.19e-04	-5.83e-04	5.58e-01	-6.09e-03	2.47e-01	8.37e-02	3.62e-01
5	1.39e-04	-2.03e-02	1.06e+00	-2.28e-01	2.41e-01	1.05e-01	6.66e-01
6	1.52e-04	-1.34e-02	2.18e+00	-8.13e-01	7.22e-01	9.78e-01	8.46e-01
7	7.66e-05	-1.98e-03	8.34e-01	-5.68e-02	1.62e-01	4.22e-02	7.53e-01
8	1.56e-04	-3.64e-03	1.21e+00	-5.55e-02	1.49e-01	3.76e-02	8.32e-01
9	9.91e-05	-9.66e-03	9.00e-01	-8.60e-02	2.23e-01	7.18e-02	7.50e-01
10	1.01e-04	3.63e-02	3.97e-01	2.08e-01	1.77e-01	5.39e-02	7.75e-01
11	-	-	-	-	-	-	-
12	1.03e-04	-1.07e-02	9.11e-01	-1.71e-01	4.04e-01	2.94e-01	6.00e-01
13	1.93e-04	3.34e-03	9.36e-01	3.45e-02	2.80e-01	1.35e-01	5.60e-01
Mean	1.29e-04	-3.53e-03	9.69e-01	-1.31e-01	2.62e-01	1.64e-01	6.63e-01
Std	3.26e-05	1.43e-02	4.34e-01	2.46e-01	1.54e-01	2.55e-01	1.47e-01

Table A.19: Healer R3; inspiratory volume linear regression (order 1) coefficients and dispersion statistics for all the participants in static conditions.

Subject	Slope	Intercept	MAE	MSE	R^2
1	7.35e-01	2.40e+02	9.09e+01	1.47e+04	8.22e-01
2	7.39e-01	4.55e+02	1.84e+02	6.02e+04	8.56e-01
3	5.85e-01	6.77e+02	2.39e+02	1.39e+05	6.00e-01
4	6.33e-01	3.47e+02	1.15e+02	2.45e+04	8.25e-01
5	3.73e-01	7.00e+02	2.40e+02	1.32e+05	3.34e-01
6	8.40e-01	3.31e+02	9.08e+01	1.43e+04	6.72e-01
7	7.75e-01	3.10e+02	1.21e+02	3.06e+04	9.09e-01
8	4.47e-01	6.87e+02	1.64e+02	6.34e+04	5.80e-01
9	4.48e-01	1.21e+03	3.08e+02	1.77e+05	5.42e-01
10	6.57e-01	5.90e+02	2.85e+02	1.72e+05	5.83e-01
11	-	-	-	-	-
12	6.62e-01	4.76e+02	2.92e+02	1.93e+05	6.88e-01
13	5.65e-01	9.28e+02	4.61e+02	4.40e+05	5.19e-01
Mean	6.22e-01	5.79e+02	2.16e+02	1.22e+05	6.61e-01
Std	1.38e-01	2.71e+02	1.06e+02	1.16e+05	1.61e-01

Table A.20: Healer R3; inspiratory time linear regression (order 1) coefficients and dispersion statistics for all the participants in static conditions.

Subject	Slope	Intercept	MAE	MSE	R^2
1	9.92e-01	2.39e-01	8.80e-01	1.80e+00	9.89e-01
2	9.94e-01	8.25e-02	2.96e-01	1.72e-01	9.93e-01
3	1.01e+00	-8.45e-02	3.41e-01	4.08e-01	9.71e-01
4	9.70e-01	4.73e-01	6.64e-01	9.80e-01	9.67e-01
5	9.52e-01	1.03e+00	1.43e+00	6.35e+00	9.17e-01
6	9.72e-01	5.93e-01	6.53e-01	1.27e+00	9.60e-01
7	9.71e-01	4.74e-01	5.52e-01	9.54e-01	9.85e-01
8	9.70e-01	5.05e-01	8.99e-01	2.08e+00	9.46e-01
9	9.70e-01	3.68e-01	4.07e-01	5.64e-01	9.56e-01
10	9.77e-01	2.94e-01	7.56e-01	2.69e+00	9.66e-01
11	-	-	-	-	-
12	9.88e-01	3.02e-01	9.79e-01	3.57e+00	8.98e-01
13	9.66e-01	4.31e-01	5.77e-01	8.98e-01	9.75e-01
Mean	9.77e-01	3.93e-01	7.03e-01	1.81e+00	9.60e-01
Std	1.45e-02	2.65e-01	3.03e-01	1.67e+00	2.72e-02

Table A.21: Healer R3; breathing rate linear regression (order 1) coefficients and dispersion statistics for all the participants in static conditions.

Subject	Slope_{Abs}	Intercept_{Abs}	Slope_{Norm}	Intercept_{Norm}	MAE	MSE	R^2
1	1.17e-04	-9.71e-03	5.35e-01	-1.04e-01	1.71e-01	4.77e-02	6.06e-01
2	7.88e-05	-3.15e-03	8.15e-01	-4.89e-02	2.67e-01	1.10e-01	4.06e-01
3	7.64e-05	-2.91e-02	1.14e+00	-5.70e-01	2.06e-01	1.29e-01	5.60e-01
4	6.31e-05	-2.39e-02	2.88e-01	-4.82e-01	1.29e-01	2.62e-02	6.22e-01
5	1.12e-04	-3.41e-02	8.19e-01	-8.29e-01	3.54e-01	2.18e-01	8.16e-01
6	1.72e-04	-5.55e-02	1.00e+00	-7.80e-01	2.38e-01	1.13e-01	7.91e-01
7	6.07e-05	6.22e-04	4.19e-01	9.97e-03	1.12e-01	2.16e-02	7.58e-01
8	1.53e-04	3.17e-02	5.95e-01	1.94e-01	1.70e-01	4.42e-02	3.91e-01
9	8.34e-05	-4.37e-02	1.09e+00	-4.44e-01	2.26e-01	8.63e-02	7.99e-01
10	1.15e-04	8.71e-02	1.10e+00	6.72e-01	1.87e-01	5.79e-02	7.21e-01
11	1.52e-04	-7.89e-03	1.95e+00	-1.74e-01	4.28e-01	2.99e-01	7.34e-01
12	5.32e-05	-1.83e-02	4.41e-01	-1.13e-01	8.13e-02	1.33e-02	7.07e-01
13	1.76e-04	-7.71e-03	1.02e+00	-5.69e-02	1.28e-01	2.89e-02	7.63e-01
Mean	1.09e-04	-8.73e-03	8.62e-01	-2.10e-01	2.07e-01	9.19e-02	6.67e-01
Std	4.16e-05	3.48e-02	4.21e-01	3.95e-01	9.42e-02	8.12e-02	1.37e-01

Table A.22: Healer R1; inspiratory volume linear regression (order 1) coefficients and dispersion statistics for all the participants in dynamic conditions.

Subject	Slope	Intercept	MAE	MSE	R^2
1	7.58e-01	2.83e+02	1.11e+02	2.68e+04	5.47e-01
2	9.09e-01	5.06e+01	1.47e+02	4.78e+04	9.19e-01
3	9.01e-01	8.42e+01	1.73e+02	7.25e+04	7.22e-01
4	6.68e-01	3.44e+02	1.26e+02	3.22e+04	8.24e-01
5	5.87e-01	5.40e+02	1.88e+02	8.25e+04	3.36e-01
6	9.98e-01	9.05e+01	1.03e+02	1.81e+04	8.93e-01
7	7.34e-01	4.22e+02	1.30e+02	3.28e+04	5.84e-01
8	8.39e-01	1.95e+02	1.12e+02	2.85e+04	8.09e-01
9	8.65e-01	4.99e+01	3.08e+02	1.59e+05	6.24e-01
10	6.88e-01	3.86e+02	2.64e+02	1.15e+05	6.20e-01
11	8.18e-01	2.00e+02	1.32e+02	3.01e+04	6.10e-01
12	8.30e-01	1.67e+02	1.76e+02	6.29e+04	7.72e-01
13	7.38e-01	3.86e+02	1.38e+02	4.13e+04	4.41e-01
Mean	7.95e-01	2.46e+02	1.62e+02	5.77e+04	6.69e-01
Std	1.09e-01	1.53e+02	5.92e+01	3.95e+04	1.67e-01

Table A.23: Healer R1; inspiratory time linear regression (order 1) coefficients and dispersion statistics for all the participants in dynamic conditions.

Subject	Slope	Intercept	MAE	MSE	R^2
1	8.89e-01	3.40e+00	1.68e+00	5.94e+00	8.34e-01
2	1.01e+00	-1.35e-01	4.97e-01	5.09e-01	9.73e-01
3	9.85e-01	4.13e-01	1.20e+00	3.17e+00	8.86e-01
4	9.86e-01	3.83e-01	1.19e+00	2.30e+00	9.22e-01
5	8.55e-01	3.34e+00	1.85e+00	7.22e+00	7.61e-01
6	9.79e-01	5.30e-01	1.02e+00	1.90e+00	9.66e-01
7	9.59e-01	8.61e-01	8.42e-01	1.31e+00	8.95e-01
8	9.94e-01	1.16e-01	5.21e-01	4.99e-01	9.59e-01
9	9.14e-01	7.96e-01	4.62e-01	4.76e-01	7.74e-01
10	9.56e-01	3.72e-01	2.30e-01	1.40e-01	9.75e-01
11	9.86e-01	4.51e-01	1.25e+00	3.41e+00	8.63e-01
12	9.86e-01	5.41e-01	1.70e+00	7.60e+00	8.64e-01
13	9.31e-01	1.45e+00	7.78e-01	9.80e-01	9.27e-01
Mean	9.56e-01	9.63e-01	1.02e+00	2.73e+00	8.92e-01
Std	4.46e-02	1.09e+00	5.00e-01	2.52e+00	6.90e-02

Table A.24: Healer R1; breathing rate linear regression (order 1) coefficients and dispersion statistics for all the participants in dynamic conditions.

Subject	Slope_{Abs}	Intercept_{Abs}	Slope_{Norm}	Intercept_{Norm}	MAE	MSE	R^2
1	1.71e-04	-3.07e-02	9.87e-01	-4.38e-01	1.94e-01	8.80e-02	7.39e-01
2	1.79e-04	-3.58e-02	1.18e+00	-3.22e-01	1.58e-01	3.97e-02	8.19e-01
3	1.44e-04	-1.71e-02	6.92e-01	-1.24e-01	8.20e-02	1.27e-02	8.50e-01
4	1.63e-04	-1.85e-02	1.24e+00	-3.34e-01	1.93e-01	6.24e-02	7.71e-01
5	1.34e-04	-3.09e-02	8.84e-01	-3.86e-01	1.99e-01	1.04e-01	7.88e-01
6	2.31e-04	-3.62e-02	1.08e+00	-4.86e-01	1.87e-01	6.26e-02	8.68e-01
7	1.30e-04	-3.12e-02	1.35e+00	-6.73e-01	1.74e-01	5.75e-02	8.79e-01
8	1.44e-04	5.91e-03	1.16e+00	1.51e-01	4.21e-01	3.29e-01	4.96e-01
9	1.43e-04	-2.24e-02	9.28e-01	-1.34e-01	1.13e-01	2.23e-02	8.94e-01
10	8.94e-05	7.12e-03	1.79e+00	8.71e-02	1.96e-01	5.63e-02	7.44e-01
11	1.24e-04	-1.90e-02	1.29e+00	-5.08e-01	3.32e-01	1.95e-01	7.52e-01
12	1.43e-04	-5.85e-02	8.48e-01	-4.67e-01	1.69e-01	5.05e-02	8.37e-01
13	1.73e-04	-3.21e-03	9.07e-01	-3.26e-02	1.59e-01	5.02e-02	7.20e-01
Mean	1.52e-04	-2.23e-02	1.10e+00	-2.82e-01	1.98e-01	8.69e-02	7.81e-01
Std	3.25e-05	1.75e-02	2.72e-01	2.41e-01	8.46e-02	8.23e-02	9.93e-02

Table A.25: Healer R2; inspiratory volume linear regression (order 1) coefficients and dispersion statistics for all the participants in dynamic conditions.

Subject	Slope	Intercept	MAE	MSE	R^2
1	5.93e-01	3.88e+02	6.66e+01	1.03e+04	5.42e-01
2	9.61e-01	-7.29e+01	7.04e+01	7.36e+03	9.38e-01
3	8.57e-01	2.33e+02	1.05e+02	1.89e+04	8.51e-01
4	7.81e-01	2.30e+02	6.31e+01	7.49e+03	9.05e-01
5	5.76e-01	3.70e+02	1.75e+02	8.16e+04	6.26e-01
6	8.61e-01	1.44e+02	6.31e+01	7.14e+03	8.42e-01
7	8.65e-01	1.44e+02	8.35e+01	1.24e+04	8.43e-01
8	9.39e-01	7.55e+01	7.70e+01	1.04e+04	8.55e-01
9	8.83e-01	1.55e+02	1.15e+02	4.10e+04	9.45e-01
10	7.77e-01	3.47e+02	1.74e+02	5.95e+04	6.99e-01
11	8.14e-01	1.61e+02	8.44e+01	1.32e+04	5.64e-01
12	8.60e-01	1.12e+02	1.22e+02	5.00e+04	6.62e-01
13	6.39e-01	4.33e+02	1.25e+02	2.78e+04	5.02e-01
Mean	8.00e-01	2.09e+02	1.02e+02	2.67e+04	7.52e-01
Std	1.20e-01	1.38e+02	3.75e+01	2.31e+04	1.52e-01

Table A.26: Healer R2; inspiratory time linear regression (order 1) coefficients and dispersion statistics for all the participants in dynamic conditions.

Subject	Slope	Intercept	MAE	MSE	R^2
1	8.75e-01	3.86e+00	1.13e+00	3.44e+00	8.24e-01
2	1.02e+00	-3.22e-01	2.81e-01	1.42e-01	9.85e-01
3	1.00e+00	3.64e-02	8.00e-01	1.16e+00	9.43e-01
4	9.54e-01	9.87e-01	5.59e-01	7.15e-01	9.50e-01
5	8.34e-01	4.73e+00	3.00e+00	2.26e+01	6.76e-01
6	9.66e-01	1.08e+00	1.19e+00	2.41e+00	9.33e-01
7	9.89e-01	2.96e-01	7.65e-01	9.84e-01	9.39e-01
8	9.80e-01	3.71e-01	4.26e-01	3.11e-01	9.67e-01
9	9.83e-01	3.02e-01	6.38e-01	1.65e+00	9.59e-01
10	9.63e-01	3.43e-01	2.31e-01	1.36e-01	9.83e-01
11	9.72e-01	8.77e-01	1.17e+00	2.34e+00	8.79e-01
12	9.55e-01	1.32e+00	1.31e+00	4.32e+00	8.74e-01
13	8.93e-01	2.39e+00	1.10e+00	2.40e+00	8.34e-01
Mean	9.53e-01	1.25e+00	9.70e-01	3.28e+00	9.04e-01
Std	5.11e-02	1.46e+00	6.81e-01	5.71e+00	8.33e-02

Table A.27: Healer R2; breathing rate linear regression (order 1) coefficients and dispersion statistics for all the participants in dynamic conditions.

Subject	Slope_{Abs}	Intercept_{Abs}	Slope_{Norm}	Intercept_{Norm}	MAE	MSE	R^2
1	9.20e-05	-2.18e-02	6.51e-01	-4.20e-01	1.35e-01	2.97e-02	8.54e-01
2	1.17e-04	-5.99e-02	6.35e-01	-4.45e-01	1.15e-01	2.19e-02	7.75e-01
3	7.04e-05	-1.75e-03	4.45e-01	-1.60e-02	9.14e-02	1.59e-02	6.20e-01
4	5.89e-05	-9.65e-03	2.76e-01	-1.01e-01	4.13e-02	3.10e-03	7.87e-01
5	-	-	-	-	-	-	-
6	5.30e-05	-9.93e-03	7.58e-01	-6.04e-01	2.15e-01	7.26e-02	8.18e-01
7	6.29e-05	-1.45e-02	6.86e-01	-4.16e-01	1.45e-01	3.61e-02	9.06e-01
8	1.25e-04	-2.47e-02	9.68e-01	-3.76e-01	1.76e-01	5.39e-02	7.57e-01
9	7.07e-05	-2.36e-02	6.42e-01	-2.10e-01	1.02e-01	2.01e-02	8.68e-01
10	5.83e-05	8.66e-02	2.30e-01	4.97e-01	1.24e-01	2.04e-02	4.11e-01
11	-	-	-	-	-	-	-
12	5.11e-05	-5.52e-03	4.52e-01	-8.85e-02	1.72e-01	1.08e-01	5.08e-01
13	1.30e-04	-4.31e-02	6.29e-01	-4.44e-01	1.23e-01	2.69e-02	7.92e-01
Mean	7.41e-05	-1.06e-02	5.31e-01	-2.19e-01	1.20e-01	3.40e-02	7.36e-01
Std	3.53e-05	3.37e-02	2.52e-01	2.87e-01	5.59e-02	2.94e-02	2.49e-01

Table A.28: Healer R3; inspiratory volume linear regression (order 1) coefficients and dispersion statistics for all the participants in dynamic conditions.

Subject	Slope	Intercept	MAE	MSE	R^2
1	7.71e-01	2.36e+02	1.01e+02	3.77e+04	5.37e-01
2	9.75e-01	-5.80e+01	1.12e+02	2.16e+04	9.09e-01
3	9.74e-01	7.08e+01	1.13e+02	2.67e+04	9.43e-01
4	8.75e-01	1.40e+02	6.89e+01	8.44e+03	7.31e-01
5	-	-	-	-	-
6	9.56e-01	1.06e+02	7.16e+01	1.10e+04	6.69e-01
7	8.06e-01	3.07e+02	1.18e+02	2.47e+04	8.17e-01
8	8.25e-01	2.70e+02	1.30e+02	3.27e+04	7.31e-01
9	9.21e-01	8.02e+01	1.29e+02	3.10e+04	9.42e-01
10	8.45e-01	1.69e+02	1.85e+02	5.93e+04	7.20e-01
11	-	-	-	-	-
12	6.20e-01	4.44e+02	2.06e+02	1.29e+05	5.50e-01
13	7.05e-01	4.20e+02	1.57e+02	4.47e+04	5.08e-01
Mean	7.73e-01	1.82e+02	1.16e+02	3.56e+04	7.32e-01
Std	2.55e-01	1.51e+02	5.24e+01	3.22e+04	2.49e-01

Table A.29: Healer R3; inspiratory time linear regression (order 1) coefficients and dispersion statistics for all the participants in dynamic conditions.

Subject	Slope	Intercept	MAE	MSE	R^2
1	8.48e-01	4.85e+00	1.99e+00	8.52e+00	7.13e-01
2	1.02e+00	-2.64e-01	4.31e-01	3.61e-01	9.53e-01
3	9.97e-01	9.67e-02	6.37e-01	8.76e-01	9.71e-01
4	9.25e-01	2.12e+00	9.04e-01	1.38e+00	8.69e-01
5	-	-	-	-	-
6	9.06e-01	3.24e+00	1.68e+00	6.46e+00	8.29e-01
7	9.81e-01	3.68e-01	6.06e-01	7.91e-01	9.26e-01
8	9.89e-01	2.14e-01	7.31e-01	1.07e+00	9.52e-01
9	8.80e-01	1.86e+00	1.01e+00	3.06e+00	9.39e-01
10	9.95e-01	5.33e-02	1.90e-01	8.52e-02	9.87e-01
11	-	-	-	-	-
12	9.09e-01	2.29e+00	1.59e+00	8.21e+00	7.89e-01
11	9.05e-01	2.15e+00	1.28e+00	3.18e+00	8.28e-01
Mean	9.41e-01	1.41e+00	9.21e-01	2.83e+00	8.87e-01
Std	1.65e-01	1.53e+00	5.89e-01	3.02e+00	2.58e-01

Table A.30: Healer R3; breathing rate linear regression (order 1) coefficients and dispersion statistics for all the participants in dynamic conditions.

B | Appendix B: Bland-Altman plots of Pooled data

B.1. Pooled analysis on the three L.I.F.E. devices and intra-subject variability.

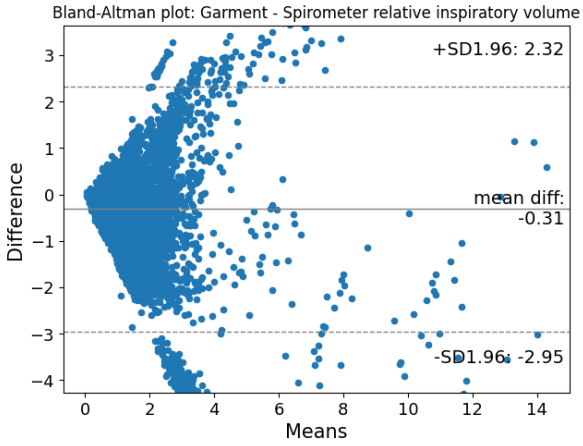

(a) Relative ΔV_{insp}

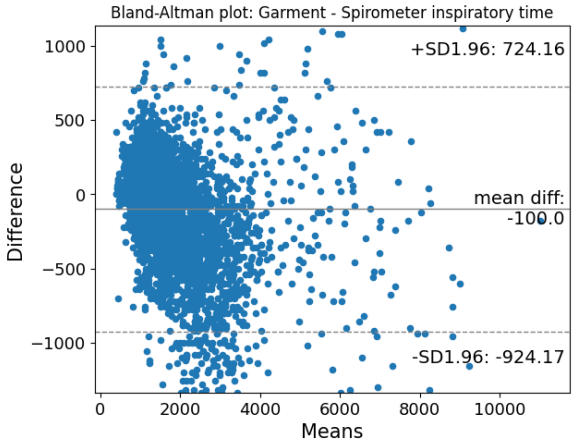

(b) T_{insp}

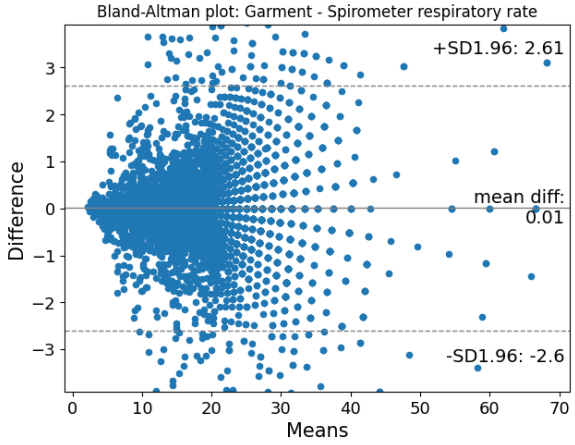

(c) f_B

Figure B.1: Bland-Altman plots of the parameters of interest relative to L.I.F.E. Healer R1 garment and to all subjects.

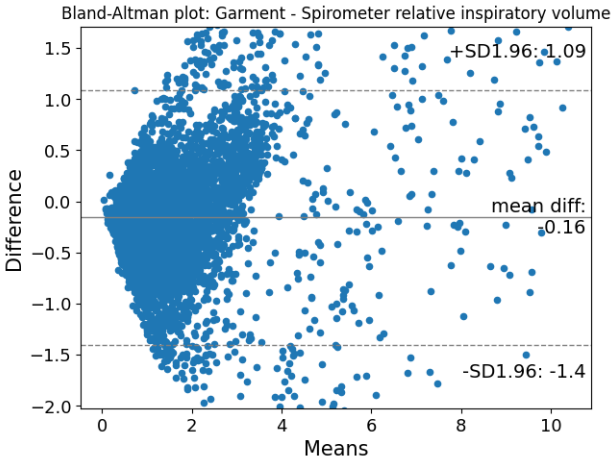

(a) Relative ΔV_{insp}

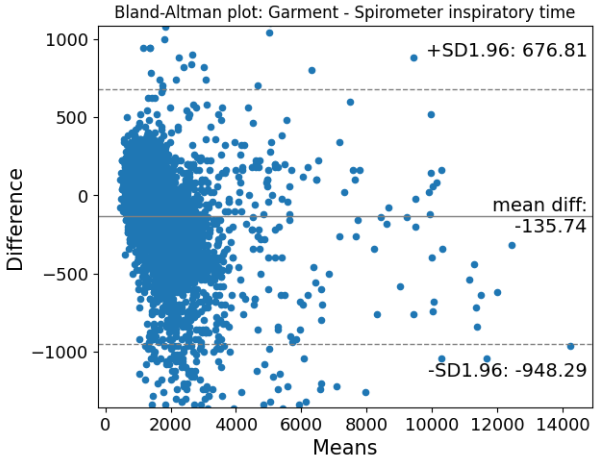

(b) T_{insp}

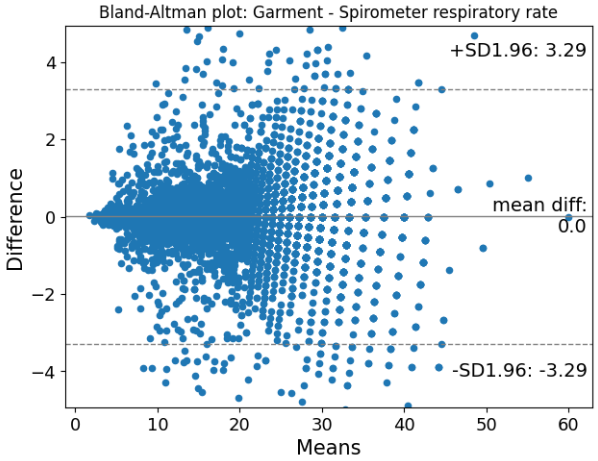

(c) f_B

Figure B.2: Bland-Altman plots of the parameters of interest relative to L.I.F.E. Healer R2 garment and to all subjects.

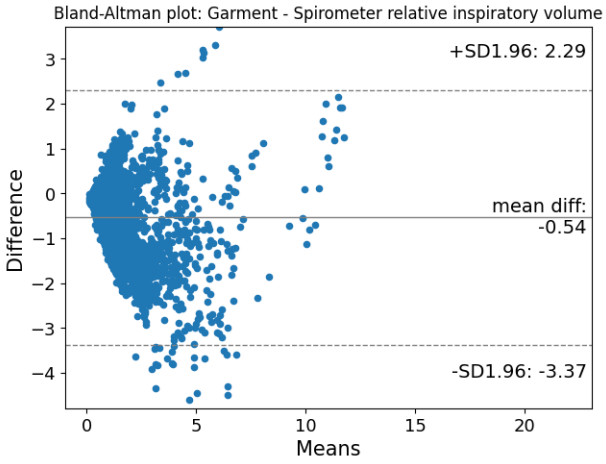

(a) Relative ΔV_{insp}

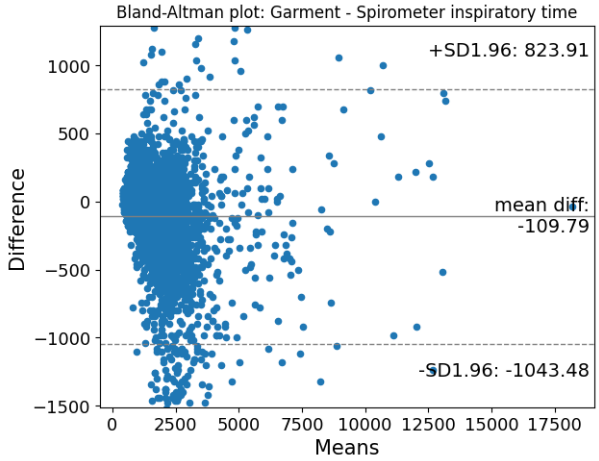

(b) T_{insp}

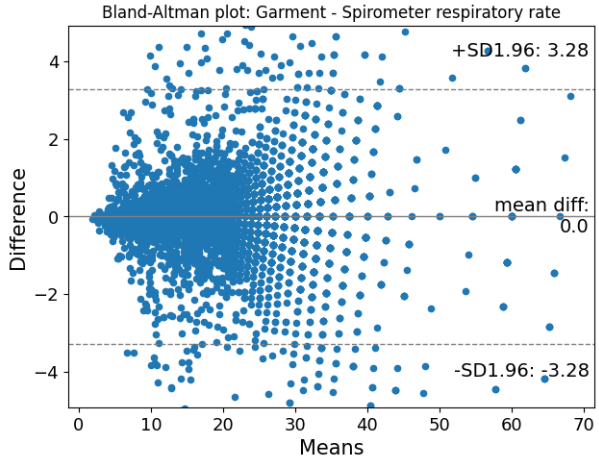

(c) f_B

Figure B.3: Bland-Altman plots of the parameters of interest relative to L.I.F.E. Healer R3 garment and to all subjects.

B.2. Data pooled by breathing in static or dynamic exercises

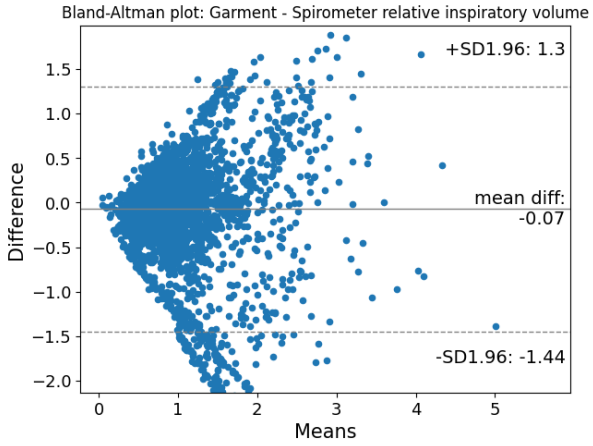

(a) Relative ΔV_{insp}

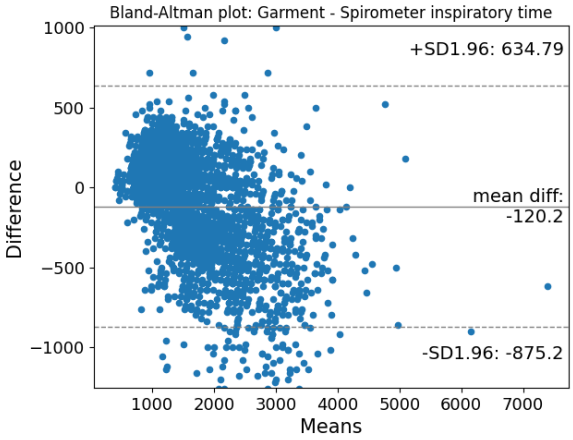

(b) T_{insp}

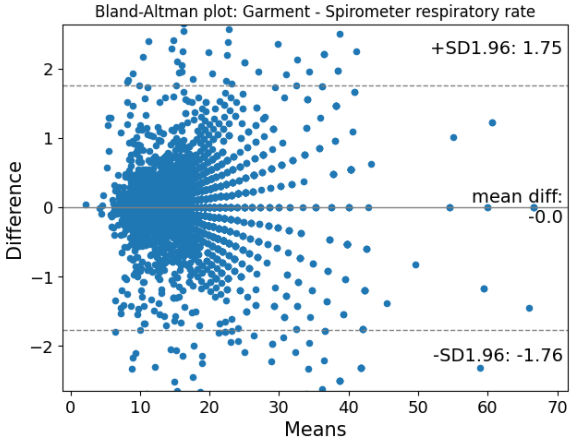

(c) f_B

Figure B.4: Bland-Altman plots of the parameters of interest relative to L.I.F.E. Healer R1 garment and to all subjects under static exercises conditions, excluding inspiratory and expiratory maneuvers-related breaths.

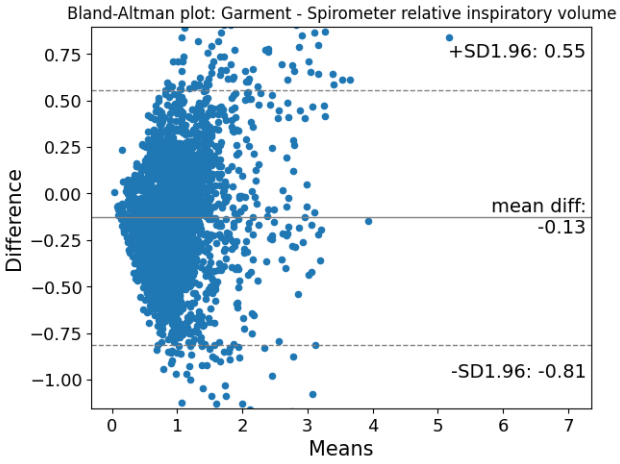

(a) Relative ΔV_{insp}

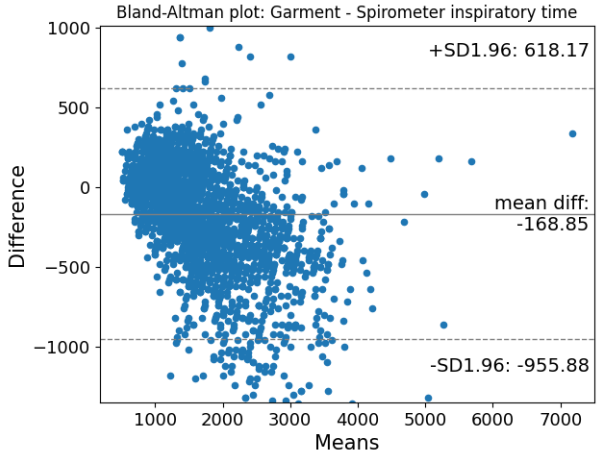

(b) T_{insp}

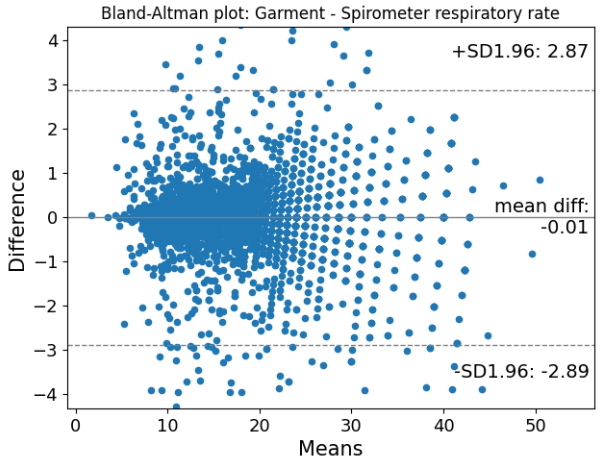

(c) f_B

Figure B.5: Bland-Altman plots of the parameters of interest relative to L.I.F.E. Healer R2 garment and to all subjects under static exercises conditions, excluding inspiratory and expiratory maneuvers-related breaths.

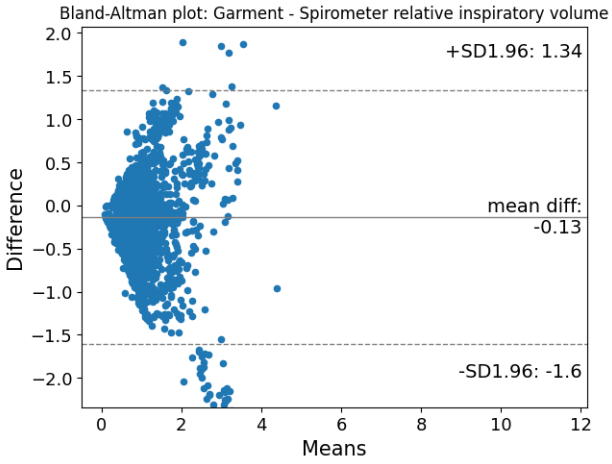

(a) Relative ΔV_{insp}

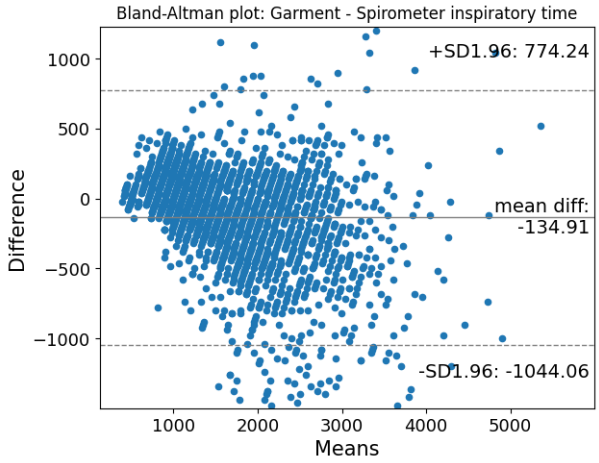

(b) T_{insp}

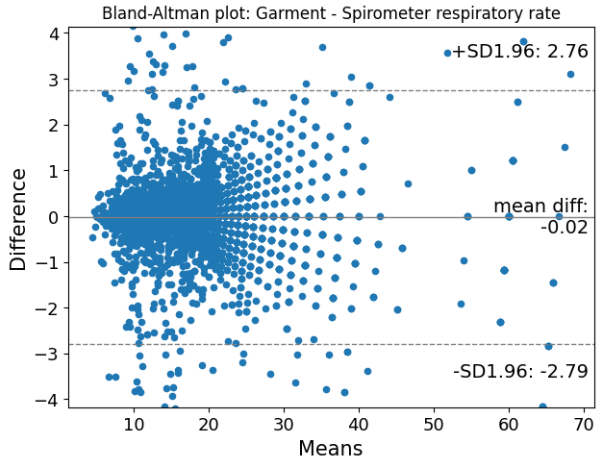

(c) f_B

Figure B.6: Bland-Altman plots of the parameters of interest relative to L.I.F.E. Healer R3 garment and to all subjects under static exercises conditions, excluding inspiratory and expiratory maneuvers-related breaths.

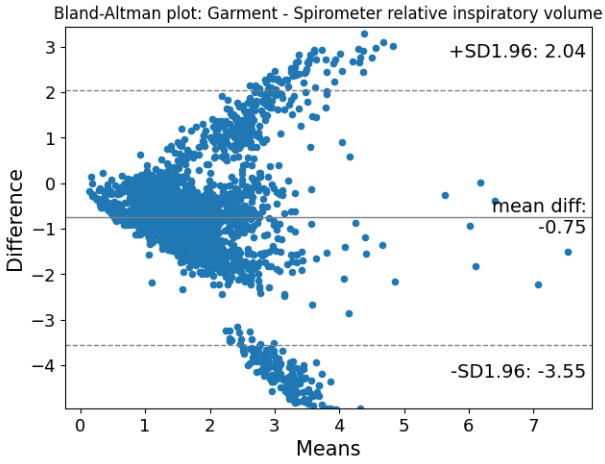

(a) Relative ΔV_{insp}

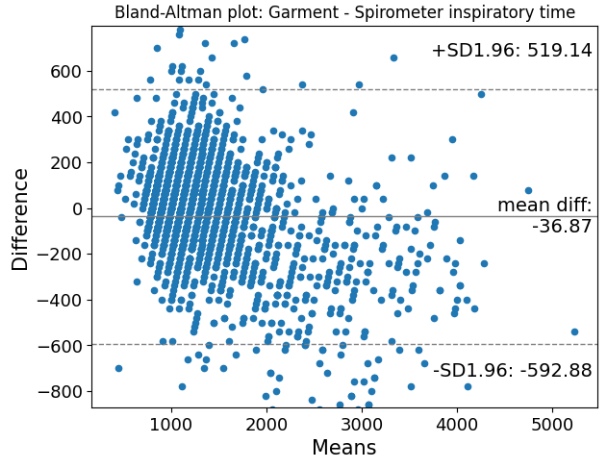

(b) T_{insp}

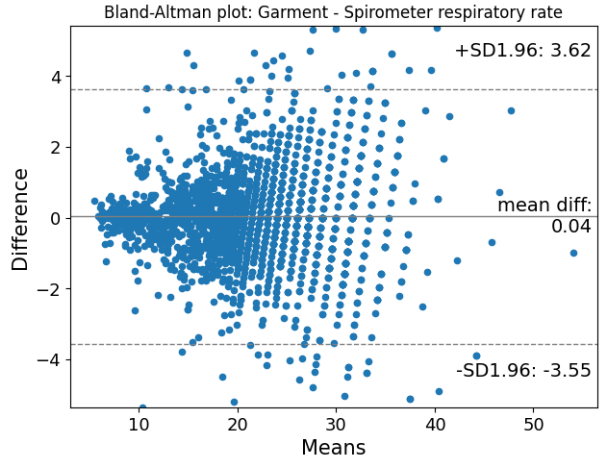

(c) f_B

Figure B.7: Bland-Altman plots of the parameters of interest relative to L.I.F.E. Healer R1 garment and to all subjects under dynamic exercises conditions.

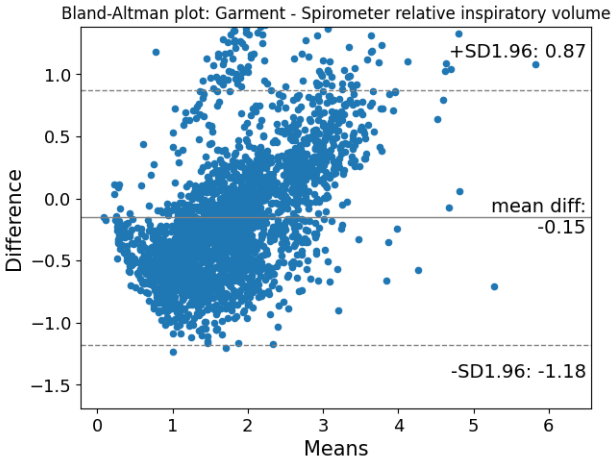

(a) Relative ΔV_{insp}

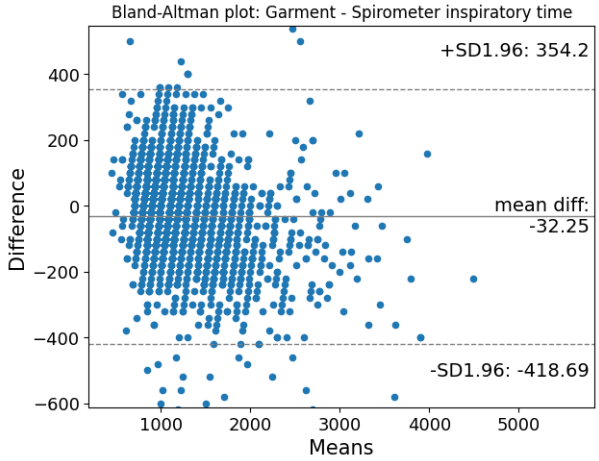

(b) T_{insp}

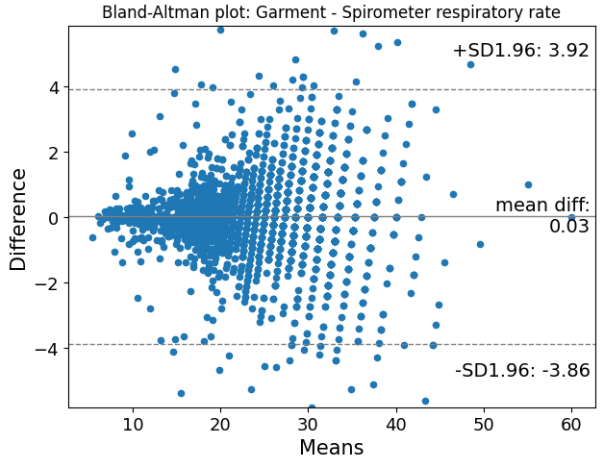

(c) f_B

Figure B.8: Bland-Altman plots of the parameters of interest relative to L.I.F.E. Healer R2 garment and to all subjects under dynamic exercises conditions.

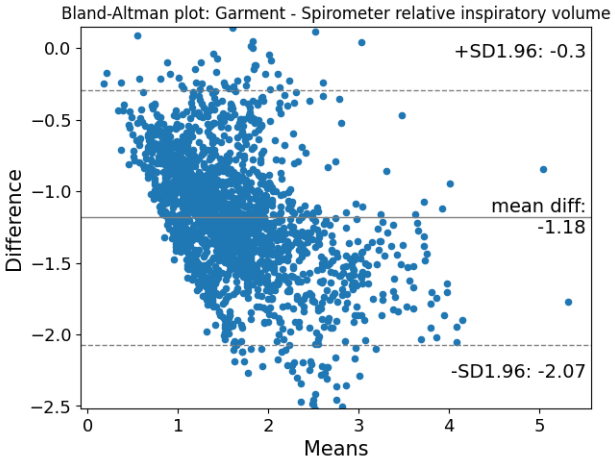

(a) Relative ΔV_{insp}

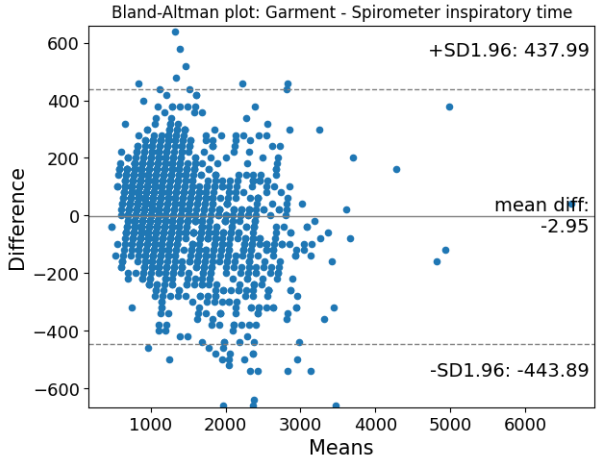

(b) T_{insp}

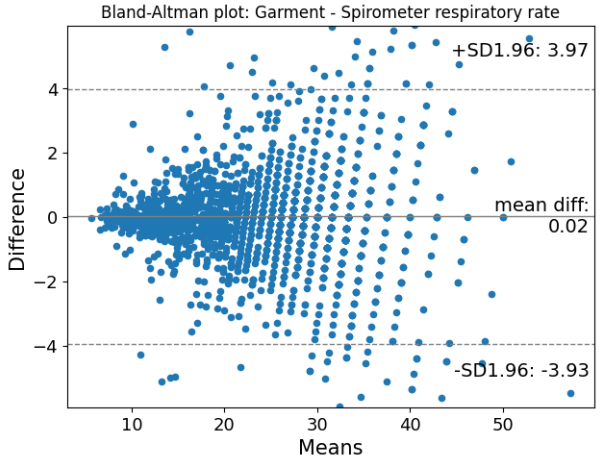

(c) f_B

Figure B.9: Bland-Altman plots of the parameters of interest relative to L.I.F.E. Healer R3 garment and to all subjects under dynamic exercises conditions.

List of Figures

List of Tables